Tyre model verification over off-road terrain

This thesis is submitted in partial fulfilment of the requirements for the degree of Master of Engineering

from the University of Pretoria

by

Martin Joachim Stallmann

UNIVERSITEIT VAN PRETORIA
UNIVERSITY OF PRETORIA
YUNIBESITHI YA PRETORIA

Denkleiers • Leading Minds • Dikgopolo tša Dihlalefi

Abstract

Vehicle dynamic simulations form a significant part of the design and development process of vehicles. These simulations are used to study and improve the vehicle's durability, ride comfort and handling capabilities. All forces acting on the vehicle are either generated in the tyre-road interface or are due to aerodynamic effects, where at low speeds the latter one can be ignored. The accuracy of the tyre model describing the forces on the tyre-road interface is thus of exceptional importance. It ensures that the simulation model is an accurate representation of the actual vehicle.

Various approaches are adopted when developing mathematical tyre models. Many of these models are developed to study the handling capabilities of passenger cars over a smooth road. Passenger car tyres are the focal point as larger tyres introduce some difficulties due to their size and load rating. Off-road truck tyres also differ in their construction which will influence force and moment generation of the tyre. Research efforts are increasing to meet the need of tyre models that can describe the behaviour of the tyre over uneven terrain with sufficient accuracy. This thesis addresses the question of whether existing mathematical tyre models can accurately describe the forces and moments generated by a large off-road tyre while driving over rough terrain.

The complexity of different mathematical tyre models varies greatly, as does the parameterisation efforts required to obtain the model parameters. The parameterization of most tyre models relies on some experimental test data that is used to extract the necessary information to fit model parameters. The selection of a suitable tyre model for a simulation is often dependent on the availability of such experimental data and the effort to identify the required parameters. In this study the parameterisation process for four different tyre models, are discussed in detail to highlight the difficulties in acquiring the test data and the effort to parameterize the model. The models considered are the One Point Contact, 3D Equivalent Volume contact, 3D Enveloping Contact and FTire model.

Experimental measurements are conducted on a 16.00R20 Michelin XZL tyre. Laboratory tests, as well as field tests, over discrete obstacles and uneven hard surfaces are used for parameterisation and validation purposes. Simulation results are compared to experimental test data to determine whether the models could be used to describe the tyre road interactions with sufficient accuracy. Recommendations are made for tyre model selection and model accuracy for simulations over rough off-road surfaces.

Acknowledgements

I would like to my gratitude to:

- My parents Walter and Christine Stallmann, for their support and aid in my masters.
- Prof. Els, for this mentorship through my postgraduate studies.
- Michael Gipser and Gerald Hofmann from COSIN, for their help and support with FTire.
- Carl Becker for his help during testing.
- My fellow postgraduate students Theunis Botha, Francios van der Westhuizen and Herman Hamersma, Bernard Linström, for their advice, support during testing and the everyday conversations that made the project so much more interesting.

"Automobiles and trucks are machines for using tyres."

- Maurice Olley, 1947

Index

List of Figures

List of Tables

Notation

Symbol	Unit	Description
A	$m2/cycles/m$	roughness coefficient
a	m	half contact lenght
b	m	half contact width
c	Ns/m	damping coefficient
c_z	Ns/m	vertical tyre damping coefficient
f		function
F_x	N	lateral tyre force
F_{xc}	N	lateral force at wheel in C-axis system
F_y	N	longitudinal tyre force
F_{yc}	N	longitudinal force at wheel in C-axis
F_z	N	vertical tyre force
F_{z0}	N	nominal wheel load
F_{zc}	N	vertical force at wheel in C-axis
I_0	kgm^2	moment of inertia about point O
k	N/m	spring stiffness
k_z	N/m	vertical tyre stiffness
l	m	pendulum length
l_s	m	tandem based length
m		measured value
m_t		measured value at index t
M_{xc}	Nm	overturning moment at wheel in C-axis system
M_{yc}	Nm	driving/braking moment at wheel in C-axis

M_z	Nm	aligning moment
M_{zc}	Nm	aligning moment at wheel in C-axis
n		road index
n_{length}		number of cams along tyre contact length
n_n		number of indices
n_{width}		number of cams across tyre contact width
p		predicted value
p_{A1}		tyre contact length parameter A1
p_{A2}		tyre contact length parameter A2
p_{ae}		length factor of cam
p_{B1}		tyre contact width parameter B1
p_{B2}		tyre contact width parameter B3
p_{B3}		tyre contact width parameter B3
p_{be}		height factor of cam
p_{ce}		ellipse response
p_{ls}		cam base length coefficient
p_t		predicted value at index t
q_{Fcx1}		tyre stiffness interaction with F_x
q_{Fcy1}		tyre stiffness interaction with F_y
$q_{Fc\gamma1}$		tyre stiffness interaction with camber
q_{Fz1}		tyre vertical stiffness coefficient (linear)
q_{Fz2}		tyre vertical stiffness coefficient (quadratic)
q_{v2}		tyre stiffness variation coefficient with speed
R_0	m	unloaded tyre radius
s_z	%	wheel longitudinal slip
S_z		vertical displacement spectral density

t		index
V_0	m/s	unloaded tyre rolling velocity, $V_o = \omega R_o$
W_0	m	nominal section width of the tyre
x_1	m	amplitude of the first displacement oscilation
x_2	m	smplitude of the second displacement oscilation
x_e	m	x value of cam
y_e	m	y value of cam
Greek letters	**Unit**	**Description**
$\dot{\theta}$	rad/s	rotation angular velocity
$\ddot{\theta}$	rad/s^2	rotation angular acceleration
$\dot{\rho}$	m/s	tyre deflection velocity
ρ_z	m	tyre deflection in z direction
ω_n	rad/s	undamped natural frequency
α	deg	wheel slip angle
γ	deg	wheel inclination angle
δ		logarithmic decrement
θ	rad	rotation angular displacement
κ	$\%$	wheel longitudinal slip
μ		standard deviation
ξ		damping ratio
π		the ratio of a circle's circumference to its diameter
ρ	m	tyre deflection
σ		mean
φ	$cycles/m$	spatial frequency
ω	rad/s	wheel rotation speed

Indices	Description
$\%RE$	percentage relative error
3D	three dimensional
3D ENV	3D Enveloping Contact model
3D VC	3D Equivalent Volume Contact model
ABS	Anti-lock Braking System
DSD	Displacement Spectral Density
ESP	Electronic Stability Program
LC1	load case 1 of the dynamic field test
LC2	load case 2 of the dynamic field test
LC3	load case 3 of the dynamic field test
$m\%RE$	mean percentage relative error
lk	linear tyre stiffness
nlk	non-linear tyre stiffness
OPC	One Point Contact model
OTR	off the road
PAC89	Pacejka 89 tyre model
PAC94	Pacejka 94 tyre model
PAC2002	Pacejka 2002 tyre model
PAC-MC	Pacejka motorcycle tyre model
RMS	root mean square
TNO	Netherlands Organization for Applied Scientific Research
TP	FTire tyre model where the tread pattern is modelled
TYDEX	tyre data exchange format

1. Introduction

"See first, think later, then test. But always see first. Otherwise you will only see what you were expecting. Most scientists forget that."

- *Douglas Adams, 1984*

Automobile design has occurred for the past 100 years. The automobile today is a highly sophisticated machine that is designed to transport passengers and cargo at high speeds over paved roads or comfortably over rough terrain. The user's requirements from an automobile are constantly changing and the expectations are ever increasing. The development of the automobile is thus progressing at an alarming rate.

The development process of vehicles is aided by incorporating simulations in the development process. Reliability and strength simulations as well as crash test simulations are currently amongst the most prominent simulations that are being performed during the development process. Vehicle dynamics simulations, to improve the handling and ride comfort of vehicles, are not currently performed to a great extent. Their significance is increasing though.

Every mathematical model used to run a simulation is an idealization and simplification of reality. Simulations that go beyond the fundamental vehicle dynamics investigations require complex multi-body simulation models. All components used in the simulation model, used to describe the real model, must be modelled with sufficient accuracy to ensure the validity of results.

The external forces acting on the vehicle form part of the components which need to be modelled accurately. These forces either result from the tyre-road interactions or the aerodynamic effects of the vehicle. The latter can be ignored at low speeds as it is largely dependent on the vehicle velocity. The behaviour of a ground vehicle, especially over off-road terrain is thus predominantly dependent on the vehicle-road interaction. Pneumatic tyres are primarily used to establish the vehicle-terrain contact interaction.

The pneumatic tyre is a complex structure that comprises dozens of components that are pressed, assembled and cured together. Modern tyres are a combination of steel, fabric and rubber. A few milestones in the development of the pneumatic tyre thus far are listed in Table 1-1. Tyre development is a continuous process. Currently, over 2.6 billion tyres are manufactured annually (Freedonia, 2012) in factories around the globe.

Ultimately the tyre is the means by which a vehicle remains controllable. Steering, acceleration and braking actions are transmitted to the road through the tyre. However, tyres are more often thought of as little more than automotive components; a small part in a larger assembly where the vehicle itself receives top billing. The pneumatic tyre should be considered as the most important component on an automobile.

Table 1-1 Tyre development milestones (Mullineux(2011) and Rill(2006))

1839	Vulcanization; Charles Goodyear
1845	first pneumatic tyre - Several thin inflated tubes inside a leather cover; Robert William Thompson
1846	First solid rubber tyre; Thomas Hancock
1888	Patent for pneumatic bicycle tyres; John Boyd Dunlop
1891	Patent for a removable pneumatic tyre; Andre and Edouard Michelin
1895	Michelin pneumatic tyres are used during the Paris–Bordeaux–Paris race; 760km: 50 tyre deflations, 22 complete inner tube changes
1899	"Long-lived" tyres, approx. 500 Kilometres; Continental
1904	First grooved tread tyre; Continental A.G.
1908	Grooved tyres to improve road friction; Frank Seiberling
1922	Steel cord tread in tyre bead; Dunlop
1943	Patent for tubeless tyres; Continental
1948	Steel-belted radial tyre; Michelin
1983	Radial tyres are standard in America, more than two decades after Europe

As depicted in Figure 1-1, the effect of the tyre on every vehicle operational characteristic is substantial. The tyre does not only support the weight of the vehicle but also has a major influence on fuel consumption, handling capabilities, safety and comfort of the vehicle.

The tyre-road interaction presents one of the biggest challenges in creating an accurate vehicle model. The tyre is a complex assembly of a variety of compounds. The resulting force generation is thus nonlinear and depends on the operating environments (road surface, inflation pressure, etc) and imposed states (slip angle, magnitude of loading, etc.). Research has focused on describing the forces generated in the tyre-road contact area for many years. Many tyre models have been developed and improved in the last few years. Most models describe the vertical and lateral tyre forces and accompanying moments. These models are mostly used in simulations which investigate the vehicle behaviour during handling manoeuvres on smooth roads. The improvement of ride comfort and safety of large off-road trucks, over rough terrain, has become more significant in the development process of heavy vehicles. The vertical behaviour was in many cases only described using empirical formulae or a one point contact spring damper model.

Noteworthy research efforts, regarding tyre models over short road irregularities, are summarized in Table 1-2. Most tyre models were developed for passenger car tyres. A large knowledge-gap exists concerning tyre models of large off-road tyres that can be applied to off road manoeuvres over rough terrain. Few publications can be found in this regard.

Schmeitz (2004) shows that researchers primarily rely on experimental laboratory test data to develop and parameterize tyre models. The developed tyre models are also validated using laboratory test data rather than field test results.
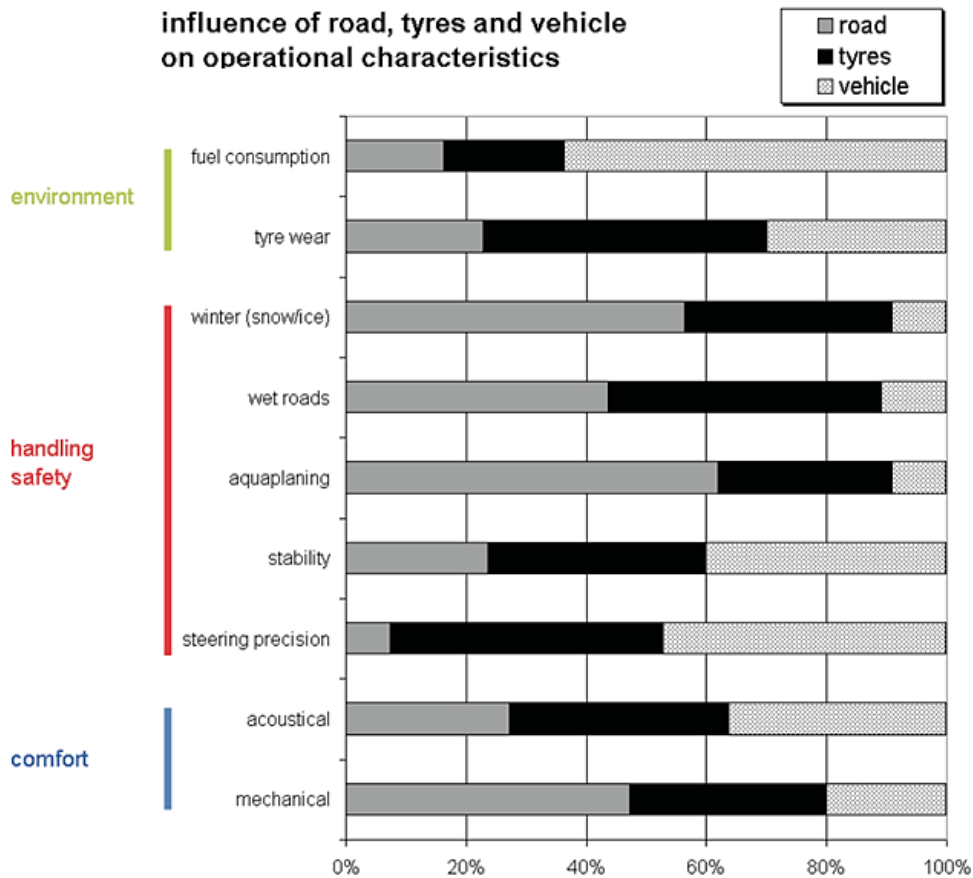
Figure 1-1 Influence of road, tyres and the vehicle on operational characteristics (Mohammadi, 2012)

Pacejka and Sharp (1991) developed a list of features that mathematical tyre models should have to be relevant and useful in vehicle dynamical simulations. The significant features include:

1. accuracy
2. range of behaviour encompassed
3. number of parameters
4. physical significance of the parameters,
5. the means by which the parameters may be obtained and the data required
6. the capability and simplicity of extension to cover behaviour outside the range used for parameter evaluation and
7. computational load

Models which possess effective combinations of the above qualities are of the greatest interest. The authors further state that to determine the accuracy of the model the following should be considered:

1. real tyres differ from each other due to manufacturing tolerances
2. tyres vary in use as the tread rubber wears away, through ageing and as the temperature and inflation pressure change
3. tyre shear force test results vary with road speed surface properties and temperature
4. many tyre tests are conducted on drums, the surface curvature of which affects the results but not in any systematic or fully understood fashion

Table 1-2 Literature on modelling the dynamic response of tyres over short road irregularities (Schmeitz, 2004)

reference	direction response				dynamic tyre model category				experiments	
	longitudinal	lateral	vertical	rotational	rigid ring	multibody	FEM	modal	laboratory	road
1987: Kao	•		•					•	•	
1987: Schulze	•		•		•					•
1988: Bandel	•		•					•	•	
1988: Gipser						•				
1988: Schulze	•		•			•				•
1988: Ushijima			•					•	•	
1993: Böhm						•				
1996, 1997: Eichler	•		•			•				•
1996, 1998: Zegelaar	•		•	•	•				•	
1996: Kamoulakos	•		•				•		•	
1996: Mousseau	•		•				•		•	
1997: Kao	•		•				•		•	
1997: Oertel	•		•			•			•	
1997: Wu	•		•				•		•	
1998: Böhm	•		•			•				•
1999: Gipser	•		•			•			•	
1999: Mancosu	•		•		•					
1999: Oertel	•	•	•			•			•	•
2000: Jansen			•		•					•
2000: Kao	•	•	•		•					•
2000: Schmeitz	•		•		•	•			•	
2001: Schmeitz	•		•	•	•				•	
2002: Belluzzo			•					•	•	
2002: Gipser	•	•	•			•			•	
2002: Olatunbosun	•		•				•		•	
2002: Pacejka	•		•	•	•				•	
2003: Sobhanie	•		•				•			
2003a: Schmeitz	•	•	•	•	•				•	
2003b: Schmeitz	•		•	•	•				•	•

Recently, the need for a tyre model that is able to accurately describe the higher frequency response during simulations has developed. Tyre models that can describe vibrational frequencies are used in the design of control systems such as ABS and ESP. These models are also aimed at improving the ride comfort, handling and durability of the vehicle. According to Antoine et al. (2005) the frequency range,

required for various vehicle-system analyses, require models to accurately predict dynamic tyre responses up to 100Hz. The specific frequency range for various vehicle systems is summarized in Figure 1-2.
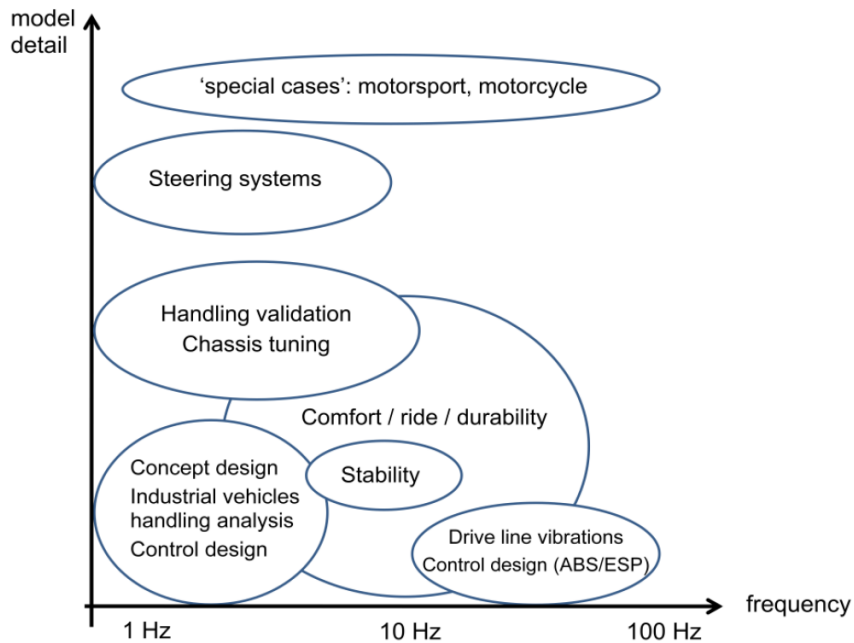
Figure 1-2 Frequency range requirements for vehicle-system analyses (Antoine et al. 2005)

This chapter will provide background information regarding tyre models (Section 1.1) and tyre testing for parameterization (Section 1.2). The motivation for this research project will be given (Section 1.3) and an outline for the remaining chapters will be provided (Section 1.4).

1.1. Tyre Models

Mathematical vehicle dynamics models are often used to aid in the development of new vehicles. These models are only useful if they can reflect reality with sufficient accuracy. The modelling of the tyre road interaction is of special importance as it influences the accuracy of the entire vehicle dynamics model. It can be said that a sufficiently accurate description of the tyre and the road is one of the most important aspects of creating a useful simulation model. All other components of the model are influenced by the forces and moments developed in the tyre contact patch. To create a balanced model the accuracy of the vehicle model should stand in a reasonable relationship to the applied vehicle- road contact model.

A wide range of tyre models and tyre contact models have been developed over the years (Schmeitz, 2004). Many of these models were developed for simulations that investigate handling manoeuvres of passenger cars, over smooth man-made roads.

Researchers have developed and validated various tyre models to be used in simulations over uneven terrain (Zegelaar, 1998). Research has shown that physical tyre models can accurately predict tyre forces. These models however require excessive computer resources and calculation times. These limitations restrict their use for vehicle dynamic simulations. More compact models, such empirical models, are

much faster and require manageable computational power. Empirical models however struggle to represent the complex tyre behaviour (Frey, 2009).

The required accuracy of a simulation varies greatly. Some simulation results are required to be very accurate. For other simulations the solution time is more important. Figure 1-3 describes the relationship between the expected accuracy and test data requirements of various tyre models that are implemented in ADAMS (MSC Software (a), n.d.).

It is not always possible to acquire enough data to parameterize the tyre model of choice. This might be due to financial or logistical constrains. By comparing different tyre models with varying complexity and parameterization effort one can determine if a simpler tyre model might be sufficiently accurate. Little has been published about the accuracy of tyre models over rough terrain.
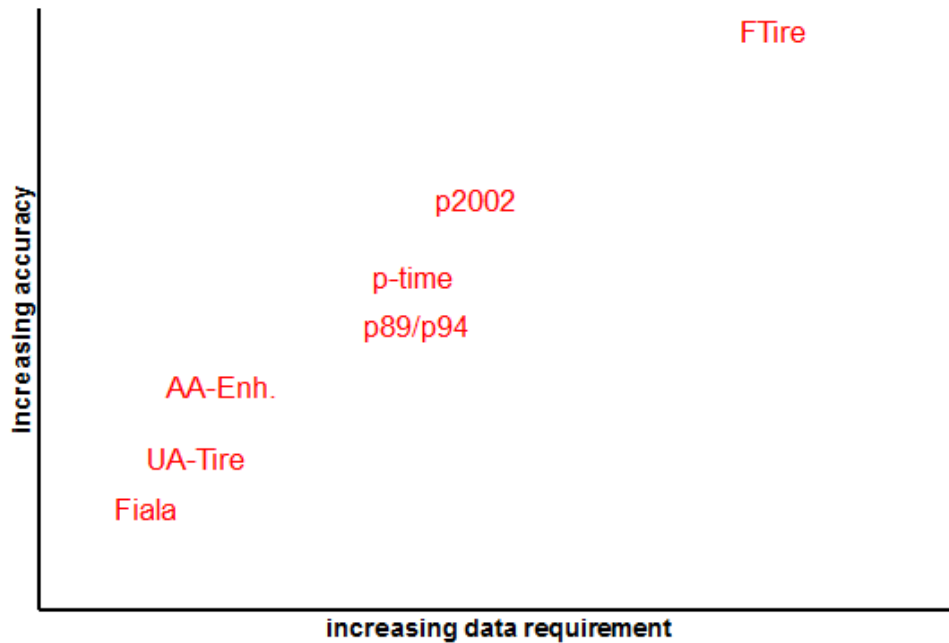
Figure 1-3 Accuracy versus test data requirements of various tyre models (Oosten, 2011)

To aid the selection of a tyre model in ADAMS the user is supplied with a tyre selection chart. The chart is shown in Figure 1-4. The tyre models are rated for various events using four classifications:

(a) Not possible/ Not realistic
(b) Possible
(c) Better
(d) Best to use

This rating scheme gives the user some indication of what tyre model should be selected. There is however also a need to give the user some indication of the expected accuracy that can be expected from the available models.

MD Adams	Event / Maneuver	ADAMS/ Handling Tire							Specific Models	
		PAC2002[1]	PAC-TIME[1]	PAC89[1]	PAC94[1]	FIALA[1]	5.2.1.[1]	UA Tire[1]	PAC-MC[1]	FTire
Handling	Stand still and start	+	o/+	o/+	o/+	o/+	o/+	o/+	o/+	+
	Parking (standing steering effort)	+	-	-	-	-	-	-	-	+
	Standing on tilt table	+	+	+	+	+	+	+	+	+
	Steady state cornering	+	+	o/+	+	o	o	o/+	+	o/+
	Lane change	+	+	o/+	+	o	o	o/+	+	o/+
	ABS braking distance	+	o/+	o/+	o/+	o	o	o/+	o/+	+
	Braking/power-off in a turn	+	+	o	o	o	o	o	+	o/+
	Vehicle Roll-over	+	o	o	o	o	o	o	o	+
	On-line scaling tire properties	+	-	-	-	-	-	-	-	o
Ride	Cornering over uneven roads *	o/+	o	o	o	o	o	o	o	o/+
	Braking on uneven road *	o/+	o	o	o	o	o	o	o	+
	Crossing cleats / obstacles	-	-	-	-	-	-	-	-	+
	Driving over uneven road	-	-	-	-	-	-	-	-	+
	4 post rig (A/Ride)	+	o/+	o/+	o/+	o/+	o/+	o/+	o/+	o/+
Chassis Control	ABS braking control	o/+	o	o	o	o	o	o	o	+
	Shimmy[2]	o/+	o	o	o	o	o	o	o	+
	Steering system vibrations	o/+	o	o	o	o	o	o	o	+
	Real-time	+	-	-	-	-	-	-	-	-
	Chassis control systems > 8 Hz	o/+	-	-	-	-	-	-	-	+
	Chassis control with ride	-	-	-	-	-	-	-	-	+
Dura-bility	Driving over curb	-	-	-	-	-	o	o	-	o/+
	Driving over curb with rim impact	o	-	-	-	-	o	o	-	o/+
	Passing pothole	-	-	-	-	-	o	o	-	o/+
	Load cases	-	-	-	-	-	o	o	-	o/+

Legend			
-	Not possible/Not realistic	*	wavelength road obstacles > tire diameter
o	Possible	[1]	use_mode on transient and combined slip
o/+	Better	[2]	wheel yawing vibration due to
+	Best to use		supension flexibility and tire dynamic response

Figure 1-4 ADAMS tyre models selection chart (MSC Software (2), n.d)

1.2. Tyre Testing and Parameterization

Most of the tyre models developed over the past two decades require experimental test data for the parameterization process. The test data is used to extract information that governs the tyre behaviour. Since all tyres have a distinctive geometry and are constructed using different materials and manufacturing processes, the tyre behaviour is unique to that tyre.

The ability of a tyre model to accurately predict the tyre behaviour is not only dependent on the modelling approach that is used. It is also determined by the accuracy and availability of measured tyre data. Since most tyre models rely heavily on the parameterization of data, the validity of the model is directly dependent on the availability of the test data. If the required data cannot be obtained the model becomes obsolete.

Tyre test rigs are widely used to obtain test data. These rigs investigate properties such as the tyre force and moment generation. Indoor and outdoor test rigs are available. Indoor tests are gaining popularity as the tests are conducted in a controlled environment and are generally more cost efficient.

Figure 1-5 shows a schematic of a tyre drum test rig and a flatbed tyre test rig. These two types are most commonly used for indoor tyre test measurements (Rill, 2006). Two different drum test setups are available. The tyre can either be on the outside or inside of the drum. The curvature of the drum itself increases or decreases the local deformation of the tyre in the contact patch. This creates variation in the

force and moment generated, which influences the behaviour of the tyre. To reduce this unwanted effect the ratio of the test drums diameter compared to that of the test tyre, must be increased.

The drum surface can either be steel or coated with a "safety walk" coating to improve the friction conditions (Rill, 2006). Modern drum tests allow caskets to be mounted on or in the drum. These caskets are filled with real pavements to simulate real road driving conditions (Schwalbe, n.d.). These drum tests are generally developed to test passenger car tyres and thus often have a maximum track width of 400mm and support tyre loads of up to five tons (TÜV SÜD, n.d.). Tyres can be tested on drums at velocities greater than 250km/h.

The tyre is generally connected to a movable hub so that changes in longitudinal slip, caster angle and camber angle can be investigated. Cleats can be mounted onto the drum to investigate the tyre behaviour over discrete obstacles.
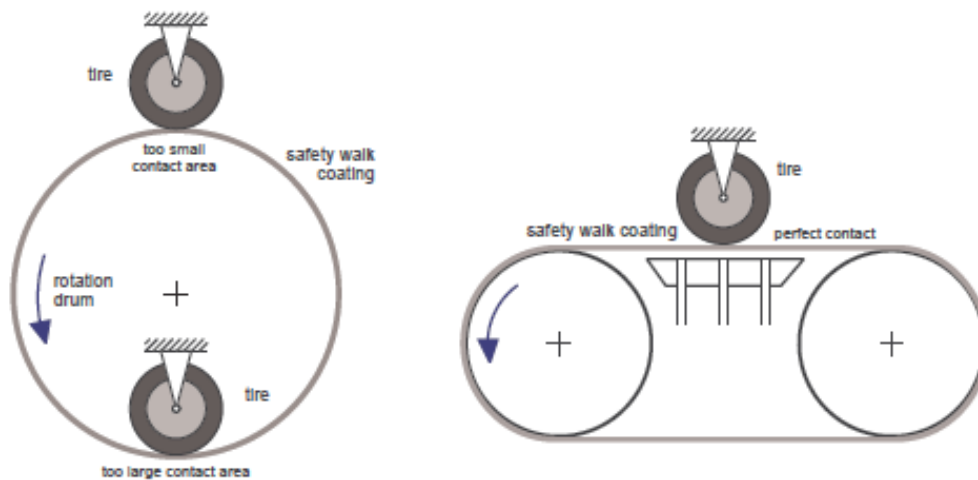
Figure 1-5 Drum and Flatbed tyre test rigs (Rill, 2006)

Drum test results are often used as parameterization data for tyre models but are more appropriately used for ranking analysis or for investigations in the relative effect of load, speed and temperature changes on the tyre behaviour. The use of the test data is limited due to the curved contact between the tyre and the test surface as well as the difficulty in achieving a test surface representative of real road surfaces. The unnatural curvature affects the tyre behaviour and influences the generated force and moment components of the tyre. To circumvent this short coming, tyre model parameterization software is being developed in such a way so as to consider the curvature effects.

Flatbed test rigs are more sophisticated than conventional drum test rigs as the tyre – road contact is flat. This is a more accurate representation of the tyre - road interaction. The belt that simulates the road is supported by two drums and is coated with an abrasive surface coating (MTS, n.d.). The coating increases the friction when compared to the uncoated steel belt however it is not identical to an actual road surface.

To support the load of the tyre, an air or water bearing is installed underneath the belt near the tyre contact patch. The tyre is connected to a movable hub to change the slip, caster and camber angle. The

test rig has a similar load and speed rating as the drum test rigs but cannot be used for extreme tyre torque measurements.

The flat bed test rig can only be used to test tyre behaviour over a flat belt and can thus not be used to perform cleat tests or be used to excite the tyre in the normal direction. To perform laboratory cleat tests on a flat surface a flat plank tyre test rig can be used.

The flat plank tyre tester consists of a main frame, flat steel plank, measuring hub, turn table, axle height and lateral position adjustment mechanism, brake, camber mechanism and a driving motor. The flat plank, simulating the road surface, is generally less than 5 m long, and can move in the longitudinal direction. Cleats are mounted onto the flat surface to conduct tyre enveloping behaviour. The disadvantage of this test rig has is that tests can only be conducted at speeds less than 0.2km/h (Cremens, 2005).

Tyre test rigs for large off road (OTR) tyres are seldom found. Tianjin Jiurong Wheel Tech Company (n.d.) has developed a tyre test rig for tyres with a wheel diameter of up to 3.2 meters. The test rig is shown in Figure 1-6. It is predominantly used to test the quality of large off-road tyres by analysing the effect that the load and number of rotational cycles have on tyre temperature and to determine the rolling resistance of the tyre.

The test rig is also used to determine the "Ton kilometre per hour" value, also known as TKPH value, of the test tyre. The TKPH value is calculated to determine the maximum work load of a tyre and is used to monitor its work so that it is not put under undue stress which may lead to its premature failure. The test rig has a drum diameter of 5 meters and can withstand tyre loads of up to 120 tons. The maximum test speed is about 70 km/h.

Figure 1-6 Large drum tyre test rig, to test large OTR tyres

Outdoor tests, also known as field tests, are generally conducted using trucks or test trailers. These trucks and trailers are equipped with a special hub on which the test tyre is mounted. Figure 1-7 shows the test trailer that is used by TNO, Netherlands, to test various tyres. The on-road tyre test rig is used to test passenger car tyres, motorcycle tyres and light truck tyres up to a maximum speed of 150km/h at a maximum normal load of 10kN (De Roon, 2006). The advantage of outdoor testing is that the tests can be conducted under real operating conditions. Tests on arbitrary road surfaces such as asphalt or concrete are

possible, as are tests under different environmental conditions including ice or rain. The disadvantages of these tests are that they are quite cumbersome and more difficult to control.

Figure 1-7 Tyre test trailer of TNO, Netherlands

Tyre test equipment which is currently available in South Africa consists of a tyre test trailer (Els & Becker. 2011). The test trailer, as shown in Figure 1-8, comprises of two core structures, the mainframe and the sub frame. The test tyre is mounted to the sub frame on the right hand side. The sub frame is in turn connected to mainframe by six load cells positioned to allow the forces and moments acting on the wheel to be calculated. The side slip angle of the tyre can be altered, ranging from -2 to 12 degrees, to investigate the lateral tyre behaviour. The trailer can be loaded with ballast so that the load on the tyre ranges from 2400kg to 5200kg. Currently no brake torque can be applied to the test tyre and the kingpin angle is fixed.

Figure 1-8 Tyre test trailer for large tyres

1.3. Motivation and Goals

To use simulations to predict the behaviour of large off-road trucks, while driving over uneven terrain, accurate tyre models are required.

A large number of tyre models have been developed that require experimental test data to be used in the parameterization process. The test data is used to extract parameters that define the tyre behaviour. Tyre test rigs, as discussed in section 1.2, are often used to acquire the required data. The test rigs are however often limited to passenger car tyres or light truck tyres. Alternative methods to obtain sufficient parameterization data, of large off-road tyre, need to be investigated.

This thesis aims to determine whether existing tyre models can be used to accurately describe the vertical behaviour of large off road tyres while driving over uneven terrain. Can a tyre model accurately describe the vertical forces, of large off-road tyre, during a simulation where off road driving manoeuvres are investigated?

This thesis attempts to address what the error range would be when using a specified tyre model. The accuracy gain versus parameterization effort compromise will also be investigated.

1.4. Thesis Outline

The outline of this thesis is as follows:

Chapter 2 contains a review of different tyre modelling approaches that are found in literature. Different modelling methods are discussed at a conceptional level. The tyre models that are implemented in the multi body dynamic software MSC ADAMS are discussed in further detail as their behaviour was investigated.

In chapter 3 the process of acquiring parameterization data is discussed. Both laboratory and field test processes are undertaken. The accuracy of the test data and the method of collection play an important role in the ability of a model to predict the tyre behaviour. The chapter will also highlight the difficulty in obtaining certain parameterization data.

Chapter 4 discusses the parameterization process of various tyre models. The data that was obtained, as discussed in Chapter 3, is used to parameterize the tyre models under investigation.

Chapter 5 focuses on the validation of the dynamic response of the tyre models. Simulation results are presented and compared to measured tyre response data over various test tracks.

Chapter 6 summarizes the research project. Improvements and recommendations for further research are formulated.

2. Tyre Modelling

"The core of science is not mathematical modelling - it is intellectual honesty. It is a willingness to have our certainties about the world constrained by good evidence and good argument."

— *Sam Harris, 2006*

Tyre modelling has been a research focus area for many years. During World War 2 an increased attempt at research was made, mostly with respect to aircraft tyres. Aircraft constructors requested information regarding the effect of normal tyre deflection on the braking force and the location of the centre of pressure between the tyre and the road (Gough & Whitehall, 1962).

Today the automotive industry has a desire to use mathematical models to aid the engineer in the development process and reduce development time and cost. Great research effort has resulted in a multitude of tyre models. The models attempt to address the need to reduce solver time and increase the accuracy of the simulation results.

In this chapter different modelling approaches will be discussed. Their advantages and shortcomings will also be outlined. Special attention will be given to tyre models that are implemented in the MSC ADAMS software platform.

2.1 Introduction to Tyre Modelling

Researchers have followed many different approaches to accurately model the tyre-road interaction. Many tyre models were developed for handling analyses only and could thus only be used on smooth road surfaces. Many of these models should rather be classified as curve fits or lookup tables that interpolate experimental test results. They are used to study the vehicle dynamic responses to steering, throttle input and braking. For these analyses the vertical force variation in the tyre is less important and simple vertical models are often used.

However, to analyse the ride comfort and durability of a vehicle over rough terrain, the vertical forces generated in the tyre become significant. Vertical forces are also extremely important when simulating handling and road holding over uneven terrain where wheel hop or loss of tyre terrain contact can be expected. The road surfaces, which are used for these analyses, are not smooth and have short wavelength obstacles. The obstacles are usually smaller than the tyre circumference.

For the simulations described above, the road profile and road contact model become vital to achieve acceptable results. To accurately describe the tyre–road interactions, different tyre models and corresponding road contact models have been developed. These contact models include one point contact models, roller contact models, fixed footprint contact model, radial spring model, flexible ring contact models, finite element models and many more.

The one point contact model is the most extensively used contact model. The modelling approach uses a single point on the road surface to represent the tyre contact patch. The tyre is generally represented by a

parallel spring and damper assembly. As discussed by Zegelaar (1998) the contact model is valid for road obstacles with wavelengths longer than 3 meters and a slope smaller than 5%. The model can thus not be used for discrete obstacles as it results in high tyre accelerations.

The roller contact model, also known as the rigid ring tyre model, was developed to filter the road input (Frey, 2009). The model approximates the tyre as a rigid ring, or disk. The tyre contact patch is represented with a single contact. Contrary to the one point contact model, the contact point of the roller contact model is not restricted to lie vertically below the tyre axis of rotation. Consequently, the roller contact model filters the road surface and small wavelength road irregularities are filtered out. This approximation is valid for very stiff tyres such as commercial truck tyres.

The fixed footprint contact model uses a static contact area where the stiffness and damping is linearly distributed. The model averages the road irregularities, resulting in a smoother road excitation (Captain et al., 1974).
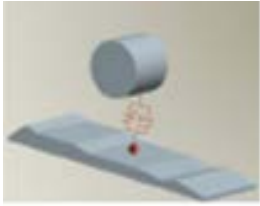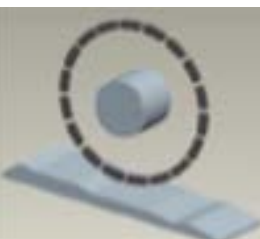
The radial spring model was developed to improve upon the behaviour of the rigid ring tyre model. The tyre is modelled using circumferentially distributed spring elements. Zegelaar (1998) states that a radial spring contact model with nonlinear digressive radial springs could be used to accurately predict the tyre behaviour over discrete obstacles.

Flexible ring contact models represent the tyre as a deformable tread band. The flexible ring is modelled as a deformable beam and is thus able to incorporate the vibrational Eigen frequencies of the tyre belt. As discussed by Zegelaar (1998) the contact model is able to show the characteristic dip in the vertical force while rolling over cleats.

Finite element models are based on the detailed modelling of the tyre structure. These models are very powerful as the tyre geometry and tyre deformation as well as different material properties are accounted for. The drawback of this modelling approach is that the solving time is generally very long and thus limits the application range.

Table 2-1 summarizes different tyre models according to the model complexity. These are the main groups of tyre models that are being used. Many tyre models are based upon these approaches or are built on a combination of these modelling methodologies.

Table 2-1 Tyre model classification according to model complexity (Einsle, 2010)

Group	Graphical representation	Description	Examples
Mathematical or characteristic model		Phenomenological -based, one point contact, various longitudinal and lateral force modelling some with a physical approach, numerically stable, in many cases real time capable, most extensively used, tyre geometry and contact area is ignored	MF-Tyre, HTyre, IPGTyre, LINES, Plesser, TameTyre, TM-Easy, PAC89, PAC94, PAC2002
Semi physical approach or brush model		Approximation of the tyre ground pressure distribution, brush element used to model ground contact, often combined with a solid ring model, in some cases the rotational motion is disregarded	Willumeit, Brit, Laermann, DYNA-TYRE, Zachow, Sharp, Mastimu
Cam or solid ring model		Combination of multiple nonlinear force elements, tyre geometry and contact area is accounted for, filtering of road surface, Eigen frequencies of the tyre belt is modelled, real time capable	SWIFT, RMOD-K 20, CTyre, CD Tyre 20,RTyre
Single flexible ring model		Elastic multi body belt model, two degrees of freedom, simplified lateral and longitudinal force modelling, able to capture the enveloping properties of a tyre	FTire (2D), RMOD-K 31, CDTyre 30, Eichler, CTyre
Flexible ring model with multiple layers		Multi layered elastic multi body belt model, modelled often with nonlinear force elements, lateral force generation due to belt dynamics, tyre geometry and contact area is accounted for, in general not real time capable	FTire (3D),RMOD-K 7.0, CD-Tyre
Finite element model		Multi layered finite element model, nonlinear material properties are often used, tyre geometry and contact area is accounted for, extremely long solving time	Brinkmeier/Nacken-Horst, DTyre,Biermann et al, Ghoreishy, Kindt et al

2.2   Tyre Axis System and Geometry

To assist with the description of the tyre forces and moments, an axis system must be defined. The axis system used in this dissertation is defined in the TYDEX-format reference manual (Unrau & Zamow, 1997). The TYDEX format, **TY**re **D**ata **EX**change format, has been developed by an international working group, consisting of car manufacturing companies and research institutes, to simplify the exchange of tyre measurement data.
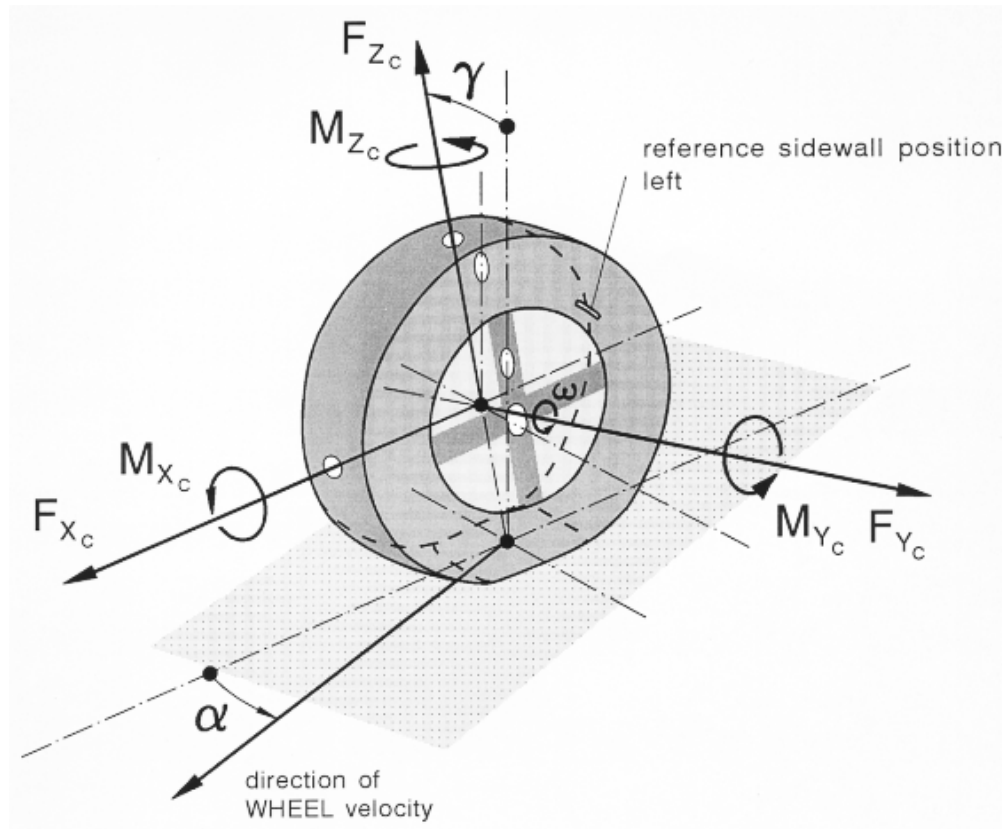
Figure 2-1 TYDEX-C axis system (Unrau & Zamow, 1997)

The TYDEX manual defines three different tyre axis systems with a positive slip and inclination angle and a positive wheel rotation speed. The origin of this axis system is fixed in the centre of the wheel, and is thus called the C-Axis system. The manual further defines the X-axis to be in the central plane of the wheel and parallel to the ground. The Y-axis turns with the inclination angle, γ, and is identical with the spin axis of the wheel. The Z-axis points upwards and also turns with the inclination angle, γ. The axis system is shown in Figure 2-1. All forces and moments are acting from the tyre to the rim. This axis system corresponds to the C-axis system as defined in SAE J 2047 (SAE International, 2013). In the SAE description the inclination angle is not included, while the TYDEX system defines this angle.

2.3   Tyre Models Implemented in ADAMS

The multi body dynamics analysis software MSC ADAMS is often used to simulate various vehicles manoeuvres. ADAMS/Tire is the module within ADAMS that is used to solve different tyre models (MSC Software (b), n.d). The following handling tyre models, incorporated in ADAMS/Tire, can be used for vehicle dynamic studies:

- PAC2002 Tyre Model
- PAC-TIME Tyre Model
- Pacejka '89 Models
- Pacejka '94 Models
- Fiala Model
- UA-Tyre Model
- 521-Tyre Model

These tyre models are primarily handling tyre models. The Pacejka models use the formulae developed by Dr H.B. Pacejka (Pacejka, Bakker & Lidner. 1987, and Pacejka, Bakker & Lidner. 1989), also known as the Magic formulae, to describe the tyre forces. These formulae describe the lateral, F_y, and longitudinal, F_x, force as well as the self-aligning torque, M_z, using the normal force, F_z, inclination angle, γ, sideslip angle, α, and the longitudinal slip, κ as input. The normal force is determined by the tyre contact model. ADAMS/Tire has four contact models that can be chosen. The contact models are:

- One Point Contact (OPC)
- 3D Equivalent Volume Contact (VC)
- 3D Enveloping Contact (3D ENV)
- Tyre cross-section profile contact method

The One Point Contact model uses a single point to represent the contact patch between the tyre and the road. This model is the default for all ADAMS/Tire tyre models.

The 3D Equivalent Volume Contact model computes the intersection volume between the tyre and the road to calculate the tyre displacement. This contact model can only be used with 3D shell roads.

The 3D Enveloping Contact model uses a series of cams to represent the tyre. The shapes of the cams correspond to the tyre contour. The model is based on the work done by Schmeitz (2004).

The tyre cross-section profile contact method is similar to the One Point Contact model but includes the cross section profile of the tyre to calculate the tyre penetration and contact position. This tyre model improves the simulation accuracy for simulations with large inclination angles, as is often the case for motorcycle simulation manoeuvres. This model is only used for simulations where motorcycle tyres are used to simulate driving manoeuvres over smooth surfaces (MSC Software (b), n.d.). It is thus not discussed in further detail in this dissertation.

 A summary of the tyre models, and their corresponding features, is shown in Table 2-2.

Table 2-2 ADAMS tyre model summary (MSC Software (b), n.d.)

tire model features		PAC89	PAC94	PAC2002	PAC-MC	Fiala	UA-Tire	521 Tire
contact methods	one-point contact (default)	X	X	X	X	X	X	X
	penetrated volume contact	X	X	X	X	X	X	X
	3D enveloping contact	X	X	X		X	X	
	tire cross-section profile contact				X			
tran-sient	linear transient (relaxation lengths)	X	X	X	X	X	X	X
	non-linear (advanced) transient			X				
belt dynamics				X				
design of experiments				X				
non-linear vertical stiffness		X	X	X	X	X	X	X
rim-road contact				X				
advanced loaded radius modeling				X				
parking torque				X				
frequency dependent stiffness (standing tire)				X				
conversion to PAC2002 with TDFT		X	X		X	X	X	
on-line scaling				X				
SmartDriver-Tire interface support		X	X	X	X	X	X	X

A second group of tyre models, which are implemented in ADAMS, are Specific tyre models. These models include:

- PAC-MC
- FTire
- SoftSoil

The PAC-MC is a motorcycle tyre model. The tyre model is described by Pacejka (2002). The tyre model can be used to describe the tyre behaviour of tyres with an inclination angle of up to 60 degrees. Large off road tyres are seldom exposed to such large camber angles. The model is thus not of interest for this study.

The SoftSoil model is used to describe the tyre-soil interaction of a tyre driving on elastic/plastic road surfaces. The model is omitted from the study as the focus is on the vertical tyre behaviour over hard uneven terrain.

The FTire (flexible structure tyre model) is a third party development by COSIN, but is supported by ADAMS and is included with a standard installation of ADAMS/Tire (Gipser, 2002). FTire is a complex tyre model that was developed for vehicle ride-comfort simulations over uneven terrain and obstacles with extremely short wavelengths. To parameterize FTire models the user is required to purchase the necessary software but the tyre model can be used without charge within ADAMS.

ADAMS/Tire supports user written tyre models. The user creates a TYRSUB subroutine that is then called by ADAMS/Tire. Many third party tyre model developers offer ADAMS add-ons. These models need to be acquired, usually at a cost.

In general ADAMS recommends that the One Point Contact, 3D Equivalent Volume Contact and the Tyre cross-section profile contact model should only be used for simulations over smooth roads with obstacles of wavelength larger than the tyre circumference. The 3D Enveloping Contact or one of the specific tyre

models, such as a FTire model, should be used for roads with smaller wavelength obstacles. This thesis investigates the performance and accuracy of various tyre models over uneven terrain, smaller that the tyre circumference.

Due to the popularity of the One Point Contact model, the thesis will also investigate this contact model. These contact models are very easy to parameterize and the parameterization is inexpensive. They may thus be useful for ride comfort simulations under conditions where the necessary parameterization data cannot be acquired. This dissertation focuses on the vertical response of a tyre while rolling over an obstacle, and not in the lateral or longitudinal behaviour of the tyre.

Magic-Formula tyre models are widely used in modelling the forces in the longitudinal and lateral direction. The latest addition to the Magic-Formula tyre models is the PAC2002 tyre model. The model contains the latest developments that have been published in Tyre and Vehicle dynamics by HB Pacejka (Pacejka, 2002). The normal force of the tyre is calculated, for a tyre deflection, ρ, as follows:

$$F_z = \left\{ 1 + q_{v2}|\omega|\frac{R_0}{V_0} - \left(q_{Fcx1}\frac{F_x}{F_{z0}} \right)^2 - \left(q_{Fcy1}\frac{F_y}{F_{z0}} \right)^2 + q_{Fc\gamma1}\gamma^2 \right\}$$

$$\left[q_{Fz1}\frac{\rho}{R_0} + q_{Fz2}\left(\frac{\rho}{R_0}\right)^2 \right]F_{z0} + c_z\dot{\rho} \tag{2.1}$$

The normal force is increased with an increase in the rotational speed, ω, and with a nonzero camber angle, γ. The normal force will decrease due to longitudinal and lateral tyre forces. The coefficients q_{Fz1} and q_{Fz2} are used to define a quadratic load- deflection curve. When q_{v2}, q_{Fcx1}, q_{Fcy1} and q_{Fcy1} are not defined, or equal to zero, the vertical force is calculated in the same way as is the case for the PAC89 and PAC94 tyre models. This thesis will analyse tyre behaviour due to road input. No torque will be applied to the tyre and the camber and slip angle will be set to zero. This leaves only the rotational speed dependency to be dissimilar from the description of the vertical force as implemented in the PAC89 tyre model.

A PAC89' tyre will therefore be used to describe the lateral and longitudinal forces and the tyre moments during a simulation. The same model will be used for all ADAMS/Tire tyre models. The dissertation will investigate the accuracy of the following tyre models and its corresponding contact model:

- PAC89 tyre model with a One Point Contact model
- PAC89 tyre model with a 3D Equivalent Volume Contact model
- PAC89 tyre model with a 3D Enveloping Contact model
- FTire model

The modelling approach of these models will be discussed in detail the following section.

2.3.1   One Point Contact Model

The One Point Contact model is the simplest and most extensively used contact model available. It represents the wheel as a spring and damper arrangement that trace a single point on the road surface that is vertically below the wheel centre. The One Point Contact model, as implemented in ADAMS/Tire

shows greater resemblance to a roller contact model. In this model the tyre and rim is considered to be a disk. The contact point is at the intersection between the wheel centre plane and the road tangent plane that has the shortest distance to the wheel centre. In this way the contact point is not constrained to be vertically below the wheel centre. This contact model is the default contact method for the Pacejka group of tyre models in ADAMS. Diagrams of both the point contact and roller contact model are shown in Figure 2-2 .

point contact   roller contact
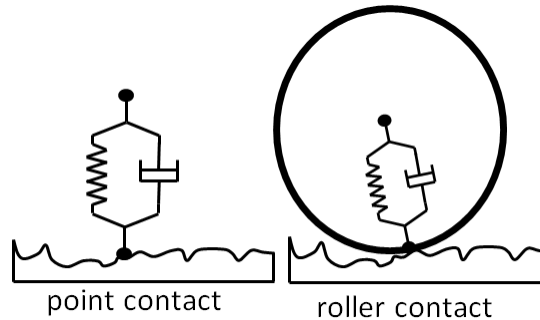
Figure 2-2 One point contact models

The contact model can be described using only three parameters, namely the unloaded tyre diameter, spring stiffness and a damping coefficient. The tyre stiffness, k_z, can either be described as linear or nonlinear while the damping can only be described with a constant damping coefficient, c_z. The nonlinear tyre stiffness can be defined, in the tyre property file, by a deflection-load curve. The deflection curve is defined by a table of tyre deflection and its resulting normal force. The table can consist of up to 100 data points. During a simulation the load deflection data points are fitted with a cubic spline curve. This allows for inter- and extrapolation of the data. The vertical force is then described by Equation 2.2.

$$F_z = k_z \rho + c_z \dot{\rho} \qquad (2.2)$$

The tyre deflection is given by ρ and the deflection velocity by $\dot{\rho}$. For small positive tyre deflections the damping coefficient is reduced and care is taken to ensure that the normal force does not become negative. If the tyre loses contact with the road the tyre deflection and deflection velocity is set to zero. This configuration ensures a zero normal force acting on the rim.

The contact force computed by the point-follower contact method is normal to the road plane. Therefore, in a simulation of a tyre hitting a pothole, the point-follower contact method does not generate the expected longitudinal force.

2.3.2   3D Equivalent Volume Contact Model

When the 3D Equivalent Volume Contact model is selected in the tyre property file the solver uses the intersection volume, between the undeflected tyre and road, to calculate the normal force. From the intersection volume the solver computes the effective normal tyre contact plane, tyre deflection, tyre to road contact point, and the effective road friction.

This contact model describes the tyre as a set of cylinders that are spaced along the width of the tyre. The user can define the outer tyre carcass shape, in the tyre property file, using up to ten points. ADAMS/Tire

assumes that the tyre carcass is symmetrical over the centreline of the tyre. When the defined carcass shape points are not equally spaced ADAMS/Tire will interpolate the data to define the same number of equally spaced data points. These data points will then be used determine the width of the discs, of which the total length is equal to the defined tyre width.

The 3D Equivalent Volume Contact model must be used with a 3D shell road. In a 3D shell road-definition-file the road is modelled as discrete triangular patches. The solver calculates the displaced volume of these patches and the tyre disks to determine the equivalent contact point of the tyre.
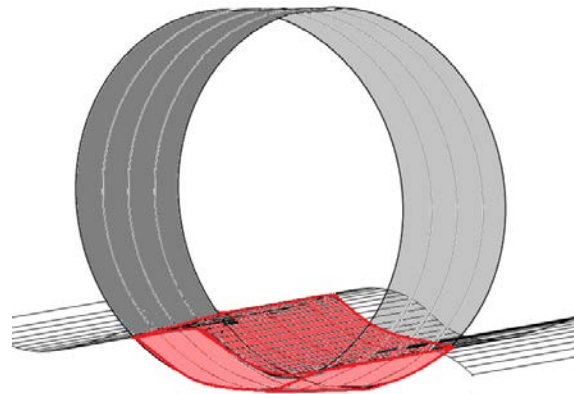
Figure 2-3 3D Equivalent Volume Contact model

The vertical force is then described by the same formula as was used in the One Point Contact model (Equation 2.2).

To parameterize the tyre model the tyre stiffness and damping need to be specified. The stiffness can be described as a constant or with an arbitrary load deflection curve. The damping is described with a constant damping coefficient. Furthermore the cross-section tyre shape needs to be defined. If no information is specified in the tyre definition file, ADAMS will assume a square cross-section. The 3D Equivalent Volume Contact model is the default contact model for simulations using a 3D shell road.

2.3.3   3D Enveloping Contact Model

To improve the accuracy of the One Point Contact model over short wavelength obstacles, the 3D Enveloping Contact model has been developed. When the tyre is negotiating an obstacle, it lengthens the input response and reduces its magnitude when compared to a solid disk. These two effects lead to a filtering of the road surface. Figure 2-4 shows the two effects and how they affect the response at the axle. Schmeitz (2004) proposed a model that uses elliptical cams to achieve a similar lengthening and swallowing effect.
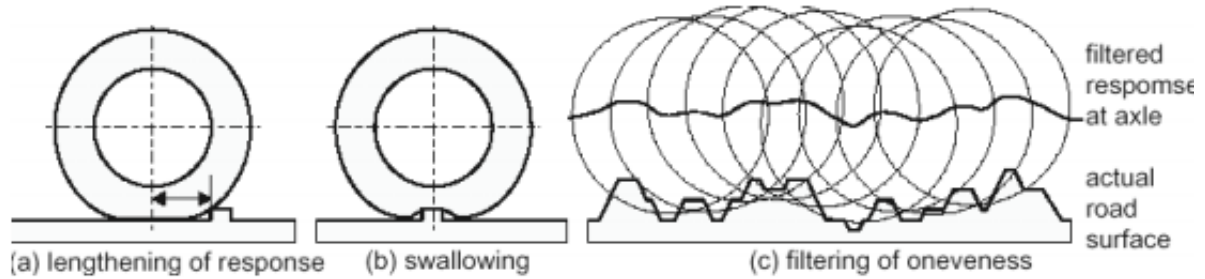
Figure 2-4 Tyre behaviour over uneven terrain (Zegelaar, 1998)

The model, as implemented in ADAMS/Tire, is based on the model proposed by Schmeitz, and is shown in Figure 2-5. The model comprises of a number of cams that are positioned in such a way that they correspond to the outside of the contact patch. Due to the shape of the cams this model is also referred to as the "tandem-egg" model. The positions and orientations of all cams are calculated during the simulation to determine the effective road height, slope, and curvature as well as the effective road camber. The effective road parameters are then used to determine the forces that are generated in the contact patch.
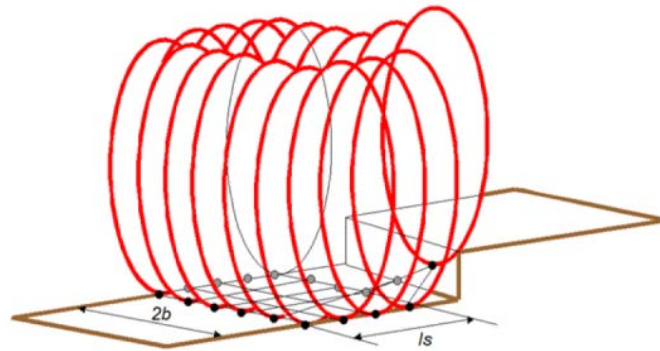
Figure 2-5 Elliptical cam model as proposed by Schmeitz (2004)

The model calculates the shape and dimensions of the contact patch for every solver step. The contact patch is defined by a length of $2a$ and a width of $2b$. The parameters used to define the load - contact patch dimension behaviour are summarized in Table 2-3. Half of the contact patch length, a, is calculated using:

$$a = p_{A1}R_0\left(\frac{\rho_z}{R_0} + p_{A2}\sqrt{\frac{\rho_z}{R_0}}\right)$$

(2.3)

where R_0 is the unloaded tyre radius and ρ_z the tyre deflection. The equation used to calculate the half contact patch width, b, is:

$$b = p_{B1}W_0\left(\frac{\rho_z}{R_0} + p_{B2}\sqrt{\frac{\rho_z}{R_0}} + p_{B3}\frac{\rho_z}{R_0}\sqrt{\frac{\rho_z}{R_0}}\right)$$

(2.4)

Similar to the equation developed by Schmeitz, the shape of the ellipsoid is given by:

$$\left(\frac{x_e}{p_{ae}R_0}\right)^{p_{ce}} + \left(\frac{y_e}{p_{be}R_0}\right)^{p_{ce}} = 1 \tag{2.5}$$

The cams are equally spaced, in the longitudinal direction, over the base length l_s. The base length is dependent on the contact length and is given by:

$$l_s = 2p_{ls}a \tag{2.6}$$

Five cams along the length of the contact patch and six across the width of the tyre contact patch showed the best performance-accuracy ratio according to Schmeitz. These tests were however done on Passenger car tyres. No information about the number of cams that should be used can be found for tyres with larger tyre dimensions.

The shape and size of passenger car contact patches differs from that of a large off-road tyre. It must still be determined if these formulae can be used to accurately describe the contact patch dimensions and the optimum number of cams for large tyres. This contact model allows for a linear and nonlinear spring stiffness description and the damping is defined by a constant damping coefficient. The user needs to specify the eleven parameters that describe the tyre contact area in the tyre definition file, if these coefficients are not specified ADAMS will use standard values.

Table 2-3 Parameters used to define the contact patch dimensions

Name	Name used in tyre property file	Explanation
p_{A1}	PA1	Half contact length dependency on sqrt(defl/R0)
p_{A2}	PA2	Half contact length dependency on defl/R0
p_{B1}	PB1	Half contact width dependency on sqrt(defl/R0)
p_{B2}	PB2	Half contact width dependency on defl/R0
p_{B3}	PB3	Half contact width dependency on defl/R0* sqrt(defl/R0)
p_{ae}	PAE	Half ellipse length/unloaded radius
p_{be}	PBE	Half ellipse height/unloaded radius
p_{ce}	PCE	Ellipse exponent
p_{ls}	PLS	Tandem base length factor
n_{width}	N_WIDTH	Number of cams across tyre contact width
n_{length}	N_LENGTH	Number of cams along tyre contact length

2.3.4 Flexible Structure Tyre Model: FTire

FTire (Flexible Structure Tyre Model) is a full 3D nonlinear in-plane and out-of-plane tyre model. The Model was developed by Gipser (1999) over the past 15 years. FTire was developed for vehicle comfort simulations and the prediction of road loads with extremely short wave-lengths obstacles but can also be used for handling simulations.

This model is based on a structural dynamics approach where the previously discussed models are based on analytical foundations. The tyre model can be seen as a very course, nonlinear finite element model. The tyre model describes the tyre belt as a flexible ring that can flex and extend in the radial, tangential and lateral directions. The belt is approximated as a finite number of rigid belt elements that are connected to each other in such a way that the movement of the elements is possible in-plane as well as out-of plane. The "belt elements" and their associated degrees of freedom are shown in Figure 2-6. In general 100 to 200 of these belt elements are used to represent the tyre.
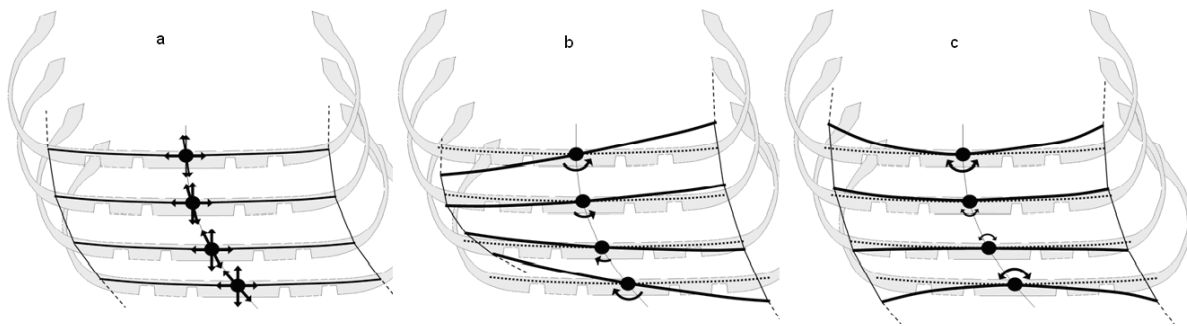
Figure 2-6 FTire belt elements degree of freedom (Gipser, n.d.)

Every belt element is again associated with a number of mass less "tread blocks", usually between 10 to 100 blocks. These tread blocks outline the tread sub-model. Tread blocks are connected to their neighbours with nonlinear stiffness and damping properties in the radial, tangential and lateral directions. These tread blocks are located along parallel lines by default. The user can however prescribe the tread pattern geometry. The tread blocks will then be placed according to the tread pattern. All 6 tyre forces and torque components acting on the rim are calculated by integrating the forces in the elastic foundation of the belt.

Due to the structural dynamics approach there are few restrictions in the applicability. FTire can deal with large or short-wave obstacles. It works out of, and up to, complete stand still, with no additional computing effort and does not require any model switch.

Parameterization of the tyre model is generally done with the FTire/Fit code (Gipser & Hoffmann, 2010). The code provides several optimization routines to minimize the error between measured results and the corresponding simulation with FTire. FTire/fit begins with an initial tyre estimate. The user can subsequently improve the tyre behaviour by supplying the parameterization program with general tyre data and experimental test data.

The general tyre data comprises of the tyre dimensions, operational pressure, mass and other physical properties. The user can then "check in" various test results to optimize the model so as to represent the

physical model. The data that can be used to improve the accuracy of the tyre model include tyre footprint images, static tyre stiffness, static cleat tests, side force slip angle measurements, dynamic cleat tests and various others. If no test data or only limited test data is available the program will use the same parameters that were loaded as the initial estimate.

Parameterization of any tyre model is always a delicate task and depends not only on the availability of parameterization data and the accuracy of the data but also on the user. This is especially true with the use of FTire/fit. The parameterization program should not be used as a "black-box-tool" where the user inputs a data set and the programs returns the tyre property file. The user is required to select and prepare the appropriate test measurements, then decide which parameters should be determined by what kind of test, and in what sequence. The process is iterative and can be time consuming.

The FTire parameterization will be discussed in extensive detail in Chapter 4.

2.4   Section Summary

Different approaches of tyre modelling were briefly discussed. Tyre models that are implemented in ADAMS/Tire were discussed in greater detail. These tyre models can be classified in two categories, the analytical contact models and the Flexible ring tyre models. The One Point Contact model, 3D Equivalent Volume Contact model and the 3D Enveloping Contact models belong to the analytical tyre models category while the FTire model is associated with the flexible ring tyre models.

The analytical contact models use different approaches to calculate an effective contact point. This point is then used to predict the tyre behaviour. ADAMS recommends that all of these contact models, with exception of the 3D Enveloping Contact model, should only be used for roads with obstacles with wavelengths larger than the tyre diameter. These contact models are however often used for simulations that have obstacles smaller than the tyre diameter due to their simplicity, fast solving time and the lack of the required parameterization data to use a more appropriate model.

In addition to the analytical tyre models a flexible ring tyre model was also discussed. The flexible ring tyre model discussed was the FTire tyre model. The model is based on a structural dynamics modelling approach. The model is complex and requires various parameterization tests to be parameterized successfully.

The following tyre models will be studied in detail in the rest of the document:

a) PAC89 tyre model with a One Point Contact model
b) PAC89 tyre model with a 3D Equivalent Volume Contact model
c) PAC89 tyre model with a 3D Enveloping Contact model
d) FTire model

3   Acquiring Parameterization Data

"It is a capital mistake to theorize before one has data. Insensibly one begins to twist facts to suit theories, instead of theories to suit facts."

-   *Arthur Conan Doyle, 1887*

3.1   Introduction to Parameterization Data

This chapter will describe the data acquisition process and the associated challenges. All tyre models require experimental test data for use during the parameterization process. The amount of test data required varies with the model.

3.2   Tyre Used

The tyre that was analysed for this project was the Michelin XZL 16.0R20 all-terrain tyre. The tyre could be used for on or off road terrain. The tyre was designed with a self-cleaning, open shoulder tread design with offset elements to increase traction on various terrains such as snow, sand or mud. Figure 3-1 shows the tyre and its tread pattern.

Figure 3-1 Michelin 16.00R20 XZL tyre and thread pattern (Michelin, n.d.)

A full width steel belt and an elastic protector ply help to protect the tyre against off-road hazards. The tyre could be used with or without a tube. The weight of the tyre carcass is 154kg and the complete wheel, including the carcass, run flat insert and rim, was weighed at 240kg. The tyre specifications and dimensions are summarized in Table 3-1.

Table 3-1 Michelin XZL specification (Michelin, n.d.)

Size description	Load Range	Max. Speed [km/h]	Loaded Radius [mm]	Overall Diameter [mm]	Overall Width [mm]	Max. Load [kg]
16.00R20	M	88	607	1343	438	6595

3.3   Laboratory Tests

The first set of parameterization data was acquired in the laboratory. These tests were conducted on a non-rolling tyre. They were mainly conducted to determine the tyre stiffness, damping parameters and contact area. The test methodology is described in subsections 3.3.1 – 3.3.5.

Laboratory testing was preferred to field tests because the experimental setup was simpler and less time consuming. This lends to an economically viable approach. Non fixed variables such as the environmental conditions can also be controlled.

3.3.1   Static Tyre Stiffness

The vertical tyre stiffness test was conducted first. The tyre stiffness was determined for three tyre pressures namely 100kPa, 300kPa and 550kPa. The recommended inflation pressure of the tyre, for cross country driving, is 300kPa. The inflation pressure of 100kPa was investigated as it is used for emergency manoeuvres over soft terrain such as sand. To investigate the tyre behaviour during high speed on road driving an inflation pressure of 550kPa was chosen.

The experimental setup is shown in Figure 3-2.
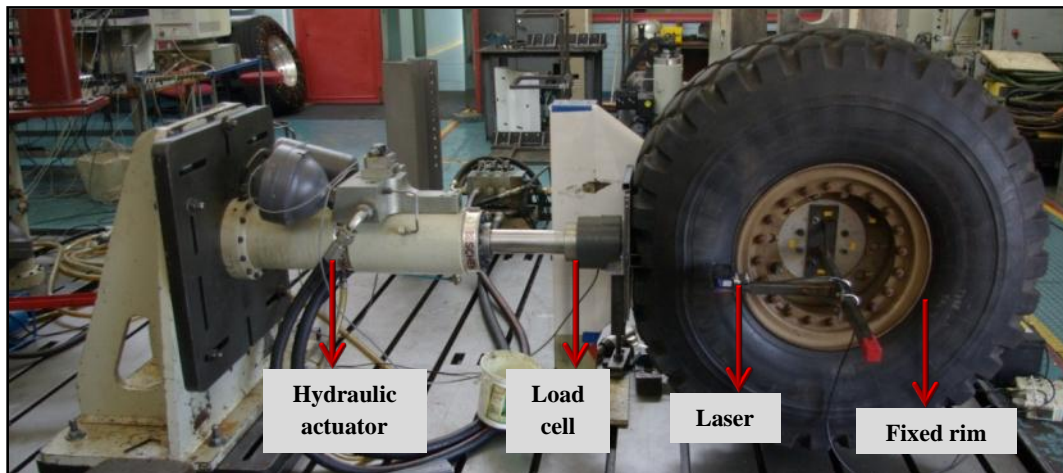
Figure 3-2 Vertical tyre stiffness test setup

The rim was fixed. A hydraulic actuator was used to compress the tyre. A large flat steel plate was used to simulate the road surface. During the test the applied load and the resulting tyre displacement was measured. To minimize the effect of elasticity in the test fixtures and floor, the tyre displacement was measured with a laser displacement instrument mounted between the rim and the flat steel plate.

Figure 3-3 shows the relationship between the applied load and resulting tyre displacement, for all tested inflation pressures. The sinusoidal displacement results in the hysteresis loop shown. The measured data is clearly nonlinear, but a linear curve fit is shown.
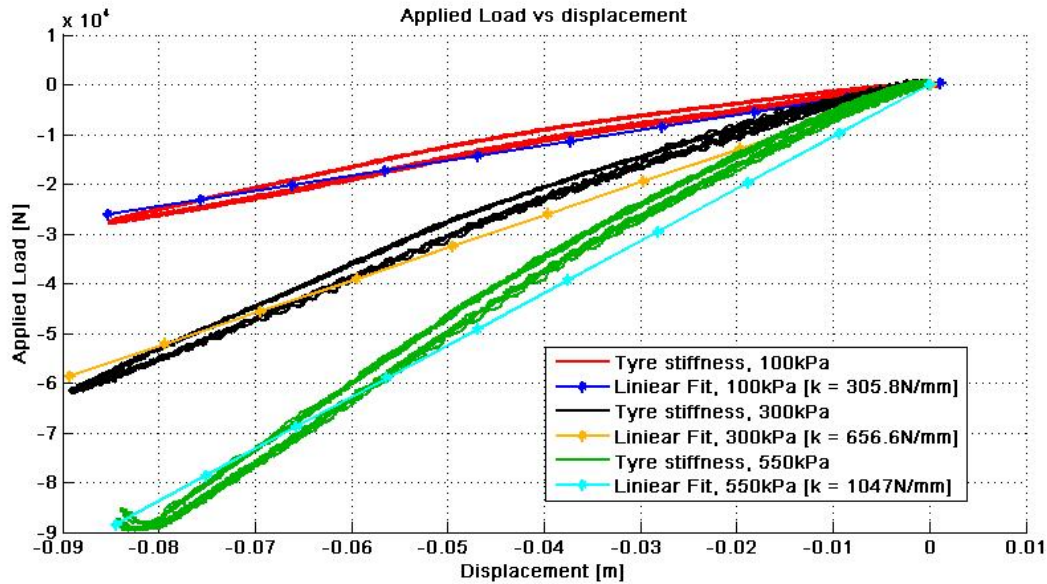
Figure 3-3 Static tyre deflection load curve

The average loads were also calculated for every 10 mm displacement, to create a nonlinear force displacement curve. The results are shown in Table 3-2. This curve would later be used to describe the nonlinear tyre stiffness in the One Point Contact model, 3D Equivalent Volume Contact model and the 3D Enveloping Contact model. These curves describe the tyre behaviour better than the linear curve fit.

Table 3-2 Tyre load deflection data

Displacement [mm]	Applied load [N], 100kPa	Applied load [N], 300kPa	Applied load [N], 550kPa
0	0	0	0
-10	-1 905	-3 496	-6 354
-20	-4 716	-9 445	-15 537
-30	-7 221	-15 559	-25 250
-40	-9 947	-21 968	-36 872
-50	-13 415	-29 011	-48 446
-60	-17 673	-37 581	-62 502
-70	-21 582	-45 717	-74 730
-80	-25 616	-54 191	-88 151

3.3.2   Static Tyre Profile

The outer contour of the test tyre was measured to describe the carcass shape required by the 3D Equivalent Contact model. Many measurements were taken to determine the outer profile of the tyre as the tyre had an irregular tread pattern.

 Figure 3-4 shows the result of two tread carcass sections and the tyre sidewall. The figure depicts the relationship between the section height and the tread width.
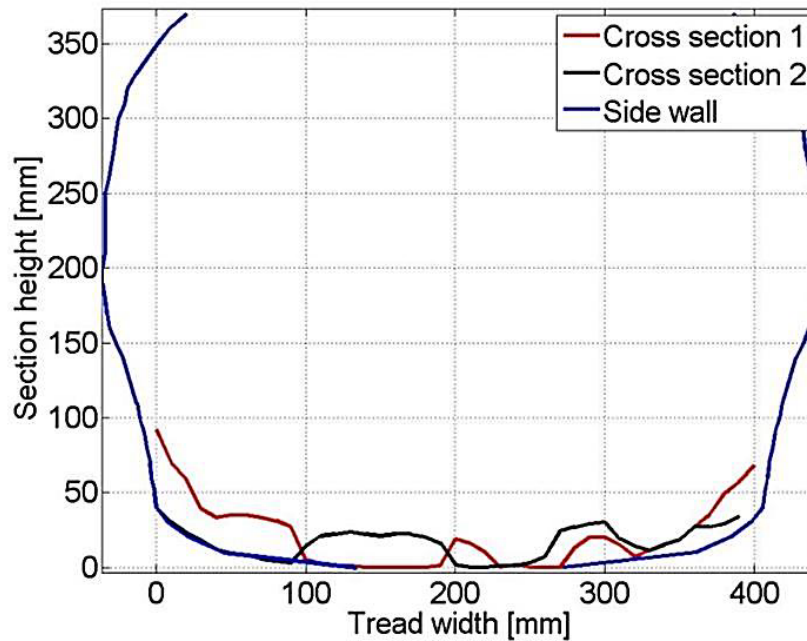
Figure 3-4 Test tyre outer contour

3.3.3   Static Tyre Contact Area

The tyre contact areas were required to parameterize the 3D Enveloping Contact models and the FTire model. An area test rig was used (Gerotek Test Facilities, n.d.). The test rig had a movable axel, on which the test tyre was mounted. It could be moved towards a bullet proof glass sheet using two hydraulic actuators. The contact between the glass and the tyre tread was visible on the opposite side of the glass. A calibrated camera was then used to capture the contact area. Figure 3-5 shows the captured image for the Michelin tyre at 500kPa at a normal load of 44.1kN
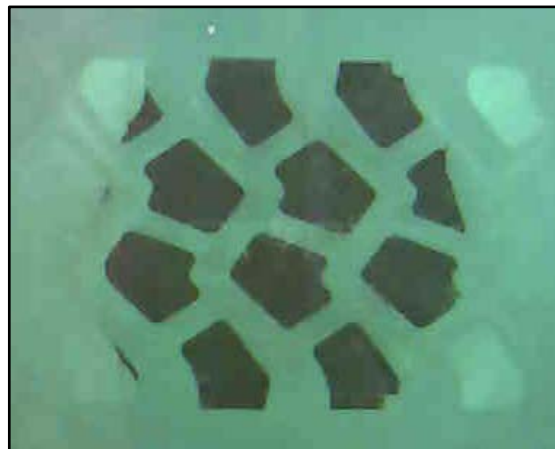
Figure 3-5 Tyre contact patch image, 500kPa, 44,1kN

Figure 3-6 shows a digital manipulation of the image, in which a scaled, black and white image of the contact area was created.
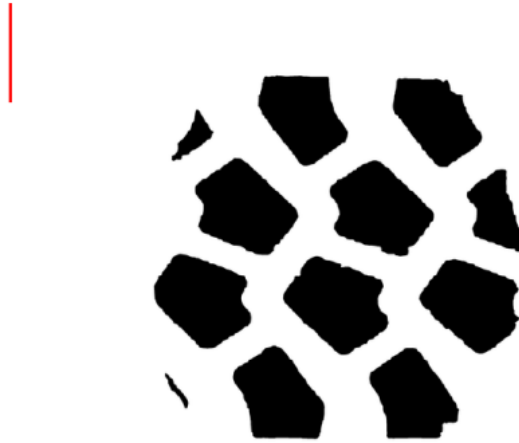
Figure 3-6 Post processed tyre contact patch

The images were then scaled using a known pixel per millimetre ratio. Another method was applying a red line with known length to the image. The latter had proved to be easier to use in the FTire parameterization process. The standard length of the line should be 100 mm and should not overlap with the tyre contact patch.

3.3.4   Static Cleat Tests

Static cleat test were used in the parameterization process of FTire to parameterize the in-plane tyre stiffness.

The test setup was similar to the setup used to determine the vertical tyre stiffness. The flat surface was replaced by cleats with various dimensions. The tests were conducted with cleats orientated in the lateral and longitudinal directions.

The dimensions of the cleats should be related to the expected tyre deflection under normal operating conditions. For a tyre where a large deflection was expected during normal operation, the cleats should be larger than for a tyre with a smaller expected deflection.

Figure 3-7 shows a static lateral cleat test.

Five different cleat dimensions were used in the parameterization of the FTire model. The dimensions of the cleats, width x height, that were chosen were:

- 25.4mm x 25.4mm
- 38mm x 38mm
- 51mm x 51mm
- 76.3mm x 76.3mm
- 100mm x 50mm

During the test the applied force and the tyre displacement was measured. The tyre was tested at an inflation pressure of 300kPa and 550kPa.
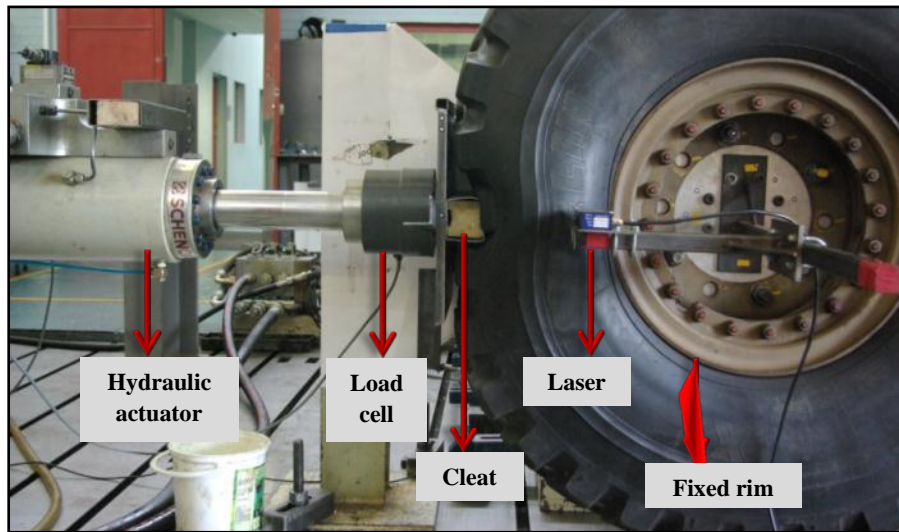
Figure 3-7 Static-cleat-test test setup

Figure 3-8 and Figure 3-9 show the results of these tests, with cleats orientated in the longitudinal and lateral direction, at 300kPa tyre inflation, respectively. It can be seen that the expected tyre stiffness declines for all static cleat tests. The decrease is more predominant with the laterally orientated cleat.
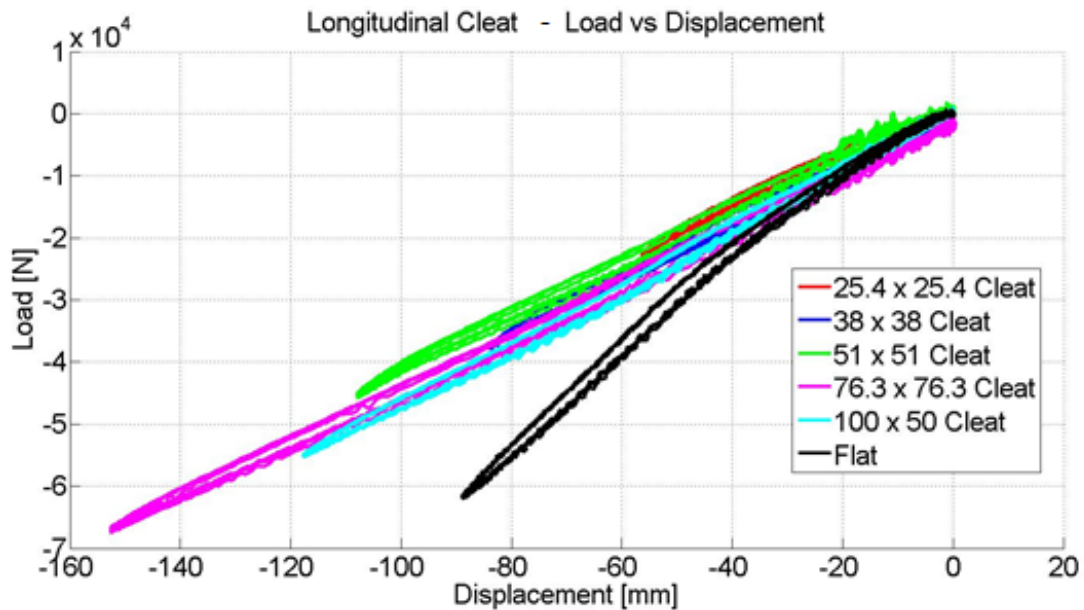
Figure 3-8 Longitudinal cleat - load vs. Displacement curve
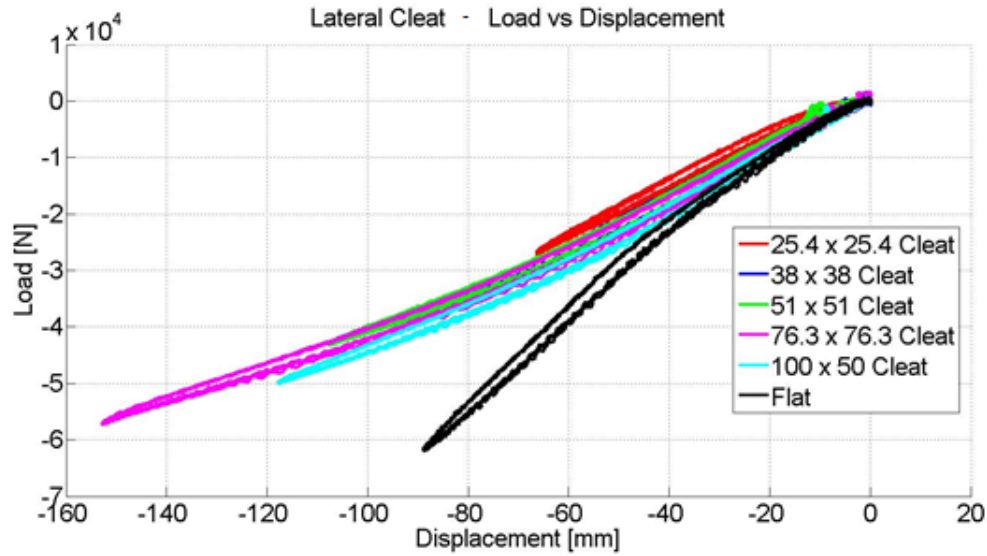
Figure 3-9 Lateral cleat - load vs. Displacement curve

3.3.5   Modal Analysis

A Modal analysis was conducted with the use of a Polytec PSV-400 Scanning Laser Vibrometer as shown in Figure 3-10. These tests were conducted to determine the frequencies of the first few vibration modes of the tyre. The tests were conducted in the lateral and longitudinal scanning surface direction. They were conducted at different impulse amplitudes to determine the linearity of the tyre at different loads.
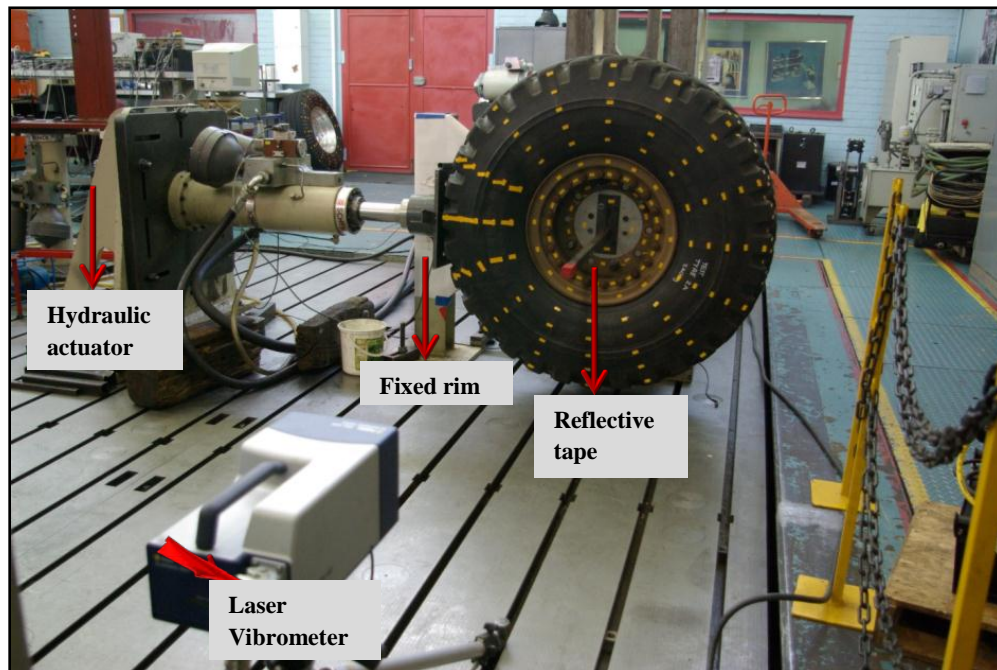
Figure 3-10 Modal analysis
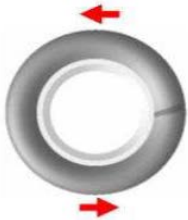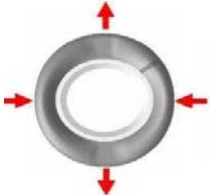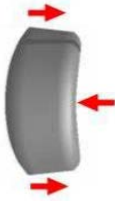
FTire Vibration mode	Vibration mode illustration	Description	Frequency [Hz], 300kPa	Damping [%], 300kPa	Frequency [Hz], 550kPa	Damping [%], 550kPa
1		natural frequency of the in-plane 'rigid-body' rotation about wheel spin axis	-	-	-	-
2		natural frequency of the 'rigid-body' movement in longitudinal or vertical direction	22.72	2.94	33.51	2.01
3		natural frequency of the 'rigid-body' movement in lateral direction	16.88	2.33	20.09	2.19
4		natural frequency of the out-of-plane 'rigid-body' rotation about any axis perpendicular to wheel spin axis	29.99	1.19	17.00	1.44
5		third natural frequency of the in plane body movement	52.39	0.54	53.77	0.06
6		third natural frequency of the out of plane body movement	43.39	0.67	45.93	0.13

Table 3-3 Tyre modal analysis results

Table 3-3 shows the modal analysis results for an impulse load of 40kN and at tyre pressures of 300kPa and 550kPa. The vibration mode shapes are organized according to Gipser (n.d.). The first mode shape represented the natural frequency of the in-plane 'rigid-body' rotation about wheel spin axis. This vibration mode could not be determined with the current test setup as the measurements were taken perpendicular to the side wall and to the contact patch of the tyre.

3.4   Field Tests

The acquisition of the required dynamic parameterization data, for large off road tyres, presents a challenge for conventional test methods. These conventional methods make use of either a roller drum test rig or a flat track test rig. They are limited to passenger cars and light truck tyres. The maximum loads of many test rigs are limited to less than 30 000N. The Michelin XZL 16.00R20 used in this study has a static load rating of 65 000N.

The second limitation is the dimensions of the test rigs. Commercial test rigs have a width of about 400 mm while the overall width of the tyre is about 435 mm. The relationship between the drum diameter and the tyre diameter is also decreased which results in an inaccurate representation of the contact patch.

To eliminate these limitations a tyre test trailer was used to acquire the experimental data. The experimental setup used for these test is shown in Figure 3-11. The test setup comprised of a large towing vehicle and the tyre test trailer. The trailer consisted of a main frame and a sub frame. The trailer can be loaded with ballast so that the static load on the tyre ranges between 2400kg and 5200kg. The wheel, with the tyre that needed to be tested, was mounted to the sub frame on the right hand side of Fig 3-11.

Figure 3-11 Dynamic test setup

The sub frame is connected to the mainframe by six load cells that are positioned to enable all the forces and moments acting on the wheel to be measured (see Figure 3-12). Since the tyre test trailer has no suspension, all the forces acting on the load cells, connecting the main frame to the sub frame, could be related to the forces that are generated in the tyre contact patch.

The tyre track width of the trailer was wider than the track width of the towing vehicle. This allowed the towing vehicle to avoid obstacles while the test trailer was towed over these obstacles. Due to the different track widths the test trailer was excited by the tyres of the trailer as they clear the obstacles while it was supported only by the towing hitch.
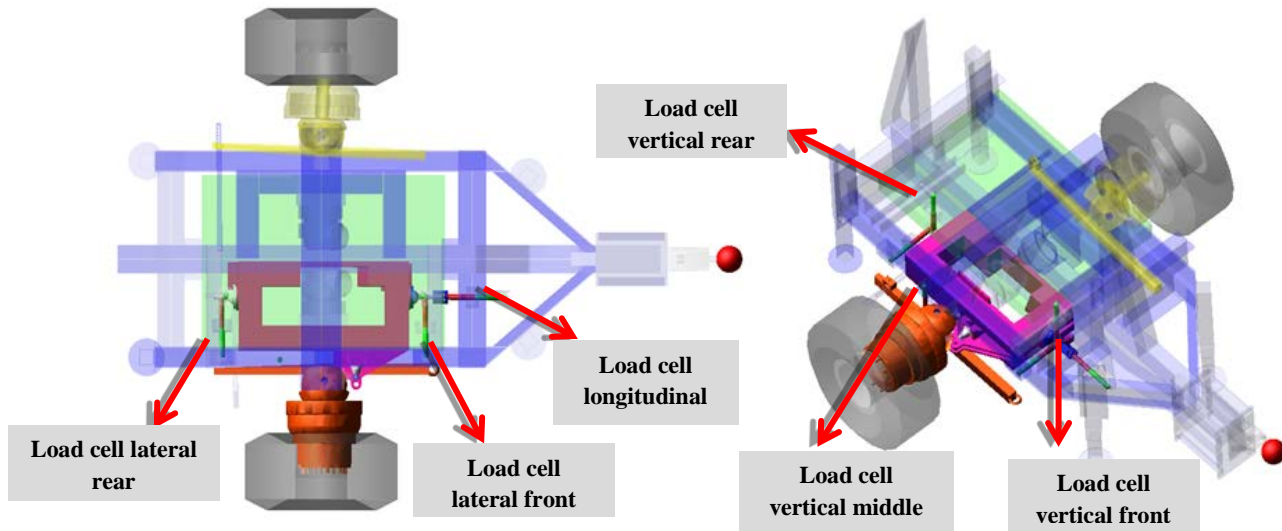
Figure 3-12 CAD model of tyre tester

The field tests were divided into two categories; dynamic cleat tests and validation tests. Dynamic cleat test were used to extract parameterization data, and will be discussed in sub sections 3.4.1 - 3.4.3. Certain test data from the aforementioned subsections was also used in the tyre model validation process. A second set of field tests was conducted of which the results were only used as validation data (see Chapter 5).

3.4.1   Tyre Damping

To determine the damping coefficient, c, of the tyres, the tyre test trailer was lifted until the wheels just lost contact with the ground. The trailer was then dropped. The vertical displacement of the rim was measured until the test trailer oscillations damped out and the trailer reached its static equilibrium again.

 Figure 3-13 shows the tyre displacements that were measured during the drop test.
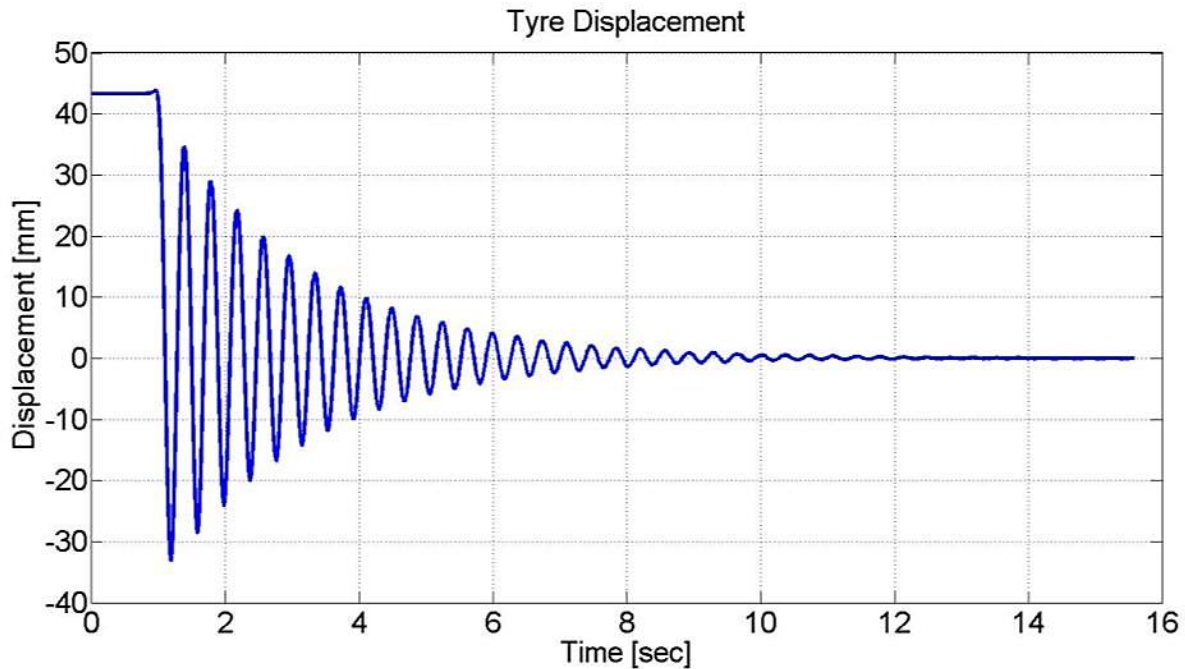
Figure 3-13 Tyre test trailer drop test result

To calculate the damping coefficient of the tyre, it was assumed that the hitch of the towing vehicle was fixed and unable to move during the drop test. The test trailer could then be approximated as a pendulum connected to the ground by a spring and a damper on the one side, and pivoting about the hitch on the other end.
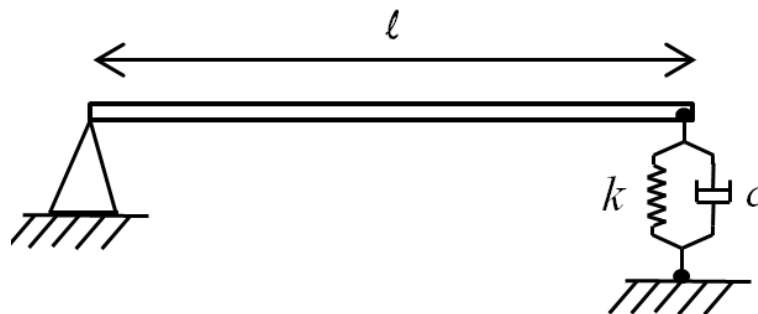
Figure 3-14 Schematic presentation of the test trailer

For small rotational displacements the small angle assumption could be made, so that $sin\theta = \theta$ and $cos\theta = 1$. The equation of motion of the pendulum is then given by:

$$I_0\ddot{\theta} + cl^2\dot{\theta} + kl\theta = 0 \tag{3.1}$$

Where I_0 is the moment of Inertia of the trailer about the axis of rotation, c the damping coefficient and k the tyre stiffness. The variable l is the distance between the hitch and the wheels. The equations can be simplified to:

$$\ddot{\theta} + \frac{cl^2}{I_0}\dot{\theta} + \frac{kl}{I_0}\theta = 0 \qquad (3.2)$$

and written in the standard form:

$$\ddot{\theta} + 2\xi\omega_n\dot{\theta} + {\omega_n}^2\theta = 0 \qquad (3.3)$$

The undamped natural frequency can then be defined as:

$$\omega_n = \sqrt{\frac{kl^2}{I_0}} \qquad (3.4)$$

The damping ratio was then given by:

$$\xi = \frac{cl^2}{2\omega_n I_0} \qquad (3.5)$$

From the measured data the logarithmic decrement of the displacement amplitudes of two consecutive oscillations could be calculated using:

$$\delta = \ln\frac{x_1}{x_2} \qquad (3.6)$$

The damping ratio could then be calculated using:

$$\xi = \frac{\delta}{\sqrt{\delta^2 + (2\pi)^2}} \qquad (3.7)$$

The damping coefficient, c, could then be calculated for the test tyre. Using this procedure the non-rolling dynamic damping coefficient for the Michelin 16.00R20 tyre, at an inflation pressure of 300kPa, was calculated as 2.66Ns/mm.

3.4.2   Dynamic Cleat Test

Cleats are discrete obstacles that are used in tyre characterization and parameterization tests. Square cleats are commonly used but other shapes are also available. Drum cleat tests are often used to parameterize tyre models such as FTire or RModK.

For the dynamic cleat test the trailer was pulled over square cleats of various sizes. Two orientations were investigated, perpendicular to the direction of travel and at a 45 degree angle. The dimensions, width by height, of the cleats that were investigated were:

- 38 x 38mm
- 50 x 50mm
- 76.3 x 76.3mm
- 100 x 100mm

Fig 3-15 shows the different cleat dimensions described above and the two orientations.

Figure 3-15 Cleats used during the dynamic cleat test

Three different load cases were investigated and are summarized in Table 3-4. Slight variations between the loaded weights are within the measurement error.

Table 3-4 Test load case

Load case	Loaded weights [kg]	Wheel load [kg]	Percentage of maximum tyre load, 6595kg [%]	Description
1	-	2375	36.0	LC1
2	3020	3895	59.1	LC2
3	5440	5095	77.3	LC3

Figure 3-16 shows a 76.3 mm cleat orientated perpendicular to the direction of travel and Figure 3-17 shows the 100mm cleat orientated at a 45 degree angle. The figures also show two different load cases, load case 2 and load case 1 respectively.

Figure 3-16 Perpendicular Cleat – 76.3 mm LC2

As was discussed in the introductory section 3.4, the tyre tester has no suspension. Due to this, the only damping associated with the test trailer is the tyre damping. The tyre damping ratio is however very small, compared to the damping ratio of a truck suspension system. Due to this the test trailer will start to oscillate uncontrollably at speeds higher than 50 km/h. Tests were thus limited to a maximum speed of 40 km/h. This is approximately half of the maximum rated speed of the tyre. The tyre was tested at 10km/h, 30km/h and 40km/h.

Figure 3-17 Oblique Cleat – 100 mm LC1

Figure 3-18 shows the results of a dynamic cleat test. The tyre test trailer was towed at a speed of 10 km/h over a 76.3 mm cleat, orientated perpendicular to the direction of travel. The test trailer was loaded with 3020 kg ballast (LC2). The top left image shows the tyre approaching the cleat. The normal force, longitudinal force and rolling moment are also shown in the figure. The vertical green line represents the instant the picture was taken. From the figure it can be seen that the highest load acting on the wheel occurs one oscillation after the tyre makes contact with the cleat. The figure also shows the highly nonlinear damping behaviour of the test tyre.
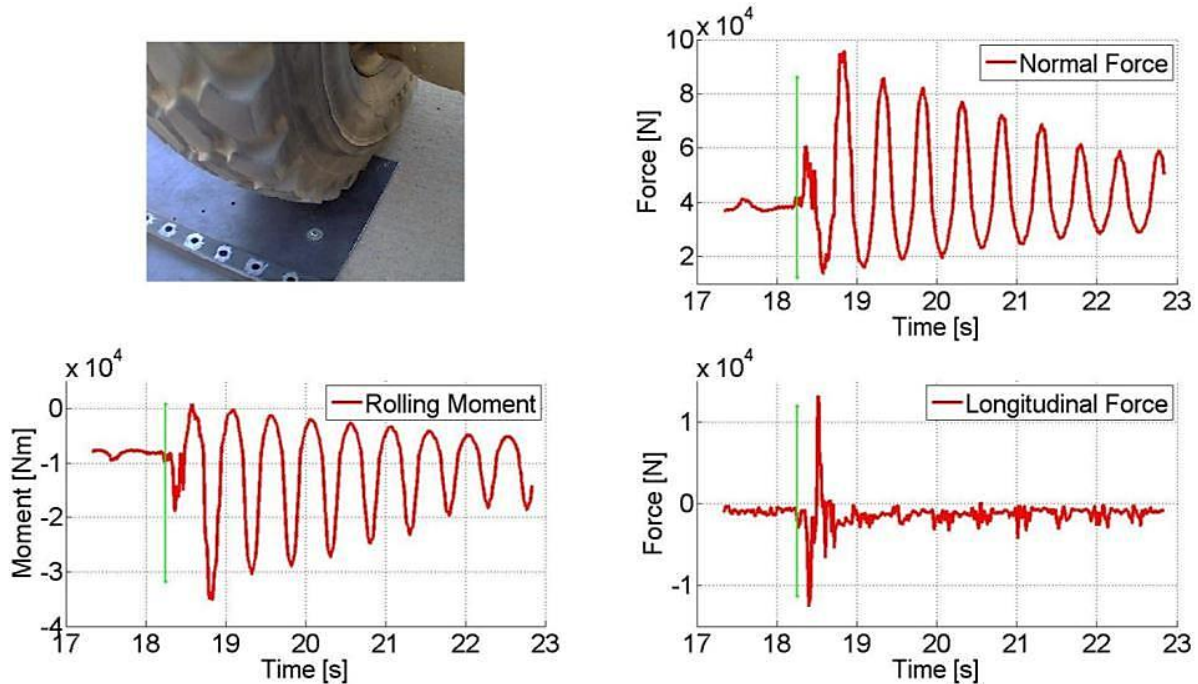
Figure 3-18 Cleat test measurement result, 76.3mm, LC2

Figure 3-19 depicts the results of a 50mm cleat test where the cleat was orientated at a 45 degree angle. The tyre tester was towed at a speed of 10 km/h over the obstacle and was not loaded with any ballast. It can again be seen that the highest loads are acting on the wheel one oscillation after the wheel has cleared the obstacle. Due to the orientation of the obstacle a lateral force is generated in the contact patch.
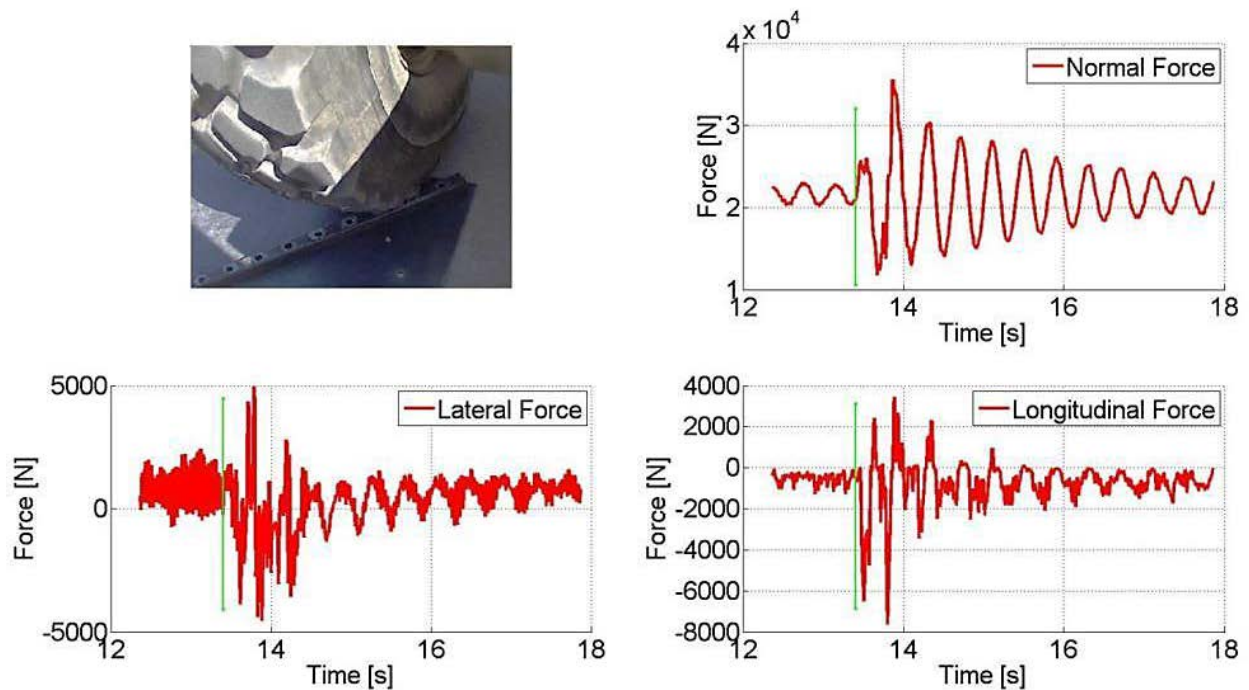
Figure 3-19 Cleat test measurement result, 50mm oblique, LC1

The tests were performed several times to ensure that the results were repeatable. The results correlated extremely well amongst the different measurements taken**.** Figure 3-20 and Figure 3-21 shows two different cleat test runs, both at 10 km/h, shown on the same graph to illustrate the repeatability of the cleat tests.

The relative error between the runs decreased with an increase in cleat size. This was expected as the orientation of the tyre as it hits the cleat, becomes less important with an increase in the cleat size. The effect of the larger tread blocks was an added complexity with the off-road tyre. It was normally considered insignificant on passenger car tyres.

The cleat tests where the obstacles were orientated at a 45 degree angle to the direction of travel showed the largest difference in correlation between tests. The difficulty arose in positioning the trailer exactly in the centre of the track when it clears the cleats. One tyre would hit the cleat before the other tyre if the trailer was not positioned in the centre.
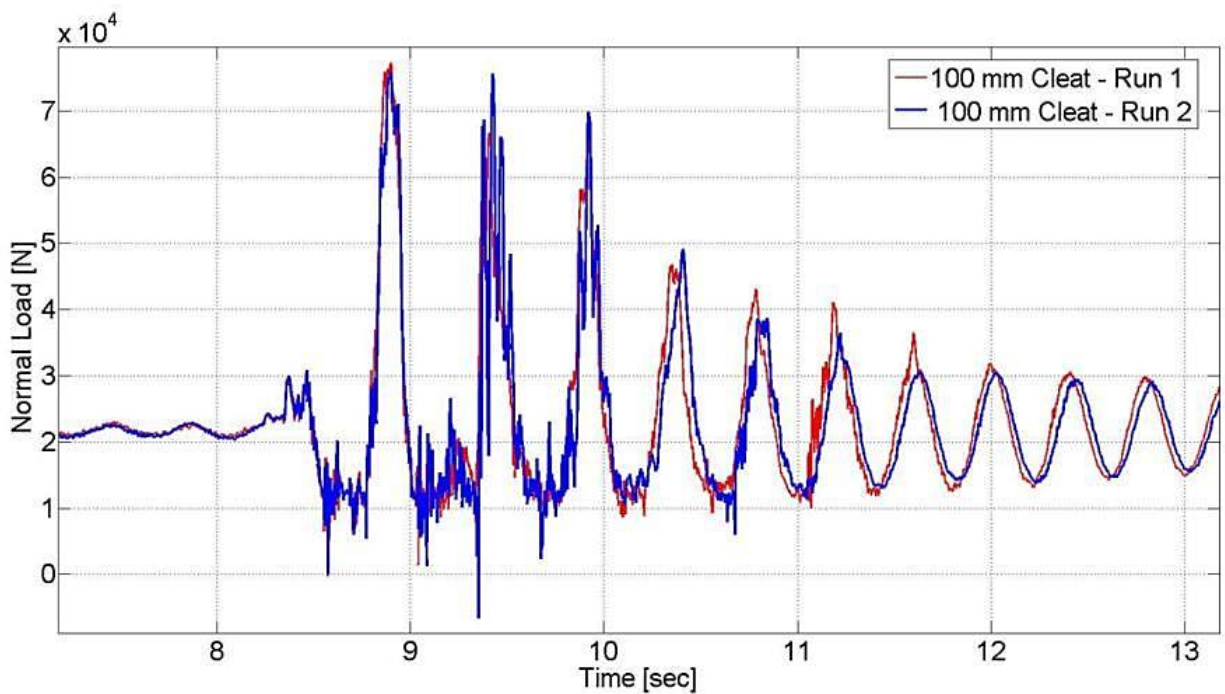
Figure 3-20 Comparison of two 100mm Cleat test, LC1
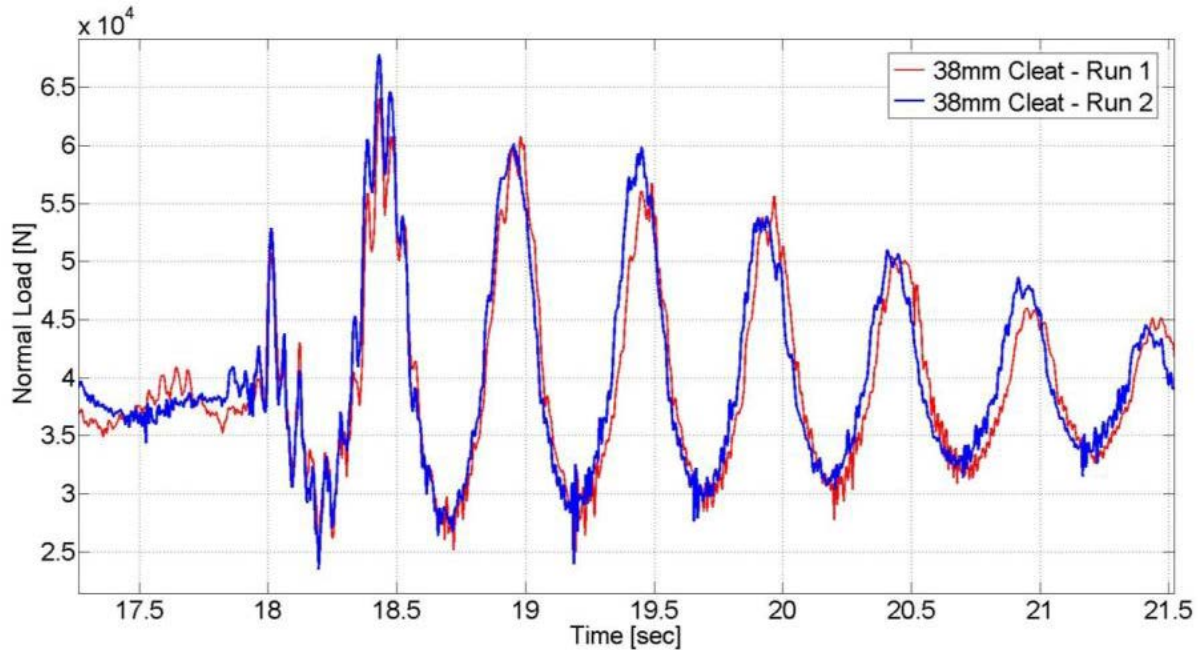
Figure 3-21 Comparison of two 38mm Cleat test, LC2

3.4.3   Validation Test

The second set of field tests were conducted to be used as validation data. Certain cleat tests were also used to validate the parameterized tyre models. Validation data would not be used in the parameterization process of the tyre. Tests that were conducted for validation purposes were:

- Trapezoidal bump
- Belgian paving
- Fatigue track
- Parallel corrugations track
- Angled corrugations track
- Increasing frequency cleats

The trapezoidal bumps are artificially made bumps with known dimensions. During the trapezoidal tests the tyre test rig was towed over the APG bumps while the towing vehicle avoided the obstacles.

 Figure 3-22 depicts the dimensions of the trapezoidal bumps that were used during the tests.
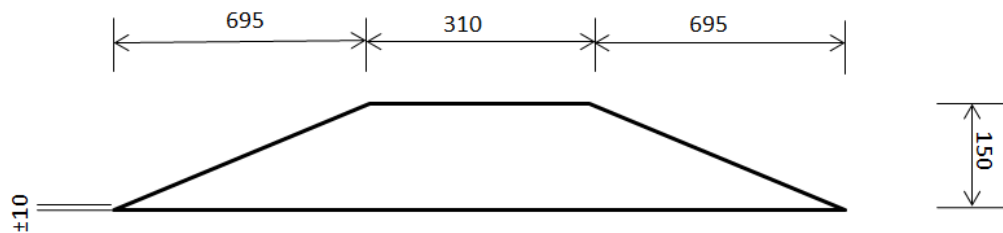
Figure 3-22 Trapezoidal bump dimensions

Figure 3-23 shows the results of a trapezoidal obstacle test conducted at speed of 4km/h. The trailer is loaded with ballast of 3020kg, LC2.
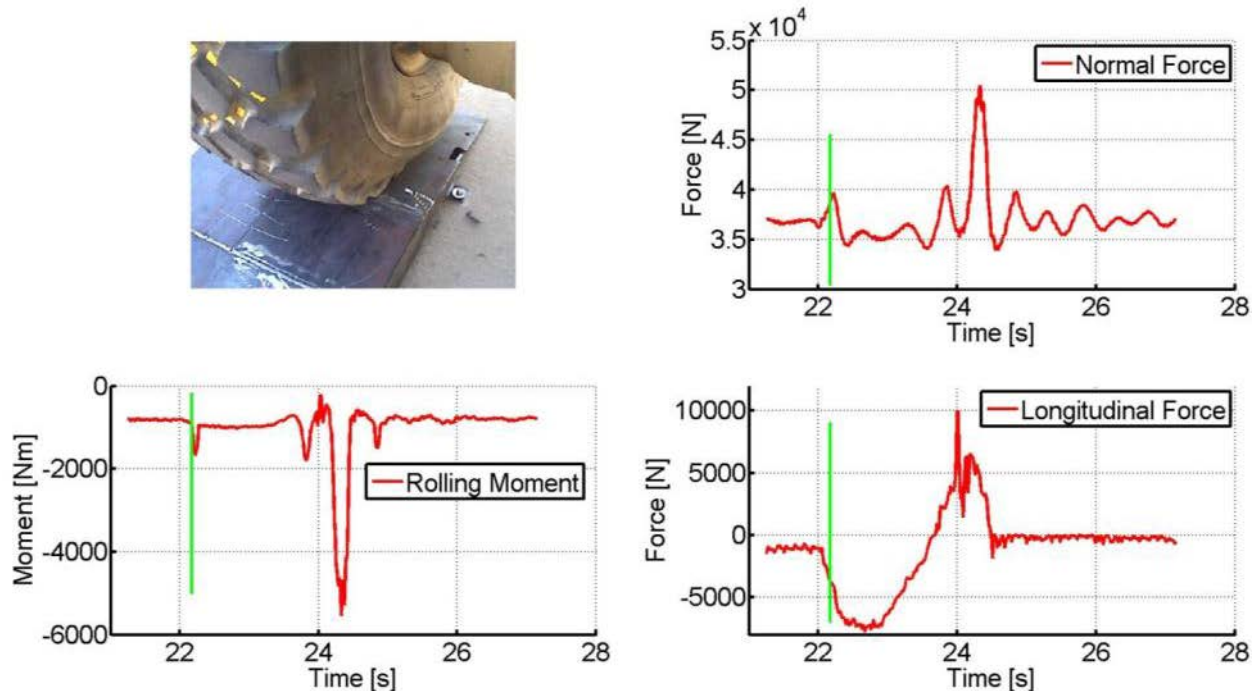
Figure 3-23 APG test, LC2

The remaining validation tests were conducted on various test tracks at the Gerotek Test Facilities (2013). The test tracks have a length of one hundred meters and a width of four meters. The right tyre was mounted to the sub frame of the tyre tester. During the test it was on the test track while the left wheel and the towing vehicle were rolling on a smooth concrete surface.

The road profiles of the test tracks were measured using the "Can-Can machine" (Becker, 2008). The "Can-Can machine" is a road profiling device that was developed by Becker, which drags profiling arms over the road surface. By measuring the angle of these arms a three-dimensional road profile can be calculated.

The arms were spaced 40 mm apart and the angle of the arms was recorded every 12mm. Using this technique the road profiles of the test tracks were measured with a resolution of 40mm by 12 mm. The measurements were then used to create curved regular grid road definition files, better known as CRG road files (OpenCRG, 2011), which could be used in simulations.

Figure 3-24. shows the CRG road representation of the validation test tracks.
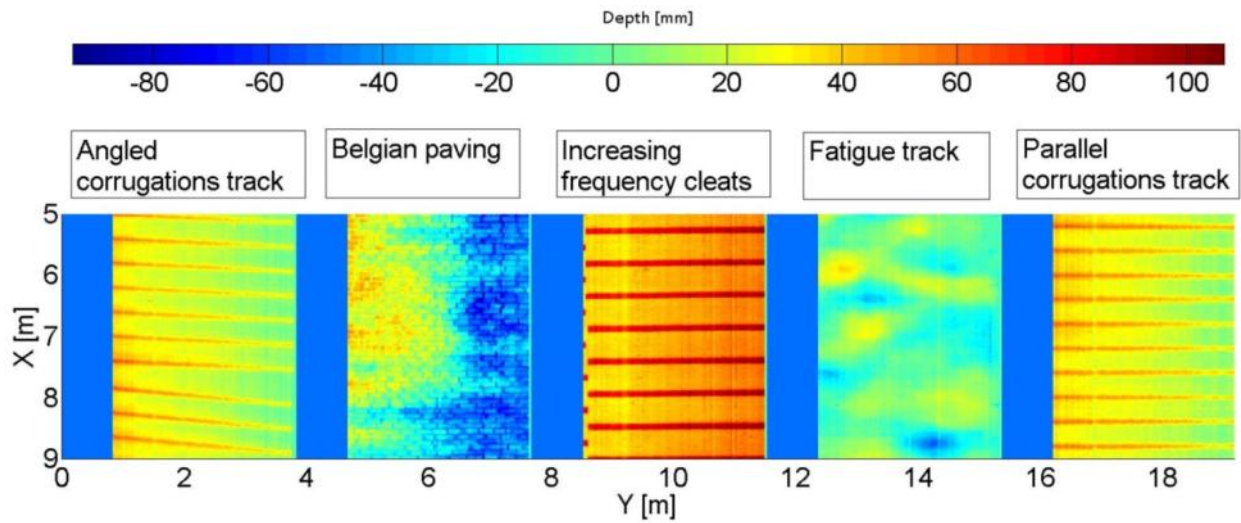
Figure 3-24 Validation test tracks

The Belgian paving, also known as the Belgian block road, was often used to test the durability and ride comfort of vehicles. The blocks on the track had a random width but a regular length of 134 mm perpendicular to the direction of travel

Figure 3-25 shows the results of a validation test on the Belgium paving.

Figure 3-25 Belgium paving validation test

Figure 3-26 shows the measured forces and moments that are generated in the test tyre contact patch during a validation test on the Belgian paving, at a speed of 5km/h with no ballast loaded on to the test trailer.
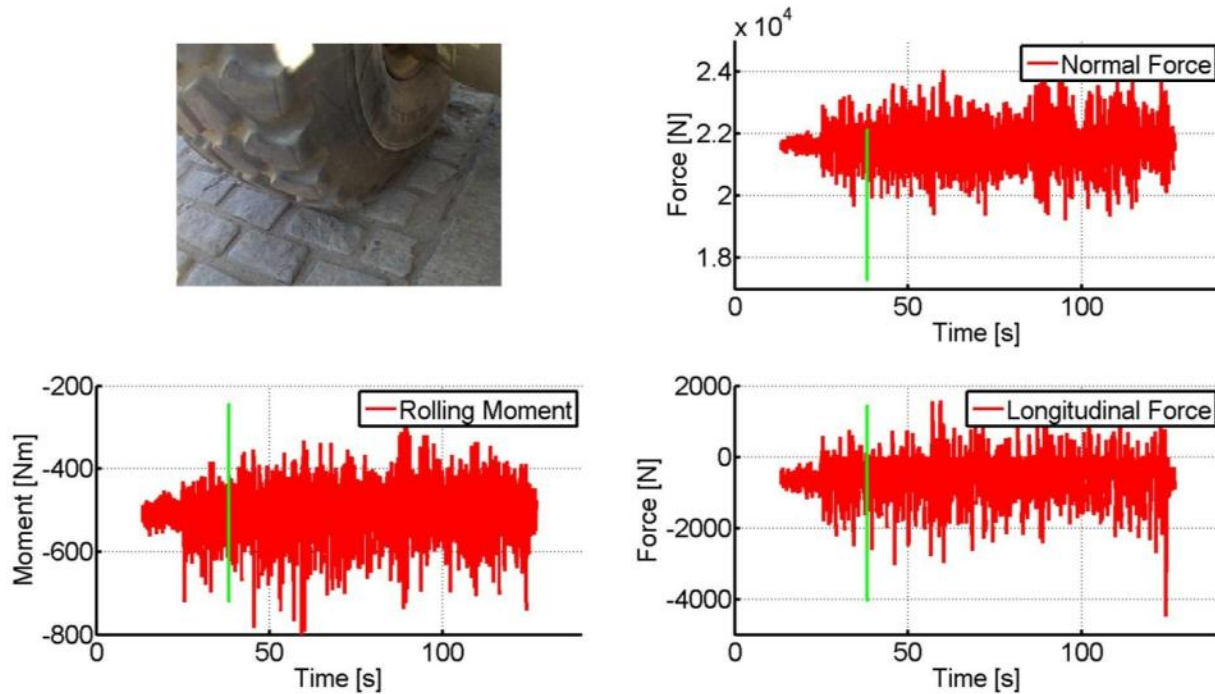
Figure 3-26 Belgian paving measurement, LC1

The roughness of a terrain was often described by the Displacement Spectral Density, DSD. A Power function or Inverse Power Law is often applied to DSD's of random roads using an equation of the following form:

$$S_z = A\varphi^{-n}$$ (3.8)

The spatial frequency range for φ , for off-road profiles, should be between 0.05 cycles/m (wavelength = 20m) and 10 cycles/m (wavelength = 0.1m) according to the ISO 8608 (1995) standard. The Roughness coefficient, A, and the Road exponent, n, can then be used to classify the roughness of the road. The method to obtain the Roughness coefficient and the Road exponent is discussed in Becker (2008).

The Roughness coefficient, A, of the test track is 3.48E-05 m^2/cycles/m while the Road exponent, n, is 1.6. Figure 3-27 shows the Displacement Spectral Density of the Belgium paving.

The Fatigue track was used to accelerate the fatigue life of vehicles and their suspension systems. The fatigue track seemed smoother than the Belgian block road but the RMS value of the track was higher. The fatigue track generated higher amplitude inputs at spatial frequencies between 0.5 and 10cycles/m but was significantly smoother below 0.5 and above 10 cycles/m, compared to the Belgian paving. The Roughness coefficient of the test track is 3.42E-05 m^2/cycles/m while the Road exponent is 2.9. Figure 3-28 shows the Displacement Spectral Density of the Fatigue track.
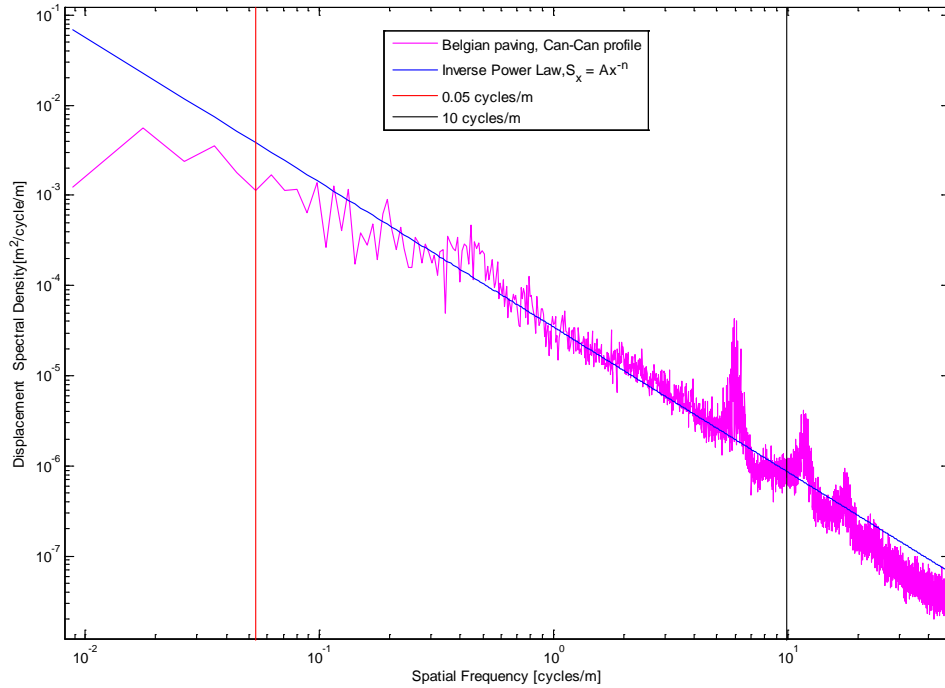
Figure 3-27 Displacement Spectral Density of the Belgium paving (Becker, 2008)
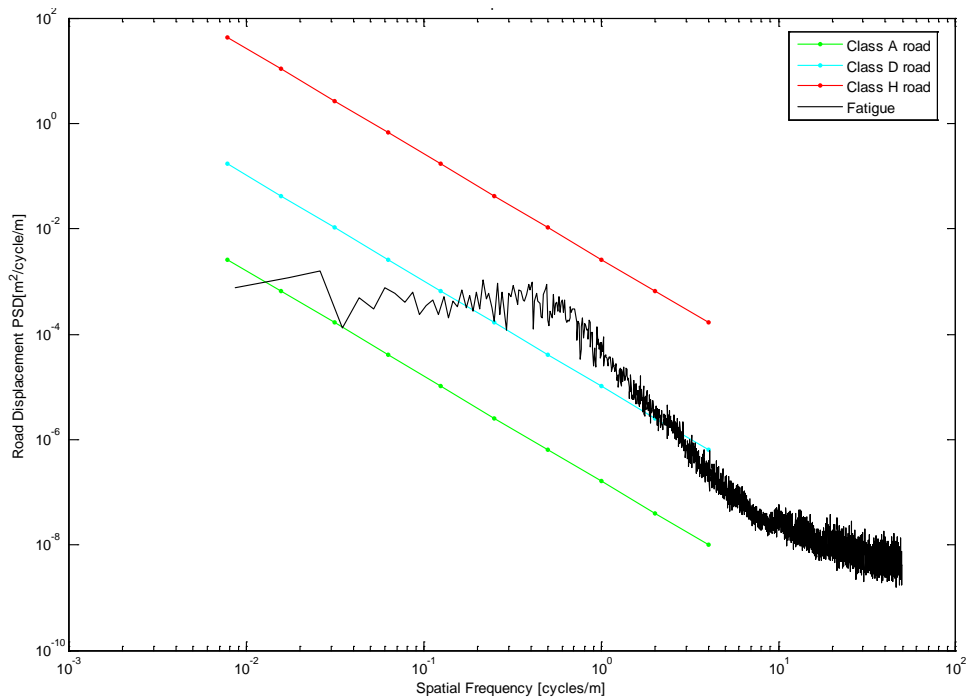
Figure 3-28 Displacement Spectral Density of the Fatigue track (Becker, 2008)

Unpaved roads often develop a series of regular bumps with a short spacing on the road surface. This phenomenon was often called a washboard road or a corrugated road. A permanent concrete test track was built at Gerotek, to investigate the effects of the road on the vehicle. The parallel and angled corrugations on the test track have an average spacing of 760 mm and a amplitude of 25mm. The Displacement Spectral Density of the Corrugations tracks are shown in Figure 3-29.
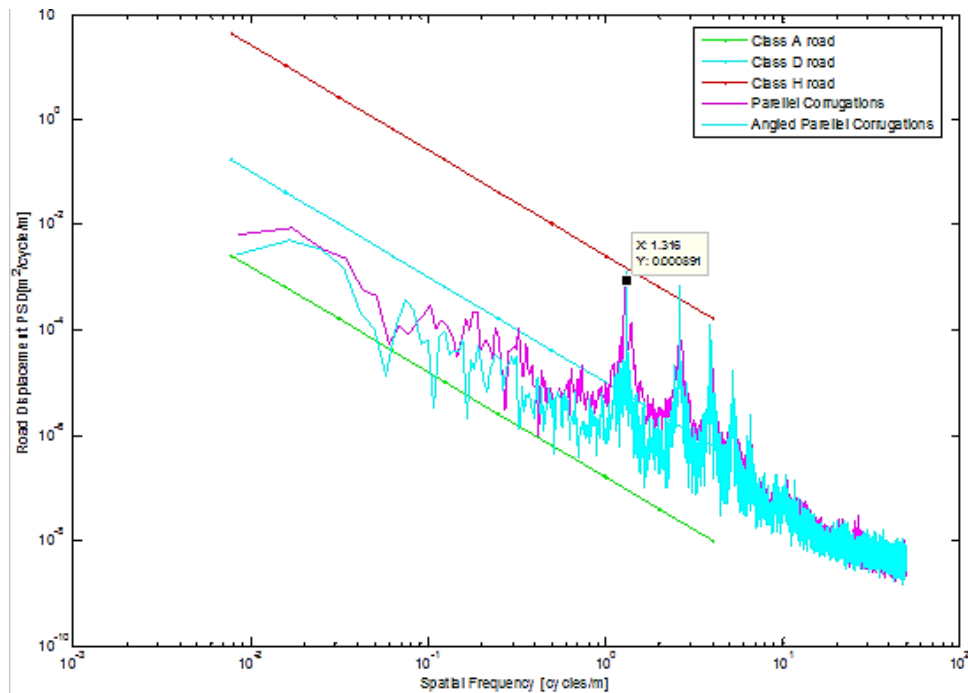
Figure 3-29 Displacement Spectral Density of the Corrugations tracks (Becker, 2008)

3.5   Section Summary

This chapter discussed the different tests that were conducted to acquire data to be used during the tyre parameterization of various mathematical tyre models and for model validation. The tests included static laboratory tests as well as dynamic field tests.

Laboratory tests were conducted on a non-rolling tyre. The static tyre stiffness was experimentally determined. The tyre carcass shape was measured and the footprint dimensions of the tyre were determined at various tyre pressures and normal loads. Tests to determine the forces that are generated when a tyre is forced onto lateral and longitudinal cleats were conducted. The tests were conducted at different inflation pressures, using cleats with different dimensions. A modal analysis was also conducted to determine the vibration modes and natural frequencies of the tyre.

A procedure to determine the tyre damping coefficient, from drop test results, was discussed. Dynamic cleat tests were conducted to be used during the parameterization and validation process. The repeatability of the parallel cleat tests was exceptionally good while the angled cleat tests did not show the same agreement. This was due to the difficulty found in positioning the test trailer exactly in the centre of the track to ensure that both wheels make contact with the cleats simultaneously.

The chapter also discussed the validation field tests that were conducted. The tests were used to validate different mathematical tyre models. The field tests were conducted on various road surfaces found at the Gerotek Test Facility (Gerotek Test Facilities, 2013). Tests were conducted on the Belgian block road, Fatigue track, increasing frequency cleats, parallel and angled corrugations.

4 Parameterization of the Tyre Models

"If you have a procedure with 10 parameters, you probably missed some"

- *Alan Jay Perlis, 1982*

4.1 Parameterization Introduction

In this chapter different tyre models will be parameterized using the test data acquired in Chapter 3. The parameterization process will be discussed in detail for each contact model and for FTire.

Tyre models that will be parameterized are:

- PAC89 tyre model with a One Point Contact model (OPC)
- PAC89 tyre model with a 3D Equivalent Volume Contact model (VC)
- PAC89 tyre model with a 3D Enveloping Contact model (3D ENV)
- FTire model

The selected tyre models were all implemented in ADAMS. For all Pacejka tyre models the contact model defines the vertical behaviour of the tyre model.

4.2 One Point Contact Model

The One Point Contact model is the simplest of all investigated contact models. The normal force can be calculated using a linear spring, with stiffness k_z, and a constant damping coefficient, c_z. The normal force is given by :

$$F_z = k_z \rho + c_z \dot{\rho} \qquad (4.1)$$

The data from the static deflection versus load test, as shown in Figure 3-3, could be fitted with a linear curve fit to determine a spring stiffness of 659.6 N/mm. It was determined that the linear fit was not a accurate representation. The root mean squared error between the linear fit and the measured data was 2938.4N.

A load deflection curve was defined in the tyre property file to improve the accuracy of the representation. When a load deflection curve is defined in the tyre property file, the solver would disregard the defined linear spring stiffness and interpolate the defined data, or extrapolate if necessary, to determine the normal load. The nonlinear load deflection data was acquired by calculating the mean load at every 5 mm tyre deflection.

The damping in the tyre was measured using the drop test method as discussed in section 3.4.1. The damping in the tyre was calculated as 2.66 Ns/mm.

Using these parameters two different tyre definition files were created, one with linear vertical tyre stiffness and another where the tyre stiffness is described with the load deflection curve.

4.3 3D Equivalent Volume Contact Model

The 3D Equivalent Volume Contact model is the default contact model when a 3D shell road is used in an ADAMS simulation. This contact model makes use of the same parameters as the One Point Contact models. In addition to these parameters the contact model requires a description of the carcass shape. If the carcass shape was not defined in the tyre definition file the solver would use a square carcass shape.

A more comparable carcass shape could be defined in the tyre property file by defining a set of points in the shape table. The carcass shape was defined using fractions of the tyre radius and width. The carcass shape was assumed to be symmetrical and only needed to be defined for one half of the tyre width. The relative width of the tyre must be given in ascending order from 0.0 to 1.0, where the value 0.0 corresponded to the centreline of the tyre. The measured outer contour, as shown in Figure 3-4, was used to determine the required ratios. A maximum of 10 points could be used to describe the carcass shape in the tyre property file.

Table 4-1 shows the calculated values that are used to describe the tyre shape in the tyre definition file. The carcass shape is shown in Figure 4-1.
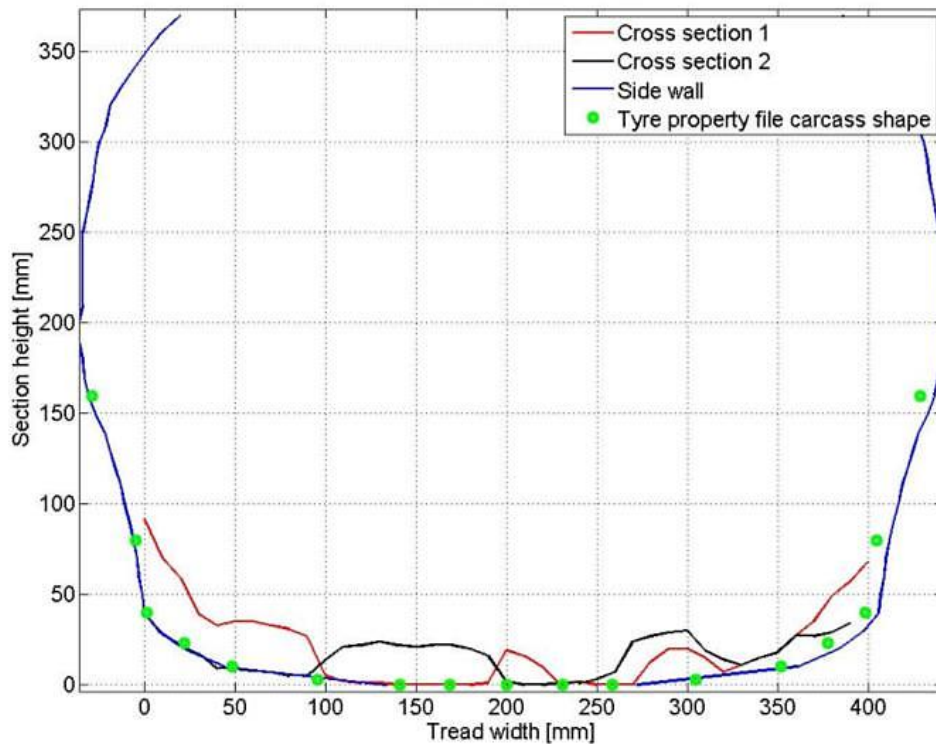
Figure 4-1 Test tyre outer contour as defined in the tyre property file

Table 4-1 Carcass shape

Radial	Width
1	0
1	0.137
1	0.2557
0.9956	0.4566
0.9854	0.6621
0.9665	0.7763
0.9417	0.8676
0.8834	0.895
0.7669	1

4.4   3D Enveloping Contact Model

The 3D Enveloping Contact model was based on the work done by Schmeitz (2004). To model the enveloping behaviour of the tyre, while rolling over a cleat, Schmeitz proposed a cam model. The cams were arranged on the outline of the contact patch. The contact model calculated the size of the tyre contact patch during each iteration step, to determine the effective height, slope, road curvature and effective road camber for the tyre model. The road profile, in the contact patch, was thus averaged.

The tyre stiffness and damping was described in the same way as was the done in the One Point Contact tyre model. The tyre stiffness could be described using a linear tyre stiffness or with a load deflection curve. The damping behaviour was described using a constant damping coefficient. The contact patch was described by three parameter sets; the contact patch dimensions, the cam dimensions and the number of cams used.

The tyre contact patch dimensions were described by the half contact patch lenght:

$$a = p_{A1} R_0 \left(\frac{\rho_z}{R_0} + p_{A2} \sqrt{\frac{\rho_z}{R_0}} \right)$$

(4.2)

The measured tyre contact patch areas, as disused in section 3.3.3, were used to find the parameters p_{A1} and p_{A2}. The Parameters were determined to be 0.15 and 7.06 respectively.

Figure 4-1 shows the measured half tyre contact patch length and the fitted results.
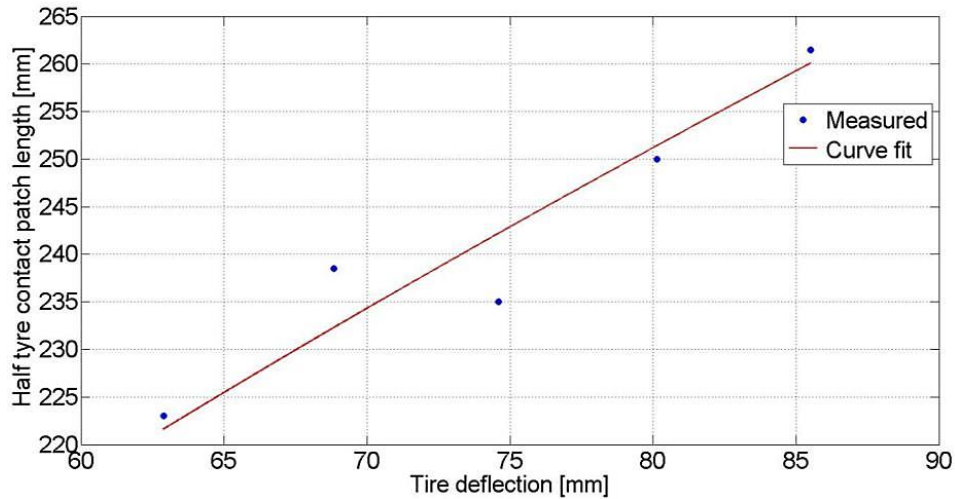
Figure 4-2 Half contact patch length vs. tyre deflection

The figure showed that the half contact patch length formula can be used to adequately describe the contact patch length. The half contact patch width is described by Equation 4.3.

$$b = p_{B1}W_0\left(\frac{\rho_z}{R_0} + p_{B2}\sqrt{\frac{\rho_z}{R_0}} + p_{B3}\frac{\rho_z}{R_0}\sqrt{\frac{\rho_z}{R_0}}\right) \tag{4.3}$$

An optimization process was used to fit this formula to the measured results. The three parameters, p_{B1}, p_{B2} and p_{B3}, were determined to be 0.0017, 16006.5 and -77819.1 respectively.

The curve fit result is shown in Figure 4-3. The figure shows that the contact width is largely independent of the tyre deflection. The curve fit, with the given formula, cannot be used to describe the tyre contact width for large off road tyres. The solver will calculate a wider contact patch for tyre deflections between 20 and 75 mm and a smaller width for tyre deflections above 75 mm. The fit can be improved when a straight line fit, or a table describing the deflection versus half contact patch width relationship, could be specified in the tyre property file.
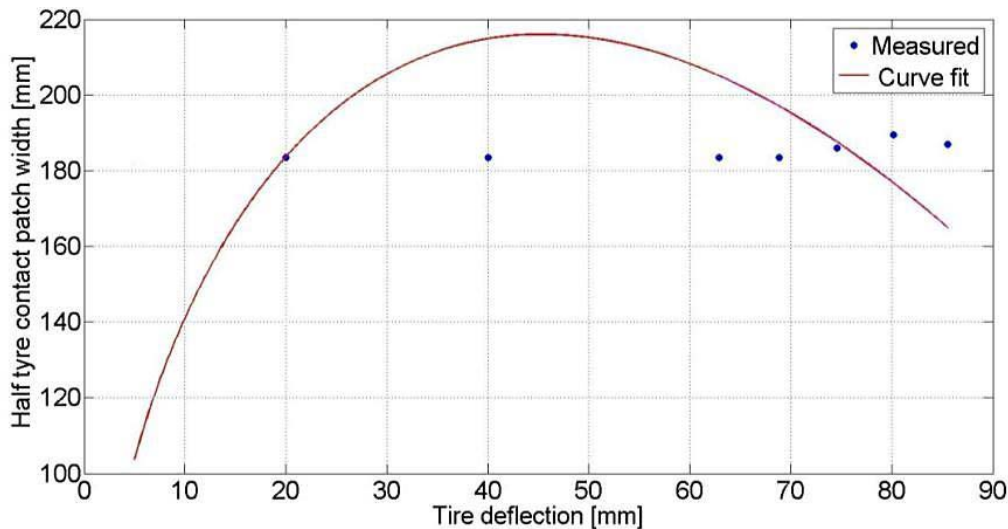
Figure 4-3 Half contact patch width vs. tyre deflection

The shape of the cams is given by:

$$\left(\frac{x_e}{p_{ae}R_0}\right)^{p_{ce}} + \left(\frac{y_e}{p_{be}R_0}\right)^{p_{ce}} = 1 \tag{4.4}$$

The coefficients p_{ae}, p_{be} and p_{ce} described the shape of the individual cam. The ADAMS help file informed the user to compare the shape of a deflected tyre with the ellipsoid shape to derive these parameters.

Figure 4-4 shows an attempt at following this procedure. The figure shows the tyre test trailer with a ballast load of 5440kg.
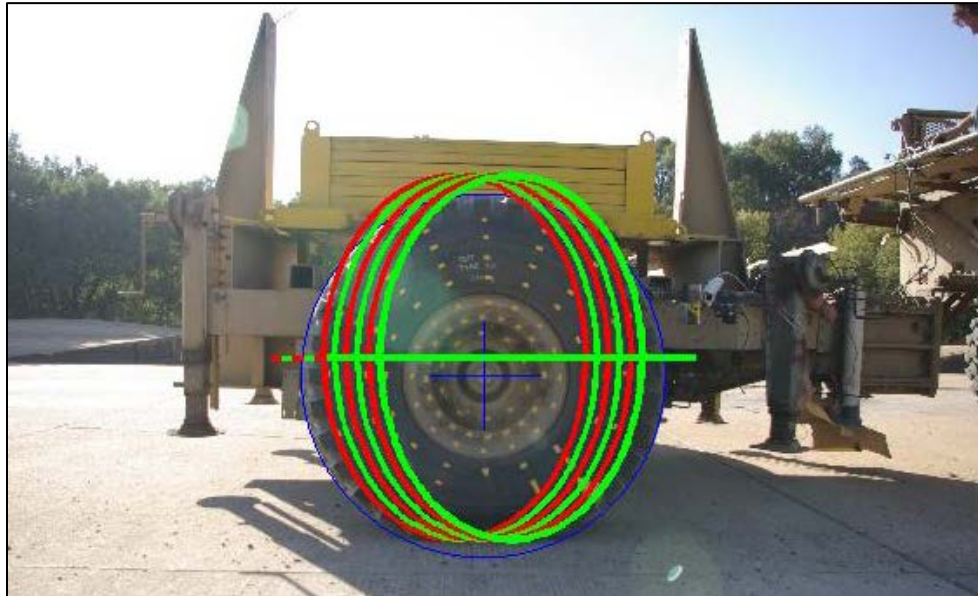
Figure 4-4 Ellipsoid shape

The shapes of the cams were only dependent on the unloaded tyre radius, not on the tyre load. The large aspect ratio of tyres made it difficult to find the correct parameters for the cams. The shape of the cams represent the tyre the best when using the values 0.72, 1 and 2 for the parameters p_{ae}, p_{be} and p_{ce} respectively.

In the lateral direction the cams were equally spaced over the entire contact width. In the longitudinal direction they were spaced equally over the base length l_s.

The base length is dependent on the contact length and is given by:

$$l_s = 2p_{ls}a \tag{4.5}$$

The tandem base length factor was chosen to be 0.9. Schmeitz has shown that 5 cams along the length and 6 along the width of the contact patch showed the best accuracy-performance ratio for a passenger car tyre. The number of cams across the contact patch width and length, for the larger tyre, were chosen to be 10 and 15 respectively. More cams were used along the contact patch length because the contact patch is longer than it is wide.

The contact patch dimensions (as would be calculated by the solver) could be compared to the measured results, by using the calculated parameters. Figure 4-5 shows the result of the comparison. The red markers indicate the contact points of the cams. The contact patch on the left shows the tyre with a 68mm tyre deflection. The figure shows that the calculated contact patch width is slightly larger than the measured result. The contact patch on the right shows a contact patch from a tyre with a deflection of 85 mm. As expected the calculated contact patch width is smaller than the measured result. The overall accuracy of the fits is acceptable.
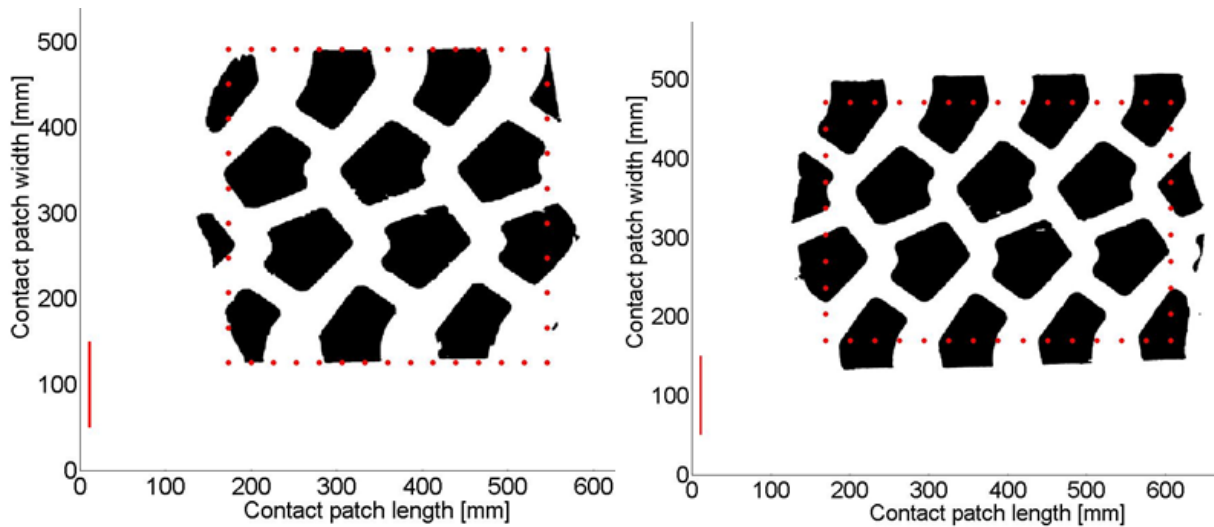
Figure 4-5 Predicted 3D Enveloping contact patch dimensions

4.5   Flexible Structure Tyre Model

The FTire model was the most complex tyre model investigated in this thesis. The parameterization of this model was also found to be the most intricate as the model contains a large number of parameters. It is required that the user understands the model structure and should be able to relate the parameters to the model behaviour. It is required of the user to obtain a sense of the parameters before a tyre model with a sufficient accuracy can be created.

The program FTire/fit is structured in such a way that it guides the user through the parameterization process. The process is summarized in Figure 4-6. The process consists of three stages namely preparation, identification/validation and finishing.

During the first stage of the parameterization a new tyre property file is created. The user provides the program with a comparable tyre property file that was used as initial estimate.

The next step is to define a cleat definition file. This file defines all the test tracks that would be used during the parameterization process. The obstacle type, called OBSTTYPE, was added to the TYDEX measurement files (Gipser & Hofmann, 2010). This allowed FTire/fit to link the measured data to a specific test track.
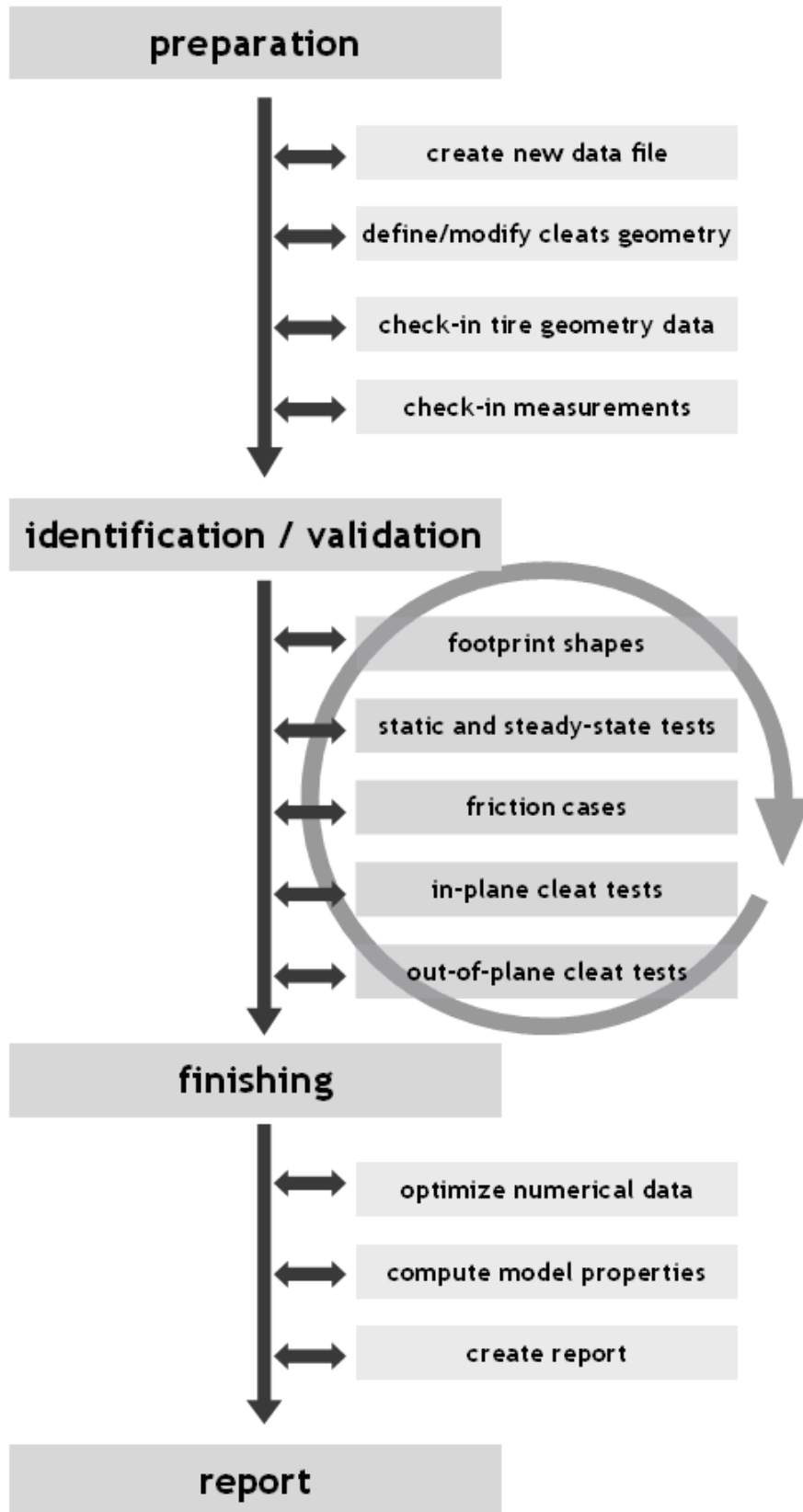
Figure 4-6 FTire parameterization procedure (Gipser, 2002)

A section of the cleat definition file is shown in Figure 4-7.

```
* A   38x38 mm    0 deg (transversal on flat surface)
* B   51x51 mm    0 deg (transversal on flat surface)
* C   76x76 mm    0 deg (transversal on flat surface)
* D   38x38 mm   90 deg (longitudinal on flat surface)
* E   51x51 mm   90 deg (longitudinal on flat surface)
* F   76x76 mm   90 deg (longitudinal on flat surface)

$obstacle_A !* 38x38 0 deg *****************************************************
 cleat_direction              0      ! [deg]
 cleat_height               38.0     ! [mm]
 cleat_length               38.0     ! [mm]
 cleat_bevel_edge_length      2      ! [mm]
 diameter                  9999      ! [m] negative if outer drum
 type drum; v vdrum/3.6; number_cleats 1; mu_factor  1.00; mu_factor_cleat 0.5

$obstacle_B !* 51x51 0 deg *****************************************************
 cleat_direction              0      ! [deg]
 cleat_height               51.0     ! [mm]
 cleat_length               51.0     ! [mm]
 cleat_bevel_edge_length      2      ! [mm]
 diameter                  9999      ! [m] negative if outer drum
 type drum; v vdrum/3.6; number_cleats 1; mu_factor  1.00; mu_factor_cleat 0.5
```

Figure 4-7 Section of the cleat definition file

The user is then asked to define the overall geometry of the new tyre model. The tyre dimensions, weight and two inflation pressures could be defined in the data file creation process.

Two different tyre pressures should be defined next. The FTire model is constructed in such a way that the same model could be used at different tyre pressures. To ensure that the model could accurately describe the tyre behaviour at various tyre pressures, the user should use test data from two different tyre pressures during the parameter identification process. Even if the tyre model would only be used with a fixed inflation pressure, the use of different tyre pressure data would ensure that the correct parameter has been optimized. The data file generation window is shown in Figure 4-8.

Due to the complexity of the tyre model, different parameters could be changed that would give the same results under certain conditions. To illustrate this situation the following example can be used:

It is known that the vertical tyre stiffness is predominantly dependent on the inflation pressure. An FTire model can be created that relies on the tyre inflation pressure to mimic the force displacement curve as was shown in Figure 3-3. The same force displacement curve can also be obtained with a tyre at lower inflation pressure, but with stiffer side walls. The tyre models would behave the same for a static load displacement test but would predict different results for other tests, such as the cleat test. This is a problem complex models are plagued with.
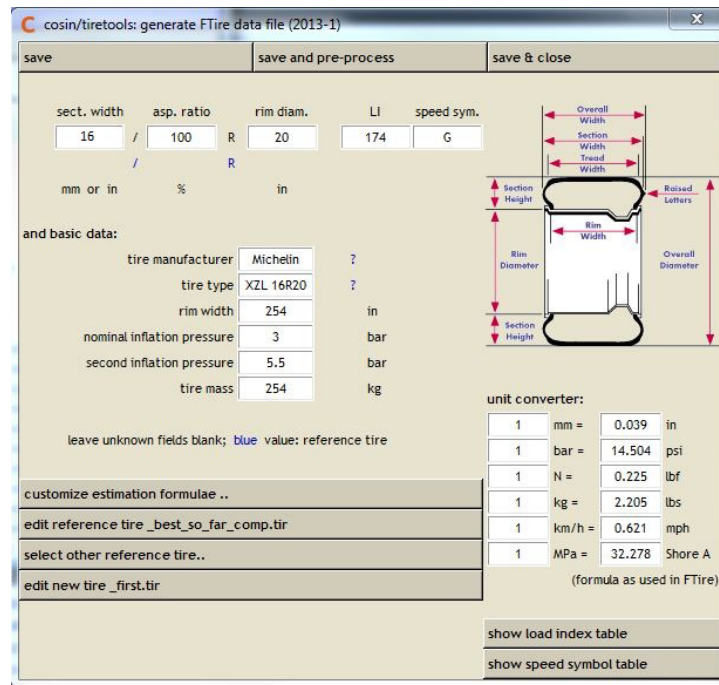
Figure 4-8 FTire data file tyre dimensions window

The final step in creating the new dataset is to "check in" all the test data that should be used during the parameterization process. During this process all the footprint bitmaps and all available parameterization test data was checked in. As discussed in Section 3.3.3 a red line of known length could be added to the bitmaps to allow the software to calibrate these files. The user would be prompted to specify the correct calibration factor, should this not be done.

In addition to footprints, the static measurement files were checked in. These files were written in the TYDEX file format and included the obstacle type that was used during the test. FTire\fit loaded each file separately and tried to automatically recognize the nature of the test. When enough information was specified in the TYDEX measurement files, the program loaded and sorted them according to the nature of the test.

After completion of the preparation step, the parameter identification process was started. It was important to follow the correct parameter identification order, especially during the first loop through the identification process.

The identification order that should be followed is:

1. Footprint shapes
2. Static and steady state tests
3. Friction cases
4. In-plane cleat tests
5. Out-of-plane cleat tests

In the first stage of the parameter identification process the tyre footprints were used. The tyre footprints holds much information regarding the tyre stiffness and shape of the tyre. The footprints were used to determine the lateral bending stiffness and the in-plane bending stiffness of the tyre belt. Should the model be able to describe the footprint shape and dimensions accurately, for all tyre loads, it would ensure that the road input to the model could be calculated accurately. An accurate representation of the road input was imperative to accurately predict the tyre behaviour. Furthermore, if the tyre model was able to reproduce an accurate set of footprints, the tyre shape and overall stiffness is modelled accurately.

Figure 4-9 shows the footprints of the test tyre at an inflation pressure of 300kPa and two different load cases. The calculated footprint shape, of the FTire model, is shown on the same figure and is indicated with a red line. From the figures it can be seen that the model is able to accurately predict the dimensions and the shape of the tyre contact patch.
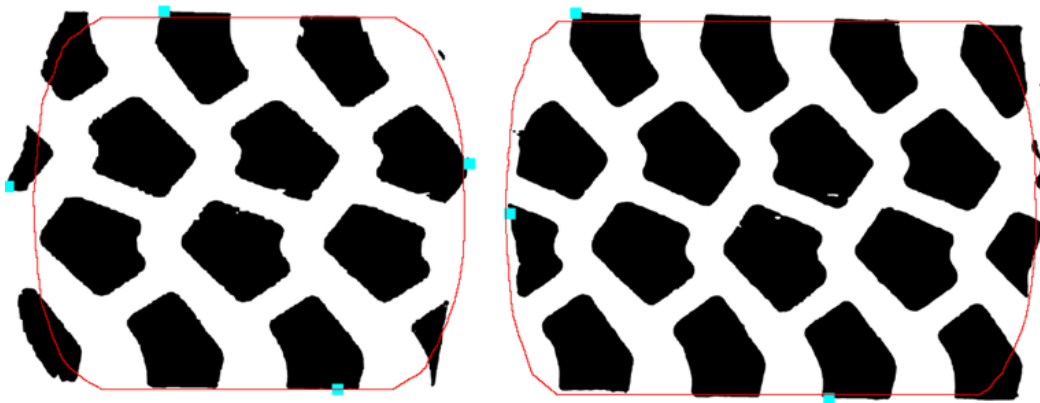
Figure 4-9 Footprint, 300kPa; left - 4000kg load; right - 6000kg load

The footprint of the tyre at an inflation pressure of 500kPa and a load of 54000N is shown in Figure 4-10. The model shows an even better fit compared to Figure 4-9.
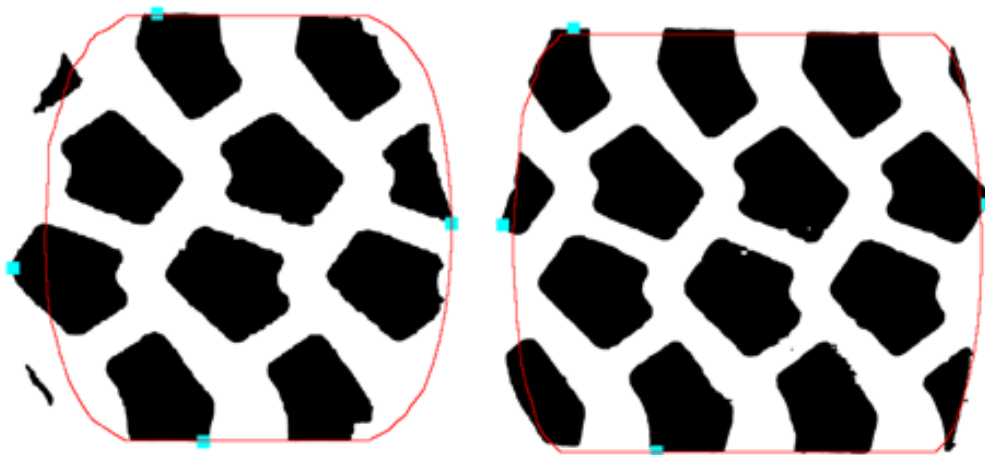
Figure 4-10 Footprint 500kPa; left - 4000kg load; right - 6000kg load

It was found that the stiffness of the tread rubber influenced the shape of the footprints. The tread stiffness was determined experimentally and was found to have a ShoreA hardness value of 60.

To identify the radial tyre stiffness parameters of the tyre model the load deflection test on a flat surface was used. Four points, two for each pressure, from the load deflection curve were used to determine the vertical tyre stiffness.
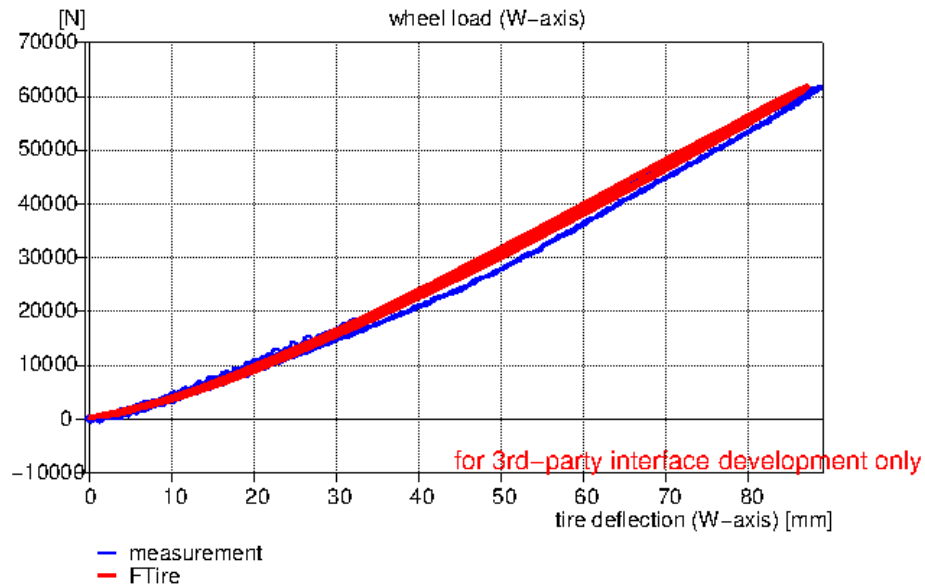
Figure 4-11 Vertical stiffness on flat surface, 300kPa inflation pressure, 0 deg camber angle
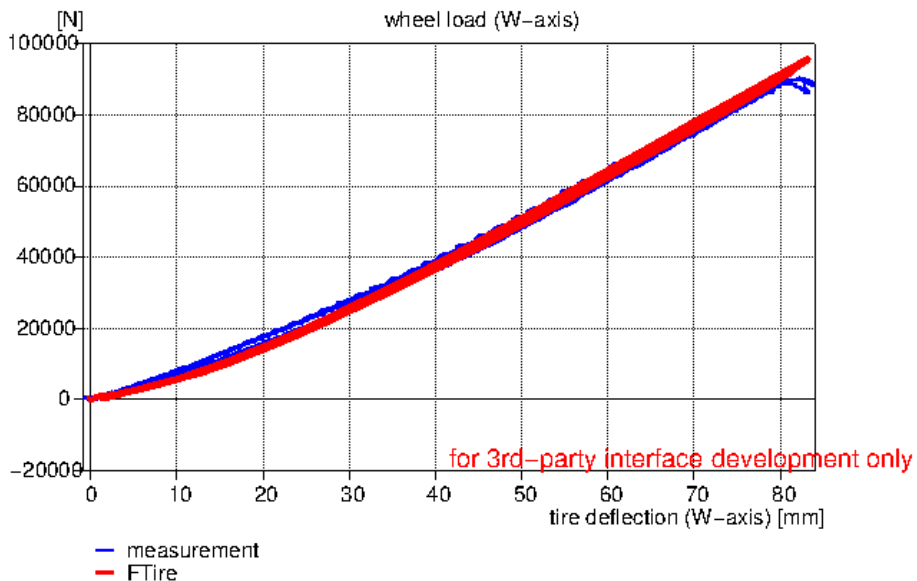
Figure 4-12 Vertical stiffness on flat surface, 550kPa inflation pressure, 0 deg camber angle

The measured and predicted static lead deflection curves are shown Figure 4-11 and Figure 4-12. Figure 4-11 shows the test results with a 300kPa inflation pressure. Figure 4-11 shows the results with a 550kPa

inflation pressure. The measured data of this test was shown in Figure 3-3. It is evident that the tyre model is able to accurately predict the load deflection curves for both inflation pressures.

The static tyre behaviour over a cleat held information about the lateral and longitudinal belt stiffness. The transversal cleat tests were used to identify the in plane belt bending stiffness.

Figure 4-13 and Figure 4-14 show that the in plane bending is largely dependent on the inflation pressure. From the figures it can be seen that the tyre model parameter is tuned until the model is capable of accurately predicting the forces on a flat surface and on transversal cleats.
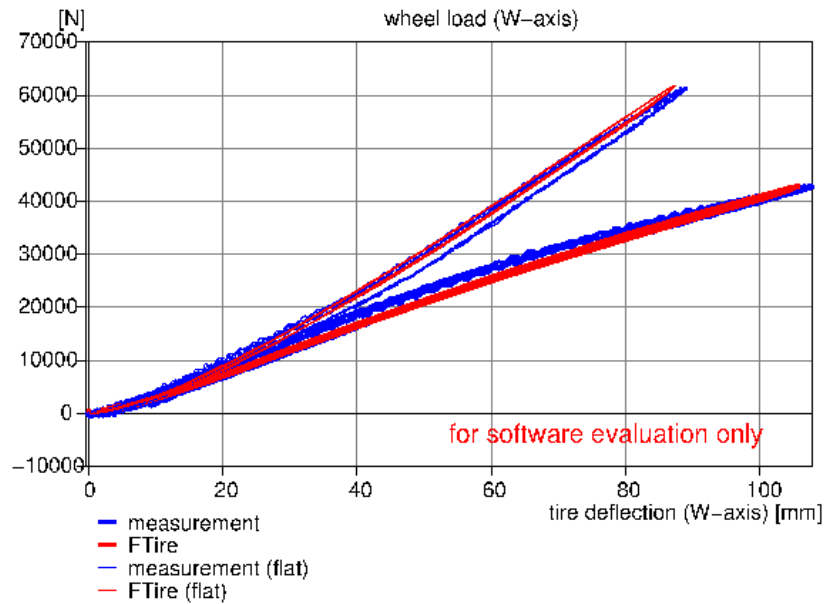
Figure 4-13 Vertical stiffness on 51x51 mm cleat, 300kPa inflation pressure, 0 deg camber angle
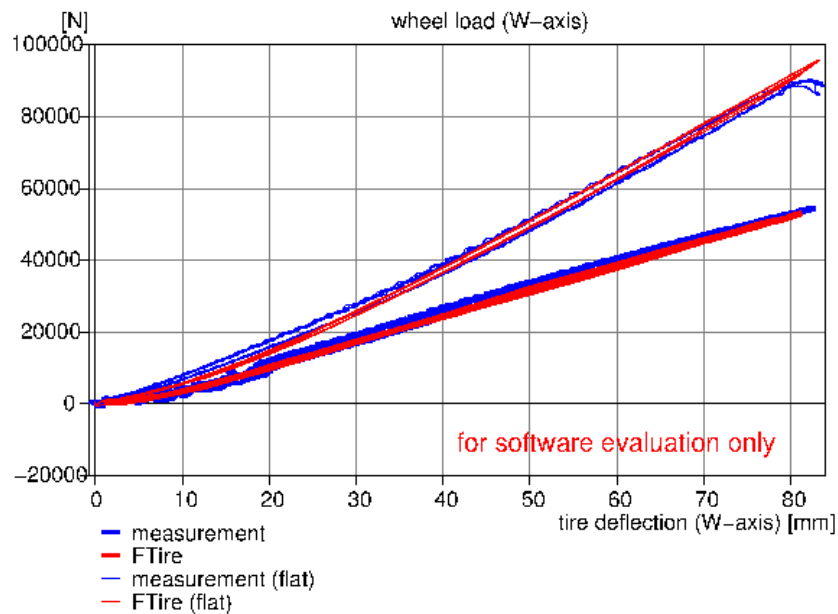
Figure 4-14 Vertical stiffness on 38 x38 mm cleat, 550kPa inflation pressure, 0 deg camber angle

The model is able to accurately predict the load deflection curve for cleats of various dimensions. Figure 4-15 shows the load deflection curve of a 76.3 x76.3 mm cleat test.
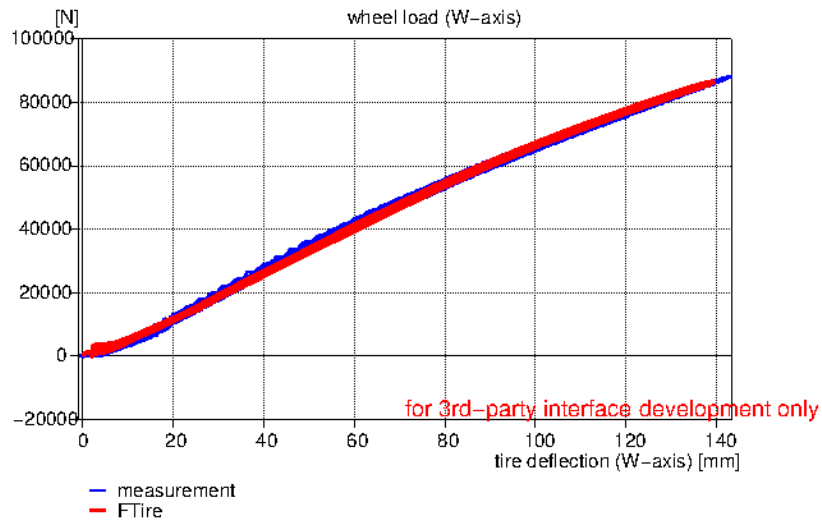
Figure 4-15 Vertical stiffness on 76.3 x76.3 mm cleat, 550kPa inflation pressure, 0 deg camber angle

The tyre model was able to capture the difference in the predicted normal force during the loading and unloading process. This indicates that the elastic hysteresis loop can be approximated with the tyre model.
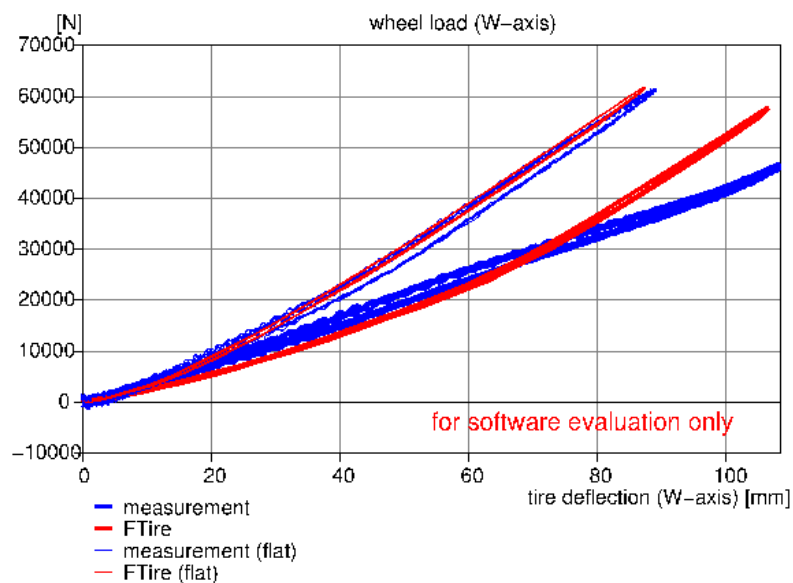
Figure 4-16 Vertical stiffness on 51x51 mm oblique cleat, 300kPa inflation pressure, 0 deg camber angle

The lateral belt bending stiffness could not be adjusted so that the measured load deflection curve was met. The measured and predicted load deflection curve is shown in Figure 4-16.

Many parameters, such as the parameter that couples the lateral and longitudinal belt stiffness's, were available to fine tune the tyre behaviour yet no combination could be found that would result in a better

representation. The tyre model behaved similar to the measured results for deflections lower than 80mm. Deflections higher than 80mm resulted in a higher predicted tyre load compared to the measured results. It is expected that such situations will seldom be found during normal operating conditions.

The parameters that are used to describe the damping behaviour of the FTire model could not be parameterized within FTire/fit. The tests that are normally used to determine these parameters were not available. The FTire/fit relied on dynamic drum cleat tests to extract the parameter values.

The damping behaviour of the tyre model is modelled using viscous damping elements between belt nodes and the rim. The damping behaviour was described, in the property file and during the parameterization process, with modal damping values. The model then tried to match these damping values. The help file (Gipser, n.d.) stated that the damping model was of limited accuracy because the rubber damping was more accurately described by frequency independent hysteresis loops. It further stated that the measured damping values are too low in many cases and should be increased to achieve similar damping behaviour between the real tyre and the FTire model.

 As no drum tests were available, the damping parameters were determined from the dynamic cleat tests by trying to match the measured tyre behaviour. These tests were discussed in section 3.4.1 and made use of a tyre test trailer. The modal analysis results were used as initial estimates of the damping values.

A tyre model was created, using the modal analysis damping values, and used in a simulation over 50 mm cleats. The simulation results were compared to the measured tyre response to determine whether the tyre showed an acceptable damping behaviour. The damping parameters were then adjusted accordingly to improve the correlation between the measured and predicted tyre behaviours.

This was a brute force method but it was found to be effective but time consuming. A concern using the described method was that the relationship between the three modal damping values could not be established. The parameters were only altered so the ratio between them remained unchanged and held the same relationship as the measured damping values. The measured and predicted tyre damping behaviours is shown in Figure 4-17 and Figure 4-18.
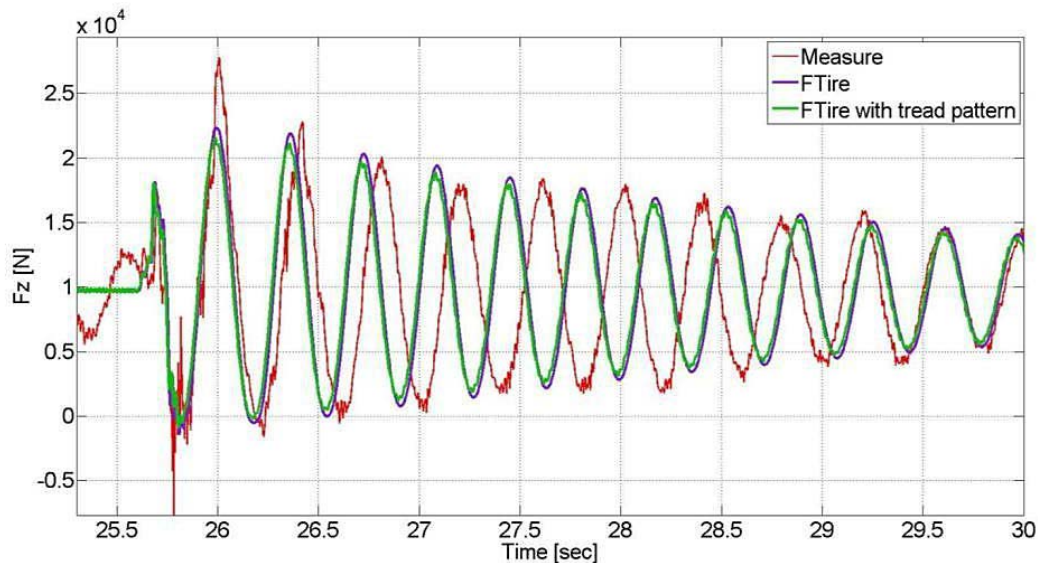
Figure 4-17 FTire Simulation result, 50mm cleat, LC1, 27km/h
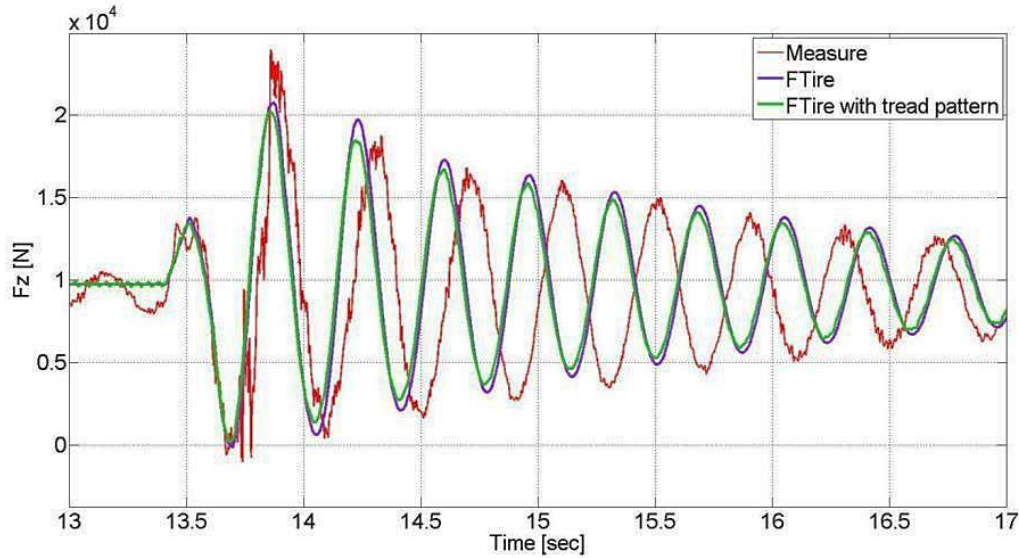
Figure 4-18 FTire Simulation result, 50 mm cleat oblique, LC1, 12km/h

Tests conducted to determine the side force slip angle relationships of the tyre were also used in the parameterization process. The force generation due to a change in the tyre slip angle did however not fall in the scope of this investigation and will thus not be discussed in detail.

The tread pattern of the Michelin 16.00R20 is shown in Figure 4-19.

Figure 4-19 Michelin XZL tread pattern

The contact nodes in the FTire model could be arranged to represent the test tyre tread pattern. It was expected that the pattern would influence the tyre behaviour, especially during tests with small wavelength road unevenness. To investigate this, an FTire model was created where the contact elements were arranged equally and a second model was created where the tread pattern was accounted for.

The graphical representation of the FTire model, where the contact elements are arranged according to the tread pattern, is shown in Figure 4-20. The figure also shows the predicted ground pressure distribution of the footprint.

ground pressure [MPa]

	> 2.4
	2.1 .. 2.4
	1.8 .. 2.1
	1.5 .. 1.8
	1.2 .. 1.5
	0.9 .. 1.2
	0.6 .. 0.9
	0.3 .. 0.6
	< 0.3

grid−line dist. 20 mm

	Tydex C	Tydex W
Fx	−2340 N	−2340 N
Fy	48 N	48 N
Fz	23411 N	24921 N = 36.5 % LI
Mx	25 Nm	−5 Nm
My	1443 Nm	−103 Nm
Mz	−13 Nm	−13 Nm

radial deflection 32.2 mm
camber angle 0.0 deg
footprint length 356.0 mm
footprint width 387.7 mm
footprint area 601.3 cm^2
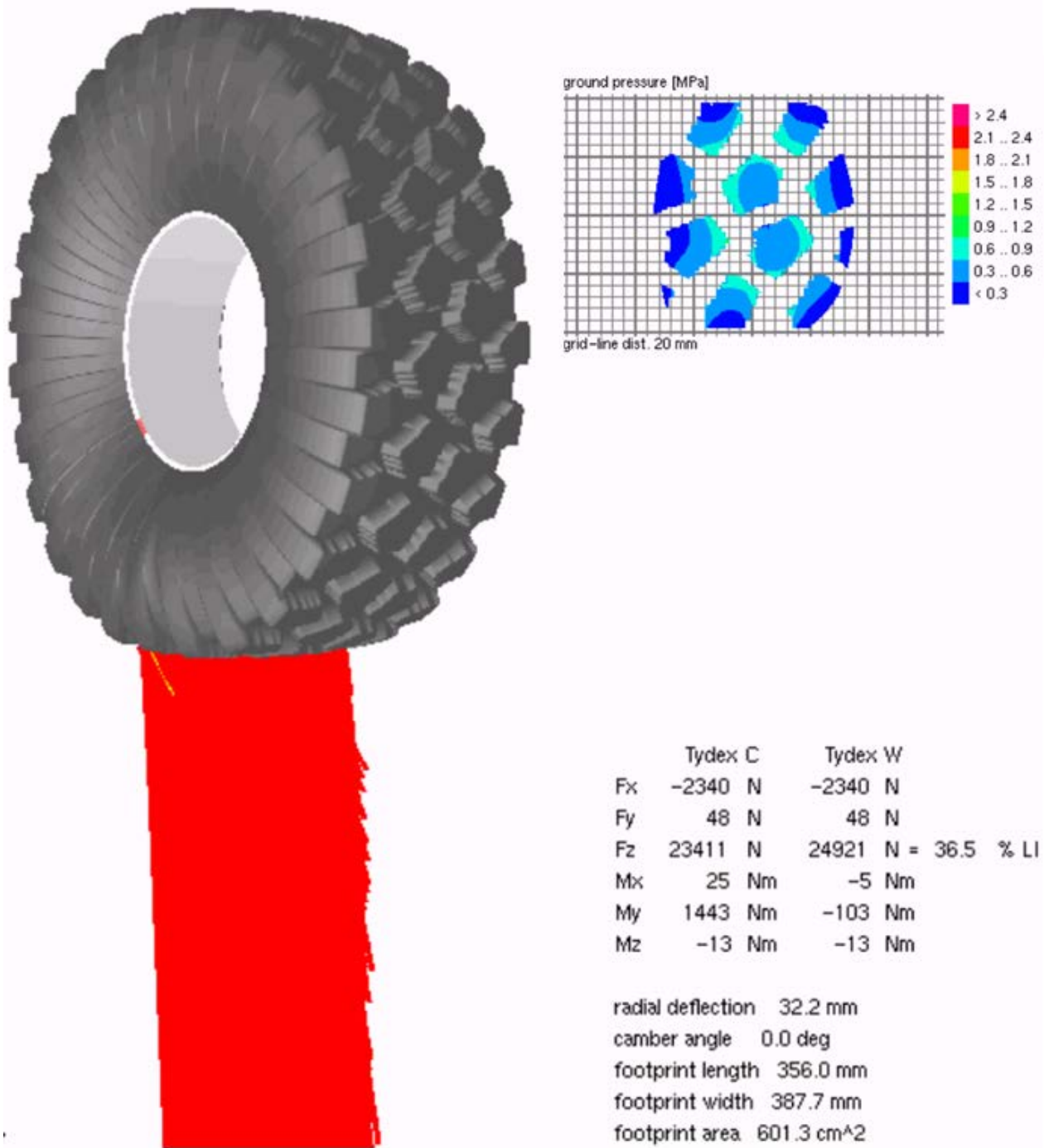
Figure 4-20 FTire model with tread pattern

4.6   Section Summary

In this section the parameterization process of three contact models, which are implemented in ADAMS, and an FTire model, with their variations have been discussed.

The contact models that are associated with the Pacejka group of tyre models were parameterized with only a few parameterization tests. The tyre stiffness and damping was described in all tyre contact models with the same parameters. The vertical tyre stiffness was obtained from a load deflection test and the tyre damping coefficient was obtained using a pendulum or drop test. The final parameter that needed to be defined for the One Point Contact model was the unloaded tyre radius.

The 3D Equivalent Volume Contact model required information about the tyre carcass shape. The carcass shape, assumed to be symmetric, was described with ten points.

The 3D Enveloping Contact model required data about the tyre contact patch width and length for a set of tyre deflections. The required information could be acquired with laboratory tests.

The parameterization process of the FTire model was found to be the most cumbersome. This was expected due to the model's complexity. When repeated multiple times, the parameterization effort is expected to decrease. The result of the parameterization process was dependent on the user and the availability of sufficient test data. The parameterization process relied heavily on experimental test data. Most parameters were defined by using static laboratory tyre tests. A tyre test trailer was used to acquire experimental field test data. These data sets were then used to identify the parameters that determine the dynamic response of the tyre.

A wide range of additional test data could be used to improve the accuracy of the FTire model. The model was able to fit the static tyre behaviour, on a flat surface and on cleats, exceptionally well. Only the lateral bending behaviour could not be fitted accurately at large tyre deflections. The standard parameterization process relies on dynamic drum cleat tests to correct the dynamic behaviour of the tyre but this is very difficult to obtain for large tyres. A trial and error approach was therefore used to find the damping parameters of the tyre from results obtained using the tyre test trailer.

5   Validation of Tyre Models

"*Wide acceptance of an idea is not proof of its validity.*"

- *Dan Brown, 2009*

5.1   Validation Introduction

The validation process is an important part of any mathematical model created to emulate physical systems. In the process simulation results are compared to experimental test data. The datasets are compared to determine their agreement and to find inconsistencies. Inconsistencies can then be related to the incorrect measurements or to uncertainties in the model. Inaccuracies in the measured data may arise from altering measurement conditions or due to inaccurate instruments. Uncertainties in the simulation model can be related to the either the model inputs, the numerical approximations or in the model itself.

Many different validation metrics have been developed (Kat and Els, 2012) and are used to quantify the agreement between two data sets. Two different approaches are often used. The first compares the data sets at every data point and calculates an error vector, such as the relative error metric. Others specify the agreement between the data sets as a single value, such as the root mean square error. The validation metrics that calculate a single value are preferred as it simplifies the comparison between different runs. These values are however often misleading as they lack the ability to justify the complex relationships.

The validation metrics that will be used to describe the agreement between the measured and simulation result will be based on the root mean square error and the relative error validation metrics. To aid the validation process it has been found useful to compare the root mean square error (RMS) between the two signals. The RMS error is a cumulative error prediction metric for a given data set that calculates a single measure of the predictive power. The RMS error is a good measure of accuracy but is scale dependent and should thus only be used where scaling is not a problem.

$$RMS = \sqrt{\frac{1}{n_n}\sum_{t=1}^{n_n}(p_t - m_t)^2} \qquad (5.1)$$

Where scaling is a problem the relative error should be used rather than the absolute error. The relative error divides the absolute error by the magnitude of the exact value. The relative error, between the measured and predicted values, can be expressed as a percentage to simplify the interpretation. The equation to calculate the relative error, RE, between a measured, m, and predicted, p, value is given in Equation 5.2. It is assumed that the measured data is the "real" or correct value. To determine a single value that describes the accuracy of the agreement the mean of the RE vector, m%RE, can be calculated.

$$\%RE = \left|\frac{p - m}{m}\right| \times 100 \qquad (5.2)$$

The data validation of this thesis will be divided into two sections in order to quantitatively describe the overall error between the measured and predicted data. The first section will discuss the ability of the tyre

models to predict the vertical forces over discrete obstacles and cleats, and the second section will discuss the simulation agreement over uneven hard road surfaces.

To relate the measured forces of the load cells to the generated tyre forces, the weight of the sub frame and the accelerations of the centre of mass, of the sub frame, are required. During the tests the acceleration of the centre of mass, of the sub frame, could not be measured directly. Measurements of an accelerometer mounted on the sub frame could not be used due to excessive noise during the measurements. In this chapter the measured and simulated load cell measurements will thus be compared.

5.2   Discrete Obstacles

The dynamic response of different tyre models, while driving over discrete obstacles, was used to validate these mathematical models. These tests excited the tyre once, at a known instance, which simplified the tyre response investigation. The behaviour of the tyre could be classified into three sections; before the impact, during the impact and the response after the impact.

The tyre response before the impact did not hold much information. The tyre was rolling over a smooth road surface. Only the equilibrium tyre forces and moments could be analysed. The tyre behaviour during impact was the most important section. The tyre was excited during this time and the response influenced the tyre behaviour after the impact. The ability of the tyre model to accurately capture the road input and to determine the response could be investigated during this segment. The third segment described the behaviour of the tyre after it cleared the obstacle. This section was important as it indicated the ability of the tyre model to capture the damping behaviour of the tyre but does not have much practical value as the road input is again smooth.

The data describing the tyre behaviour while negotiating the obstacle (during impact) would be classified as the first section while the second section would describe the resulting tyre response to this disturbance. Dividing the data sets into two sections simplified the task of determining the validity of the different models as it allowed the differentiation between the ability to capture the road input and the resulting behaviour to be made.

Figure 5-1 shows both sections as described in the paragraph above. The blue dashed line shows the first section, where the tyre is in contact with the obstacle, while the green dashed line shows the response, or second section. The figure shows two different measurements, taken during the 50 mm dynamic cleat test. The load on the tyres during the test corresponds to load case one (LC1) and the test velocity was 18 km/h.

The results correlated very well between the tests runs. Five error metrics were used to quantify the error between the two measurements. Three metrics described the correlation during the cleat contact and the remaining two described the correlation of the tyre response after the tyre negotiated the cleat.

The first metric used was the percentage relative error of the cleat disturbance. The percentage relative error vector was calculated for the measured and simulated results. The mean was then calculated to determine a single value, the mean percentage relative error, or m%RE.
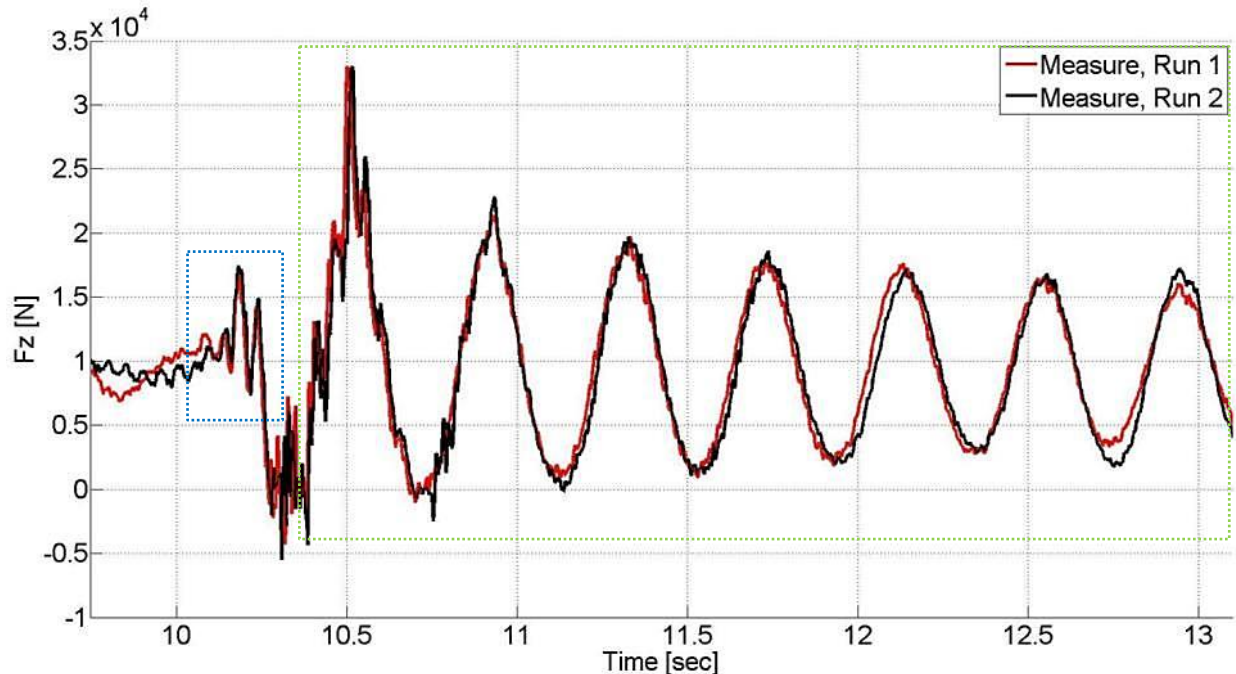
Figure 5-1 Normal load measurements of two 50mm cleat tests, LC1, 18km/h

The first metric used was the percentage relative error of the cleat disturbance. The percentage relative error vector was calculated for the measured and simulated results. The mean was then calculated to determine a single value, the mean percentage relative error, or m%RE.

The second metric that quantified the ability of the tyre model to capture the tyre behaviour was determined by calculating the maximum error present in less than 80% of the data. This measure indicates that 80 percent of the data would have an error below the defined error margin. This error metric was indicated as 80%RE. This metric was a good indication of how wide the error range is.

The third metric to be used was the root mean square error. This error metric was widely used and delivered good results when scaling was not a problem.

The two metrics used to quantify the correlation of the response were the mean percentage error and the root mean square error of the oscillation peaks. For the response validation, the relative and absolute errors were only calculated for the peaks of the oscillatory response that followed the cleat impact. They were not calculated for all recorded data points. This was necessary as the response during simulations and during experimental tests did not have the same oscillatory period. Due to this occurrence a direct time domain comparison was not possible.

The main focus of this investigation is to determine whether existing tyre models are able to accurately predict the tyre behaviour over rough terrain. During the validation process special attention should be given to the section where the tyre negotiates the obstacle. During this time the tyre is excited in the same way as it would during a test over uneven terrain where the tyre will be excited continuously. The free tyre response is thus of lower importance during validation over rough terrain compared to the road exciting response.

The measured and simulated tyre response of the tyre during a 50mm cleat test is shown in Figure 5-2. The test results were used in the parameterization process and will thus not be used to validate the models.
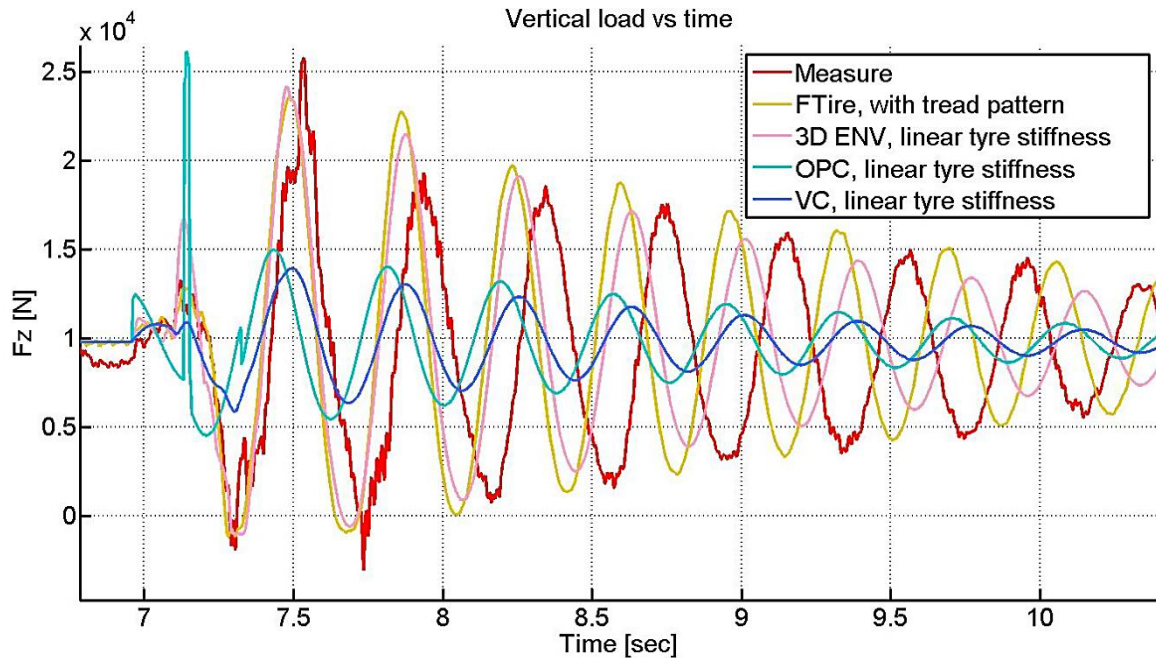
Figure 5-2 Simulation results, 50mm cleat, 12km/h, LC1

The figure shows that the period of the trailer oscillations were larger in the measured results compared to the simulation results. This could be attributed to the way the connection between the trailer and the towing vehicle was modelled. In ADAMS the trailer hook was modelled so that the position of the hook was constrained in the vertical and lateral direction. A force was applied to the hook in the longitudinal direction to facilitate the longitudinal acceleration. The force was controlled with a PID controller to ensure that the trailer was towed over the test surface at a prescribed velocity. The rotations about all three axes were not constrained at the hook. This modelling approach resulted in a stiffer overall system when compared to reality. In reality the tow hook may move in the vertical and lateral directions as relatively small forces are applied to the tow hook due to the moment of the test trailer. The tow vehicle suspension and inertia properties will influence the magnitude of this effect. It is therefore impossible to fix the tow hook vertically and laterally in reality but the effect is assumed to be small. This does mean that the two vehicle speed in reality was not perfectly constant and could deviate slightly from the speed used in the simulation.

To investigate the accuracy of the tyre model the focus should be on the section where the tyre is in contact with the obstacle. Figure 5-3 shows a close-up view of the tyre response while rolling over the cleat. Tyre models that show good correlation, between the measured and simulated tyre response, in this section are better suited for simulations over uneven terrain. The free response of the tyre is used only to analyse the damping behaviour of the tyre models. Figure 5-3 indicates large differences between the tyre models and these effects will be discussed in more detail in section 5.2.1.
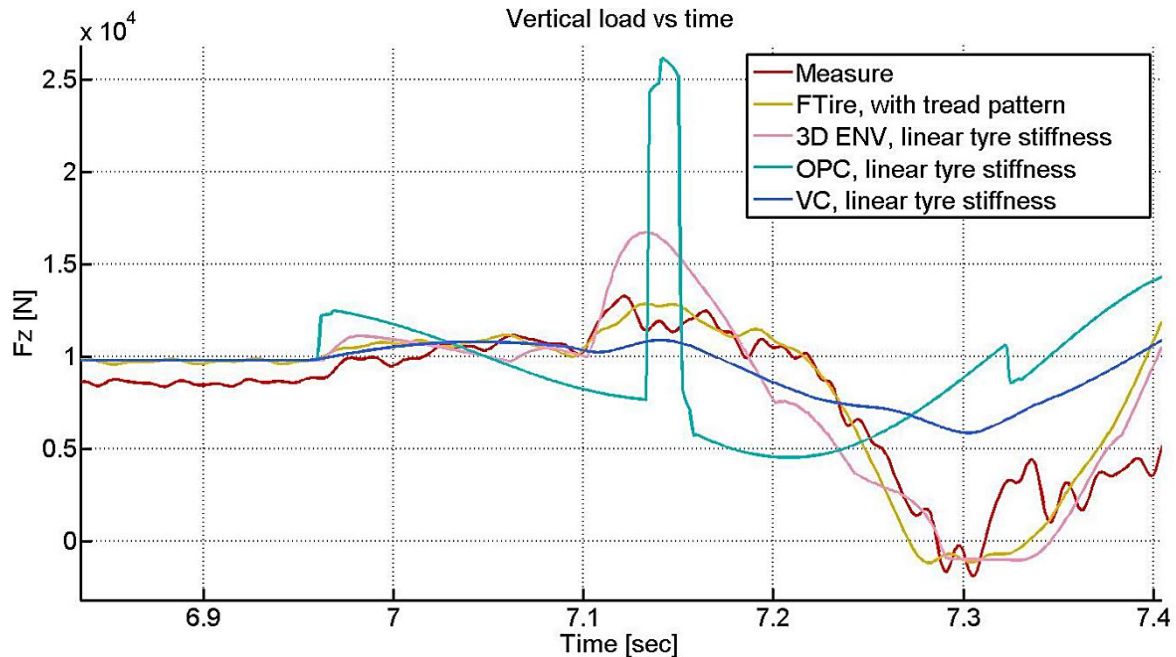
Figure 5-3 Close up on Figure 5-2

5.2.1   50mm Cleat, LC1

The 50 mm dynamic cleat test was chosen as a reference cleat size due to a similar static tyre deflection under load case 1. The 12 and 27km/h tests were used in the parameterization process of FTire.

The validation metrics were first applied to determine the repeatability of the experiments, i.e. to typical measured data as indicated in Figure 5-1. The five criteria mentioned in section 5.2 were applied to multiple measurement data sets to establish a reference for the expected validation measures.

Table 5-1 shows the result of the validation metrics of the expected normal force for different 50mm cleat test runs, at three different speeds. By visual inspection it was seen that the correlation of the two measurement data sets was exceptionally good (see Figure 5-1). This was confirmed by the validation metrics in Table 5-1.

Table 5-1 Validation measures for measured data, 50mm cleat, LC1

	m%RE, Disturbance [%]	80%RE, Disturbance [%]	RMS Error, Disturbance [N]	m%RE, Response [%]	RMS Error, Response [N]
Cleat 50 18km/h	10.4	16.2	1317	10.3	2991
Cleat 50 27km/h	25.1	33.5	3679	7.4	1853
Cleat 50 42km/h	22.9	33.0	4173	14.4	2607

ception.

The m%RE and the 80%RE, while the tyre negotiates the cleat, were calculated to be 10.4% and 16.2%. The RMS Error showed a similar good correlation and was calculated at 1314N. The validation measures for the response section supported the finding with a calculated m%RE of 10.3% and an RMS error of 2991N.

It was also noted that the correlation between two consecutive measurements decreased with an increase in the test velocity. The percentage relative error for tests at 27km/h and 42km/h were of similar magnitudes but the RMS error was slightly higher at a test speed of 42km/h. The correlation of the tyre response after it cleared the cleats was significantly better at a test speed of 27km/h when compared to the other test speed. Overall the correlation between different measurements was very good.

Figures 5-4 to Figure 5-7 show the measured and simulated vertical force response of various tyre models while negotiating a 50mm cleat. The cleat is orientated perpendicular to the direction of travel during these tests. The test trailer is towed at a constant speed of 18km/h and is not loaded with ballast.

Figure 5-4 shows the simulation results when using a One Point Contact model [OPC]. The figure shows a larger force generated by the tyre while the tyre encounters the cleat but a smaller disturbance once the cleat is passed.

This behaviour could be related to the approach used to model the tyre. The tyre was being modeled as a rigid disc which did not allow the model tyre to envelop around the cleat, so called swallowing of the obstacle. The response thus showed similarities to an impulse disturbance.
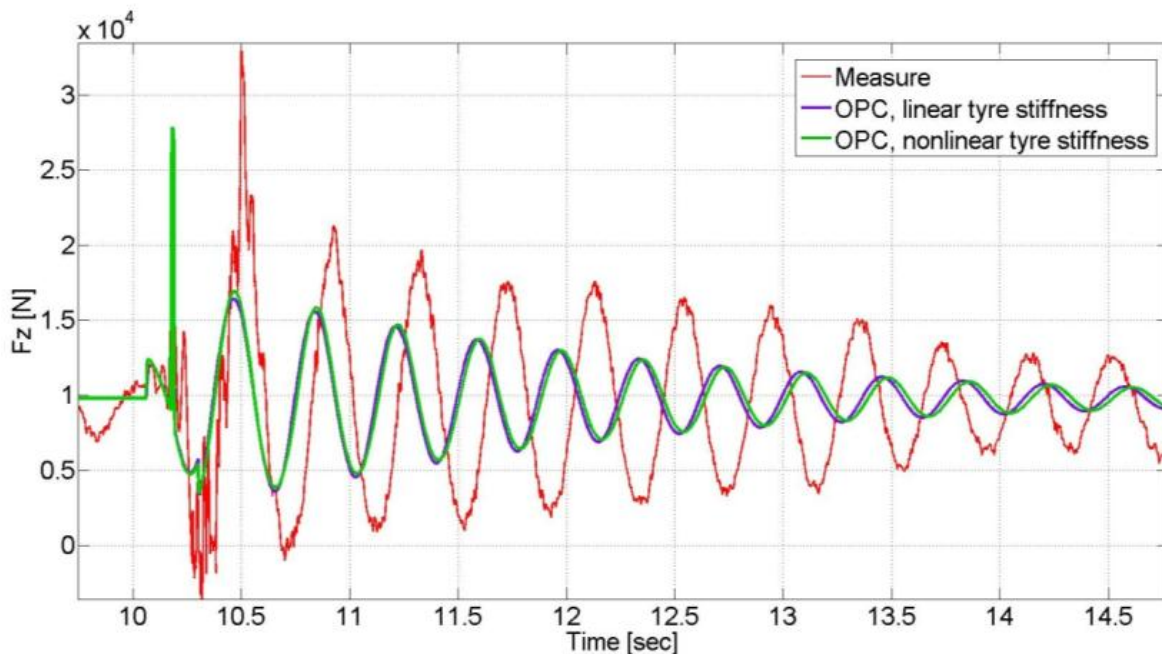
Figure 5-4 OPC simulation result, 50mm cleat, 18km/h, LC1

The figure shows the simulation result using both a linear and nonlinear tyre stiffness description. The difference between the linear and nonlinear tyre behaviours is negligible.

The 3D Equivalent Volume Contact model behaviour while negotiating a 50mm cleat is shown in Figure 5-5. The measured vertical forces do not show the characteristic peak load as was seen when a One Point Contact model was used.

While the behaviour of the tyre model, while negotiating the cleat improved, the later response did not show any noticeable improvements, compared to the One Point Contact model. The difference between the tyre model using constant tyre stiffness and a tyre model using the nonlinear stiffness description was more prominent but did not significantly alter the overall simulation result.

Figure 5-6 shows the simulation results with the 3D Enveloping Contact model. From the figure it can be seen that the modelled tyre damping is representative of the real tyre damping. The nonlinear tyre stiffness results in a slightly better correlation compared to the linear tyre stiffness description.
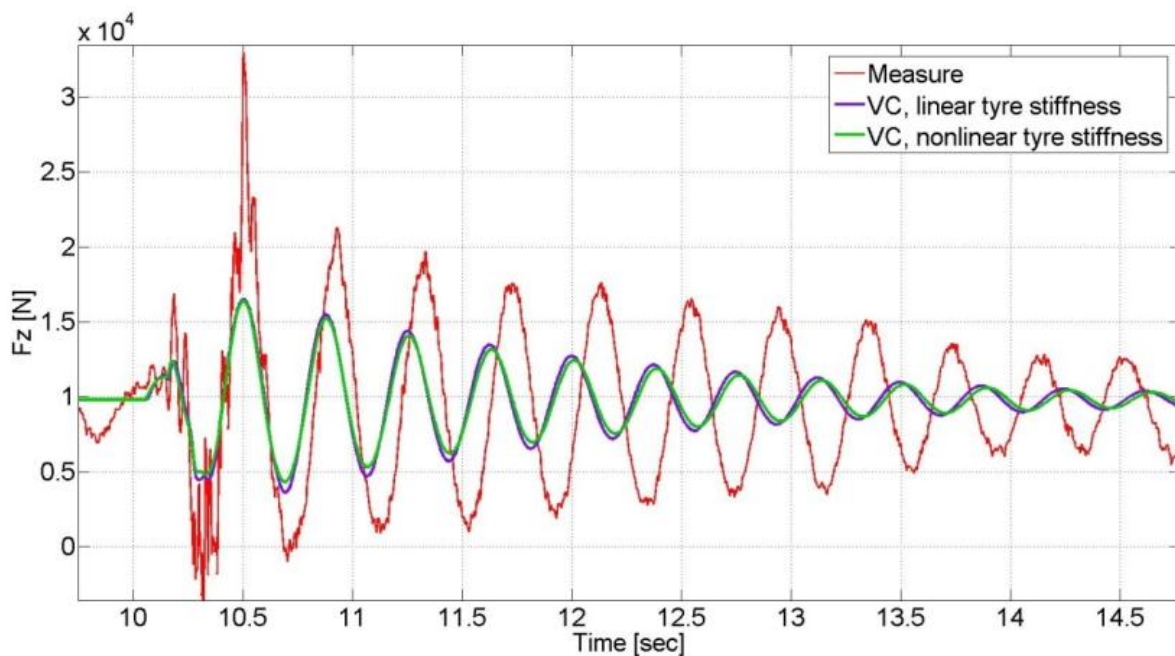
Figure 5-5 VC simulation result, 50mm cleat, 18km/h, LC1

The 3D Enveloping Contact model was developed to improve the tyre model behaviour over cleats by incorporating the lengthening and swallowing effect of a real tyre. The improved results, while negotiating the cleats, also dramatically improved the later response of the simulation.
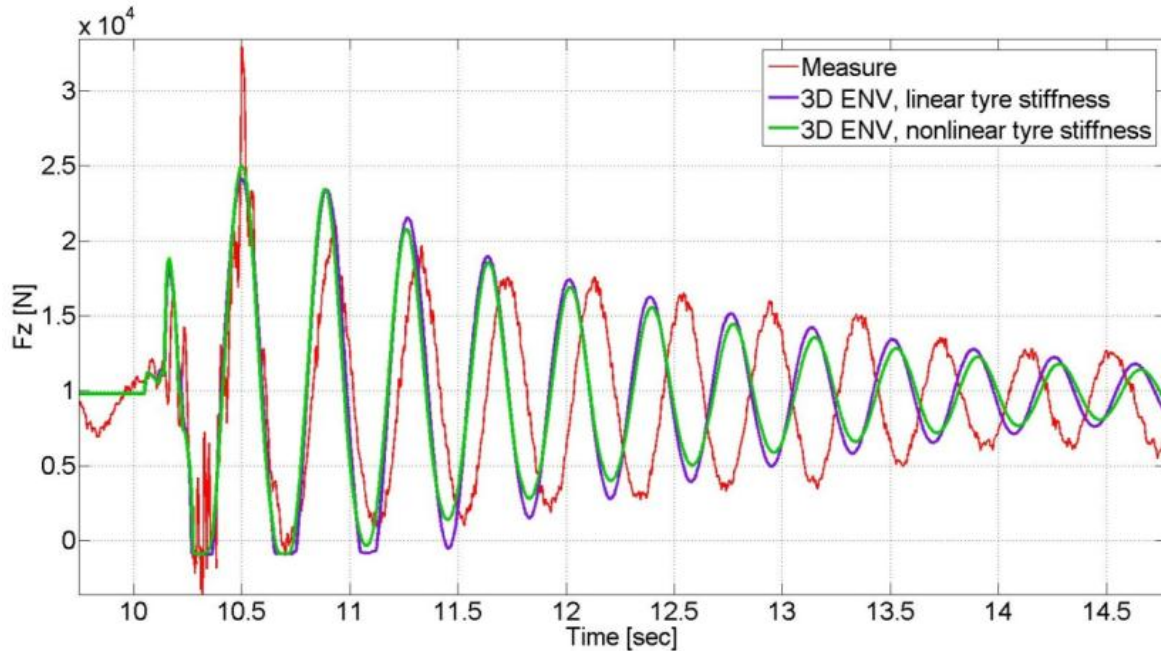
Figure 5-6 3D ENV simulation result, 50mm cleat, 18km/h, LC1

Figure 5-7 shows the simulation results when the FTire tyre model is used for a simulation over the 50mm cleat.
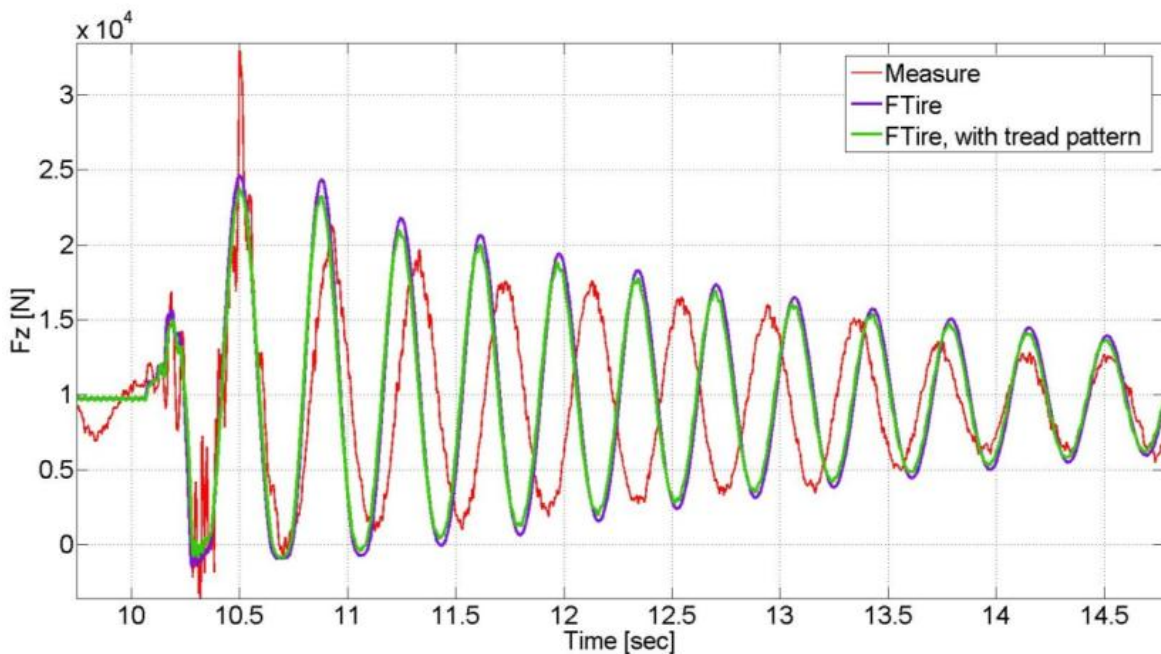
Figure 5-7 FTire simulation result, 50mm cleat, 18km/h, LC1

The FTire model replicated the measured tyre behaviour the most accurately. The response after the tyre negotiated the cleat was similar to the simulation results when a 3D Enveloping Contact model was used.

The simulation results also indicated that the tread pattern had a small effect on the simulation outcome. To evaluate the ability of the tyre models to mimic the behaviour of the test tyre the five validation metrics were calculated.

Table 5-2 shows the validation metric of the simulation results over a 50 mm cleat at a speed of 12km/h. To simplify the comparison the fields in the table were colour coded. Green indicates the best results, orange the second best results and the third best results are indicated in red. The FTire model, where the contact nodes are arranged according to the tread pattern, shows the best result for every disturbance validation metric. The FTire model, with equally spaced contact nodes, shows a marginally inferior correlation between the measurement and the simulation results. The FTire models are followed in accuracy by the volume contact models.

These measurements are an indication of the overall error but lacks the ability to give a measurement of the correct tyre behaviour. They indicated that the 3D Enveloping Contact models showed a worse performance, while negotiating the cleats, compared to the 3D Equivalent Volume Contact model. The response after the tyre negotiated the cleats was better represented with the 3D Enveloping Contact models. The 3D Enveloping Contact model with nonlinear tyre stiffness had a m%RE of 6% while the best volume contact tyre model produces an error of 34.2%. The worst model was the one point contact model.

Table 5-2 Validation metrics for tyre models, 50mm cleat, 12km/h, LC1

Cleat 50 12km/h	m%RE, Disturbance [%]	80%RE, Disturbance [%]	RMS Error, Disturbance [N]	m%RE, Response [%]	RMS Error, Response [N]
FTire	7	11	871	13	2658
FTire, TP	6	10	752	10	2256
OPC, lk	37	53	4624	35	8410
OPC, nlk	35	54	4961	32	7791
3D VC, lk	7	11	1050	34	9279
3D VC, nlk	9	16	1215	38	10490
3D ENV, lk	12	18	1775	21	7372
3D ENV, nlk	14	22	2023	6	1584
Measured	No data available				

Table 5-3 summarizes the validation metrics for the simulation results over a 50mm cleat at 18km/h as show in Figure 5-4 to Figure 5-7.

With an increase in test velocity the correlation between the measured results and the simulation results decreased for all tyre models except for the One Point Contact tyre model. The effect of an increase in the correlation error, with an increase in the test velocity, had also been present in the measured results shown in Table 5-1.

Table 5-3 Validation metrics for tyre models, 50mm cleat, 18km/h, LC1

Cleat 50 18km/h	m%RE, Disturbance [%]	80%RE, Disturbance [%]	RMS Error, Disturbance [N]	m%RE, Response [%]	RMS Error, Response [N]
FTire	16	20	2311	14	3483
FTire, TP	14	18	1974	11	3429
OPC, lk	19	39	3560	28	7175
OPC, nlk	20	40	3861	28	6992
3D VC, lk	14	21	1953	29	7278
3D VC, nlk	13	23	2023	31	7464
3D ENV, lk	19	40	3120	8	3160
3D ENV, nlk	19	35	3304	9	2842
Measured	10.4	16.2	1317	10.3	2991

Comparison between different measured result sets show a m%RE, between runs over the cleats, of 10.4%, a 80%RE of 16.2% and a RMS error of 1317N. The m%RE and the RMS error of the response is 10.3% and 2991N respectively. The FTire model and the 3D Enveloping Contact tyre models showed only marginally larger errors then the repeatability of the tests. The volume contact modes show a good accuracy over the cleats but the response after the model negotiated the cleat showed the biggest discrepancies between the measured results and the simulation results. The 3D Equivalent Volume Contact did not capture the characteristic tyre behaviour while negotiating the cleat but rather produced a result that has the lowest error.
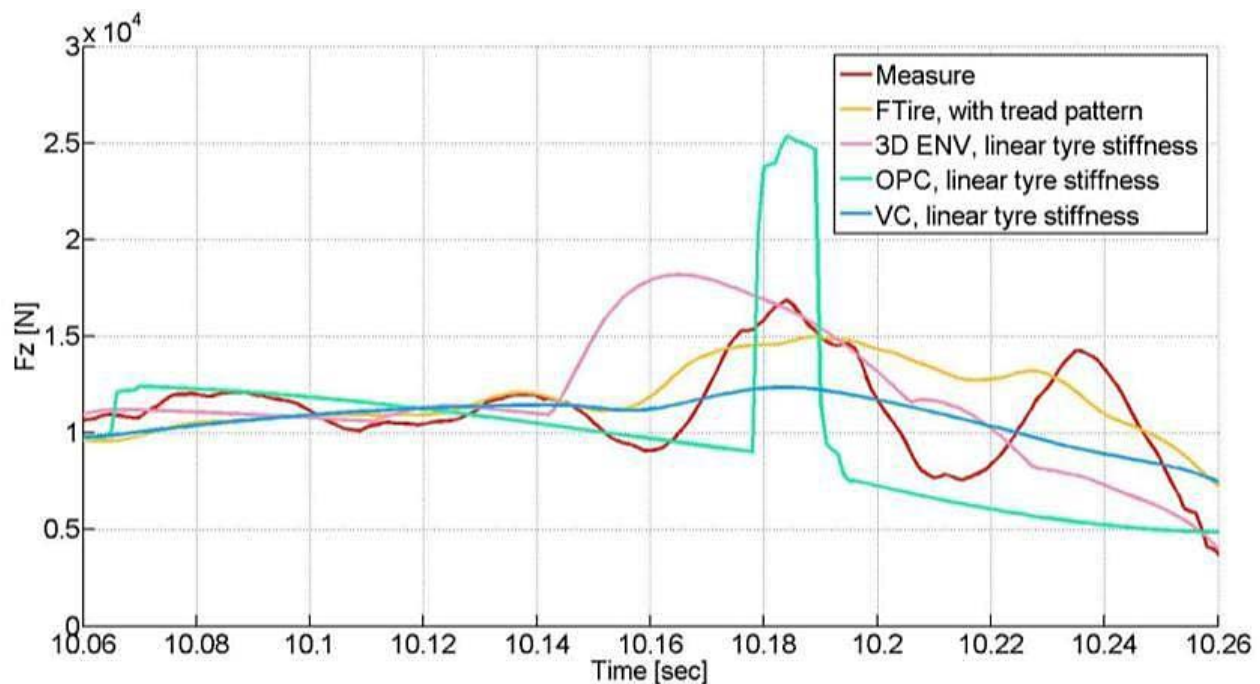
Figure 5-8 Simulation results of a 50mm cleat test, 18km/h, LC1

Figure 5-8 shows the measured and simulated tyre response while negotiating the obstacle. The FTire model captures the tyre behaviour most accurately. It captures the peak loads yet lacks the ability to match the normal force magnitudes of the troughs.

Figure 5-9 shows the percentage relative error of the simulation results. From the figure it is clear that the largest discrepancy between the measured results and the simulation results using a FTire tyre model, is occurring in the trough's. The 3D Equivalent Volume Contact model does not capture the tyre behaviour and cannot match the peaks or trough's but rather shows a highly filtered response. This behaviour leads to a misleading interpretation of the validation matrix results.

It was difficult to find an appropriate measure to quantifiably describe the accuracy of the tyre model while negotiating the cleats. Comparing the m%RE and RMS error of the tyre response after negotiating the cleat resulted in a better accuracy metric.
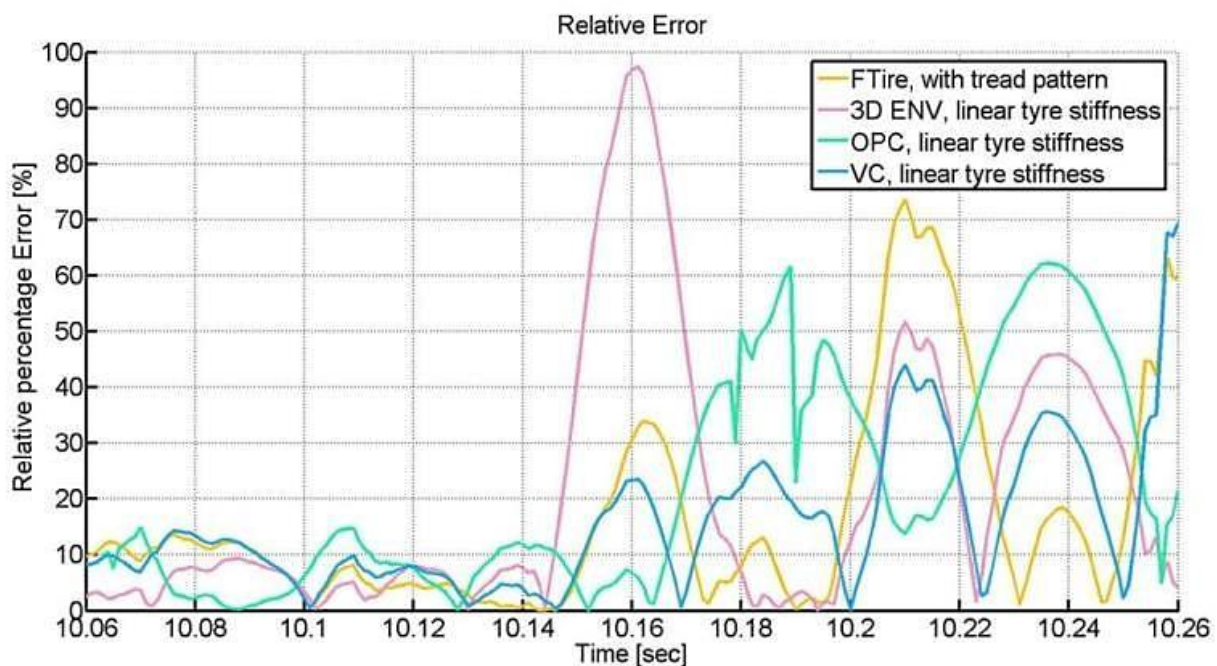
Figure 5-9 Relative percentage error of 50mm cleat simulation, 18km/h, LC1

The correlation between the measured results and simulation results decreased further when the test velocity was increased to 42 km/h (Table 5-4). The error range between the tyre models decreased so that the tyre models give similar results. The 3D enveloping tyre model produced the most promising results and had similar correlation metric results as the correlation between two different measurements. The FTire showed good performance while negotiating the cleat but relatively poor results after the disturbance.

Table 5-4 Validation metrics for tyre models, 50mm cleat, 42km/h, LC1

Cleat 50 42km/h	m%RE, Disturbance [%]	80%RE, Disturbance [%]	RMS Error, Disturbance [N]	m%RE, Response [%]	RMS Error, Response [N]
FTire	22	28	3873	17	2657
FTire, TP	22	26	3792	19	2863
OPC, lk	20	36	4711	15	2159
OPC, nlk	20	36	4744	15	2149
3D VC, lk	21	36	5007	14	2033
3D VC, nlk	21	36	5023	15	2121
3D ENV, lk	20	25	3375	9	1890
3D ENV, nlk	17	23	2902	12	2284
Measured	22.9	33.0	4173	14.4	2607

5.2.2   50mm Oblique Cleat, LC2

The validation matrix for a 50mm cleat test orientated at a 45 degree angle is shown in Table 5-5. Cleat tests orientated at an angle offer a challenge for tyre models as the model needs to interpret the road surface in three dimensions. The FTire model and the 3D Enveloping Contact model were able to predict similar forces as were established during the experimental tests. The One Point Contact and the 3D Equivalent Volume Contact model could not reproduce the measured results.

Table 5-5 Validation metrics for tyre models, 50mm cleat oblique, 12km/h, LC2

Cleat 50 oblique 12km/h, LC2	m%RE, Disturbance [%]	80%RE, Disturbance [%]	RMS Error, Disturbance [N]	m%RE, Response [%]	RMS Error, Response [N]
FTire	7	13	3793	17	7982
FTire, TP	8	15	4093	18	8756
OPC, lk	19	30	7497	38	19340
OPC, nlk	21	26	9472	31	14320
3D VC, lk	10	20	4841	34	19870
3D VC, nlk	9	19	4760	32	17740
3D ENV, lk	7	14	3664	24	11840
3D ENV, nlk	6	11	3315	20	9369
Measured	No data available				

The modelling approach of the One Point tyre model only allowed the road input to be in two dimensions while the other tyre models used the 3D road profile. Due to this constraint the One Point Contact showed the biggest error while the 3D Enveloping Contact models and the FTire tyre models showed good results.

5.2.3   76mm Cleat , LC1

Table 5-6 shows the correlation between measurements over a 76mm cleat at various test speeds. Repeatability of the test is very good at 12km/h and at 42km/h. The results of measurements at 27km/h show a relatively bad correlation. Investigations into the measured data have shown that this is due to the run up phase of the test.

The longitudinal acceleration of the test trailer was not constant which resulted in unwanted oscillations of the test trailer. This effect was noticed with various other tests, especially at test speeds higher than 20km/h. The test results with the irregular trailer acceleration were disregarded in the validation process.

Table 5-6 Validation metrics for measured data, 76mm cleat, LC1

	m%RE, Disturbance [%]	80%RE, Disturbance [%]	RMS Error, Disturbance [N]	m%RE, Response [%]	RMS Error, Response [N]
Cleat 76 12km/h	8	8	1187	7.0	4636
Cleat 76 27km/h	24	37	5666	17.8	16490
Cleat 76 42km/h	18	25	3985	6.0	1107

Table 5-7 and Table 5-8 show the validation metric of the validation tests over a 76mm cleat with a test speed of 12km/h and 27km/h respectively. In both cases the performance of the FTire model is best and shows the lowest errors. The m%RE is around 10% at 12km/h and around 20% at 27km/h. The 3D Enveloping Contact models perform equally well at both speeds and show a m%RE of 20%. The results of the 3D Equivalent Volume Contact model while negotiating the cleat is found again in the 76mm cleat test. The response error metrics show that the contact model cannot be used to accurately describe the tyre response.

Table 5-7 Validation measures for tyre models, 76mm cleat, 12km/h, LC1

Cleat 76 12km/h,LC1	m%RE, Disturbance [%]	80%RE, Disturbance [%]	RMS Error, Disturbance [N]	m%RE, Response [%]	RMS Error, Response [N]
FTire	12	20	1653	11	3475
FTire, TP	10	17	1444	10	3629
OPC, lk	37	58	6353	38	13590
OPC, nlk	40	57	7625	32	11270
3D VC, lk	10	14	1284	30	13040
3D VC, nlk	10	16	1364	41	15670
3D ENV, lk	18	35	3120	10	39960
3D ENV, nlk	21	25	3658	11	3729
Measured	8	12	1187	7.0	4636

Table 5-8 Validation metrics for tyre models, 76mm cleat, 27km/h, LC1

Cleat 76 27km/h,LC1	m%RE, Disturbance [%]	80%RE, Disturbance [%]	RMS Error, Disturbance [N]	m%RE, Response [%]	RMS Error, Response [N]
FTire	20	32	3639	16	5538
FTire, TP	19	28	3385	15	5832
OPC, lk	31	52	7053	33	11090
OPC, nlk	42	53	9478	33	10660
3D VC, lk	16	25	3137	31	10390
3D VC, nlk	15	22	3098	32	10570
3D ENV, lk	20	33	3908	13	6550
3D ENV, nlk	21	32	4150	12	5821
Measured	24	37	5666	17.8	16490

5.2.4   100 mm Cleat oblique, LC1

Table 5-9 shows the validation metrics for oblique 100mm cleat test. The table shows the error metrics for simulations with a test speed of 12km/h. The FTire models were the only models that show acceptable results. The FTire model shows the best results at both test speeds.

Table 5-9 Validation metrics for tyre models, 100mm cleat oblique, 12km/h, LC1

Cleat 100 oblique 12km/h, LC1	m%RE, Disturbance [%]	80%RE, Disturbance [%]	RMS Error, Disturbance [N]	m%RE, Response [%]	RMS Error, Response [N]
FTire	9	14	1644	28	10130
FTire, TP	8	14	1590	28	10260
OPC, lk	62	113	11970	45	18050
OPC, nlk	74	122	15710	38	17110
3D VC, lk	11	15	1843	38	15010
3D VC, nlk	11	17	2002	37	13950
3D ENV, lk	11	15	1950	43	16130
3D ENV, nlk	11	17	2030	41	15200
Measured	No data available				

5.2.5   Trapezoidal Bump

Figure 5-10 shows the measured and simulation results while the trailer negotiates the 150mm trapezoidal bump. The FTire model reproduces the measured results most accurately. The 3D Equivalent Volume Contact model also shows an acceptable behaviour.
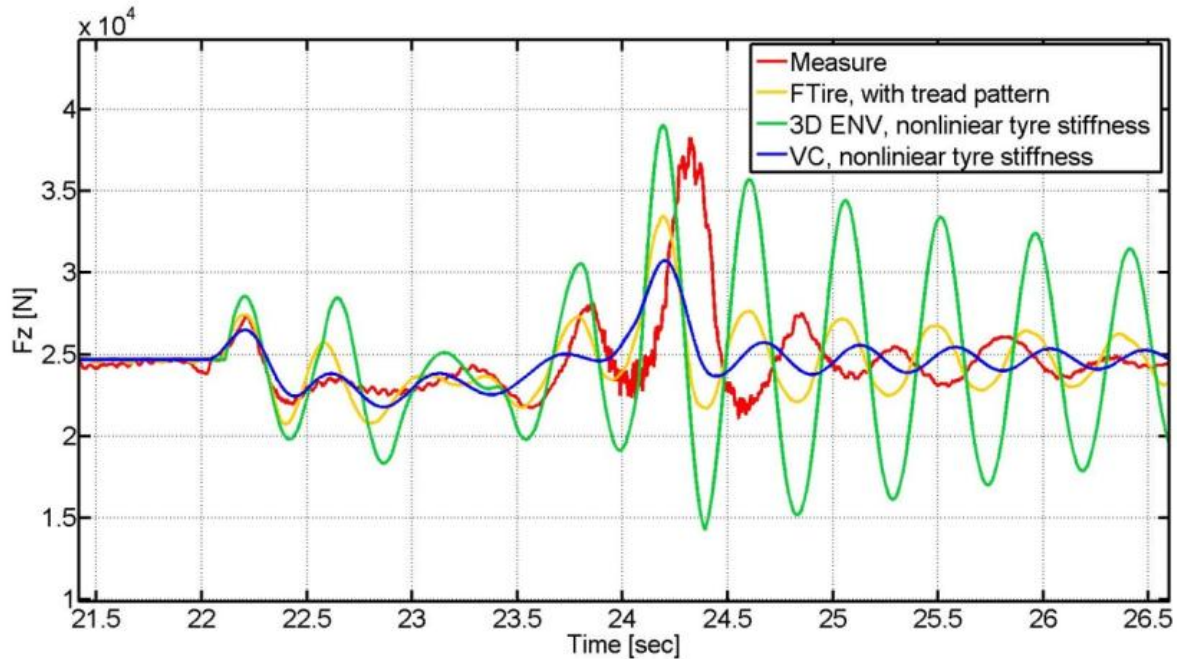
Figure 5-10 Simulation results of a 150mm trapezoidal bump, 3km/h, LC2

Table 5-10 shows the validation metrics for the test. The table confirms that the FTire model shows the best correlation.

Table 5-10 Validation metrics for tyre models, 150mm trapezoidal bump, 3km/h, LC2

Cleat 100 oblique 12km/h, LC1	m%RE, Disturbance [%]	80%RE, Disturbance [%]	RMS Error, Disturbance [N]	m%RE, Response [%]	RMS Error, Response [N]
FTire, TP	4	6	1113	26	8380
OPC, nlk	25	40	7187	38	11770
3D VC, nlk	4	6	1127	35	9290
3D ENV, nlk	8	14	2307	33	10014
Measured	No data available				

5.3   Hard Terrain

A mathematical tyre model should be capable of describing the tyre forces over individual discrete obstacles and over an uneven road to be meaningful. These test surfaces range from smooth roads with potholes to rough off-road terrain.

In this section the tyre model behaviour over different test tracks at the Gerotek Test Facility will be discussed. The test tracks are discussed in chapter 3 and include the Belgian paving, Fatigue track and the Corrugation tracks. The profiled tracks are shown in Figure 3-24.

Comparing measured and simulation results to determine whether the model can accurately describe the tyre forces while rolling over the test tracks, is challenging. The results of a Belgian paving test, at a test velocity of 5km/h, is shown in Figure 3-26.

Typical simulation results are indicated in Figure 5-11. The direct time domain comparison is problematic as a small change in the tyre path during the simulation could result in a different input condition. m%RE and RMSE accuracy metrics also failed. The only conclusion that can be made from Figure 5-11 is that the 3D Enveloping Contact model gives unacceptable results.
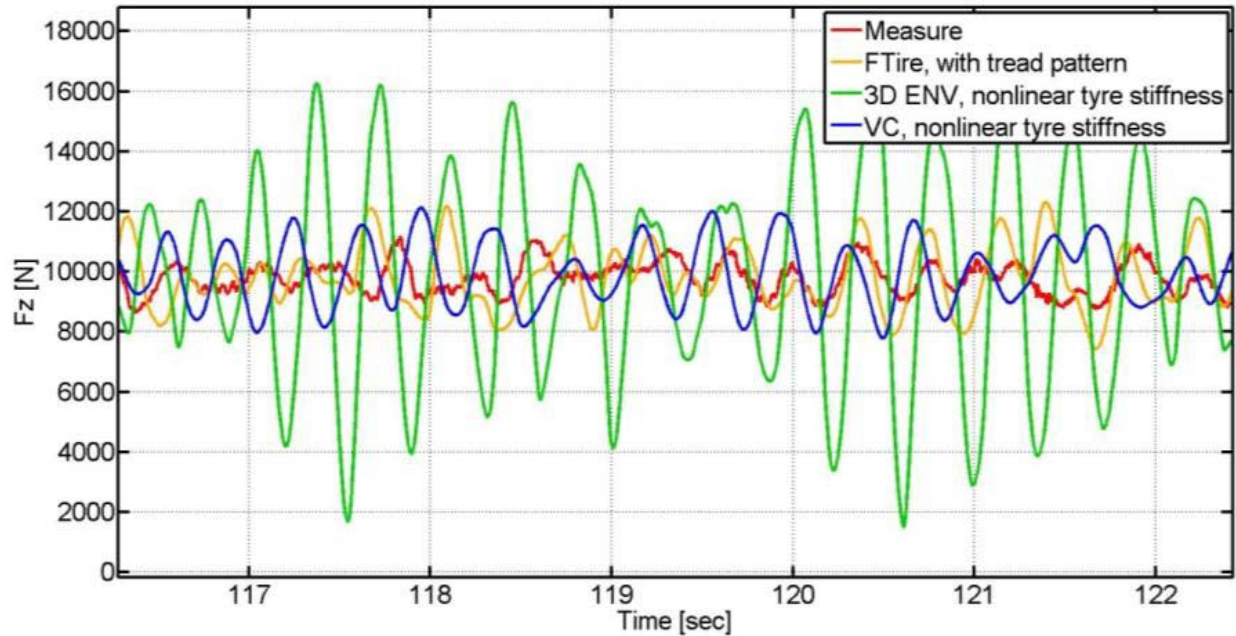
Figure 5-11 Simulation results of the Belgian paving test track, LC1, 3km/h

The results were therefore analysed using the probability theorem rather than applying a time domain comparison. The probability that a load case was found in a data set was calculated.

The normal distribution, also known as a Gaussian distribution, is a continuous probability function that is often used is statistics for real-valued random variables whose distributions are not known.

Figure 5-12 shows the scaled normal distribution fit of the measured normal force during a Belgian paving test. The fit shows a good representation of the measured data and equally good results were found for many simulation results.

Figure 5-12 Normal distribution fit to measured Belgium paving test, LC1, 3km/h

The normal probability function is given by:

$$f(x) = \frac{1}{\sigma\sqrt{2\pi}} e^{-\frac{(x-\mu)^2}{2\sigma^2}} \qquad (5.3)$$

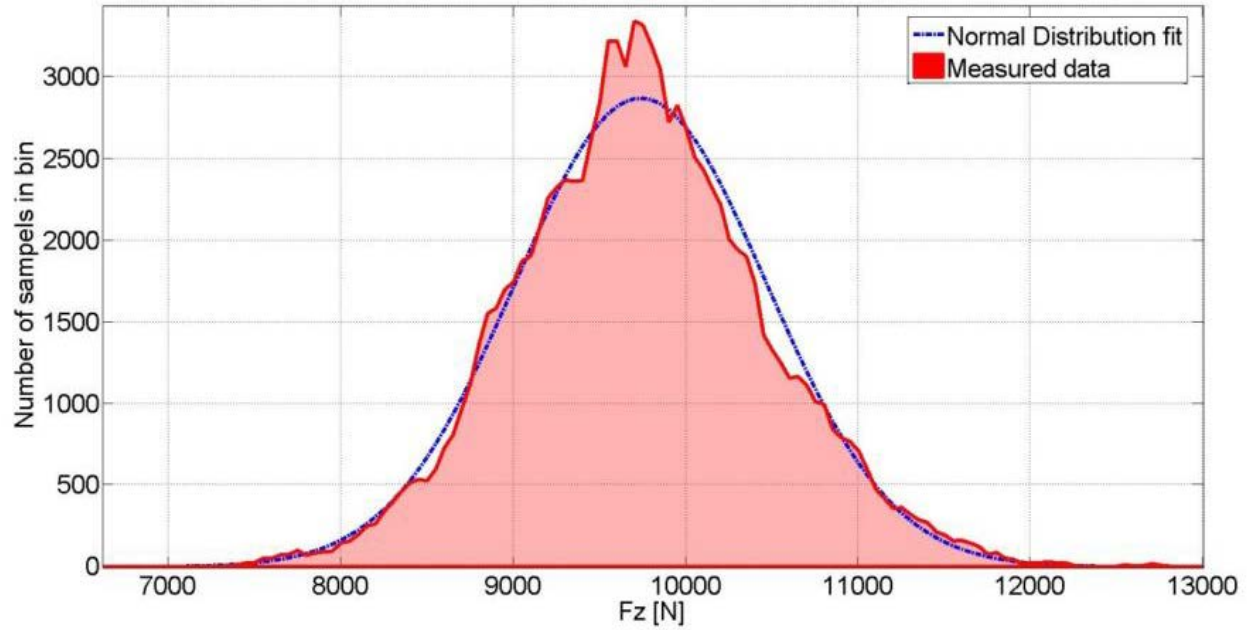The parameter μ is the mean of the distribution. The parameter σ is the standard deviation and the variance of the data set is given by σ^2. The behaviour of the dataset can then be described with only two parameters, mean and standard deviation. These parameters can then be used to compare the simulation results with the measured data.

The percentage error, of the standard deviation and the variance, for the measured and the predicted values were calculated using Equation 5.4.

$$\%E = \left(\frac{p-m}{m}\right) \times 100 \qquad (5.4)$$

The mean values of the measured and simulation results were similar to the static load. A large difference would be found when the ratio of ground contact loss differed between the simulation and the actual test. It could also have indicated different damping behaviours.

The standard deviations of the data sets held more information about the accuracy of the tyre model. This effect was illustrated in Figure 5-11.

 Figure 5-13 shows a hypothetical normal distribution of a reference system and two models. The data sets in the figure have the same mean but different standard deviations. The standard deviation is the smallest for Model 1 data set and the largest for the Model 2 data. If the probability density function represents the normal force while driving over uneven terrain, the time domain response of Model 1

shows a smaller normal force response than the normal force response of the reference model. Similarly the response of Model 2 would show a larger oscillatory response than the reference model.
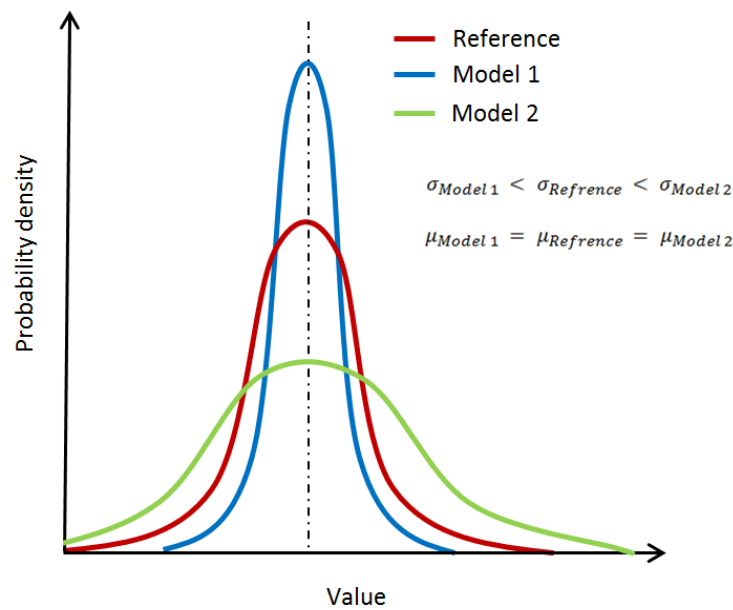

Figure 5-13 Hypothetical probability density

The linear and non-linear description of the tyre stiffness did not have a significant effect on the accuracy of the simulation results, as shown in the simulation results of the cleat tests. The same was shown for simulations over test tracks. In many cases it was found that the nonlinear tyre stiffness description had resulted in a slightly better accuracy.

The following sections only discussed tyre models with nonlinear tyre stiffness. The FTire model, where the tread pattern is accounted for, showed largely the same results as the model where the contact nodes are arranged equally. It showed a higher frequency content, similar to the measured test data, and was thus discussed in the following sections.

5.3.1 Belgian paving

The Belgian block paving is used to evaluate the ride comfort of vehicles. The road surface incorporates unevenness over a wide range of the spatial frequencies, from the uneven block itself to unevenness that has a spatial frequency of a few meters.

A section of the time domain response was shown in Figure 5-11. From the figure it can be seen that no tyre model is able to capture the higher frequency response as is present in the measured data.

Figure 5-14 shows the normal load probability density to determine whether the tyre models are able to predict the response over the multifaceted surface. The probability densities show great resemblance with a normal distribution. This is proven by the good normal distribution fit.
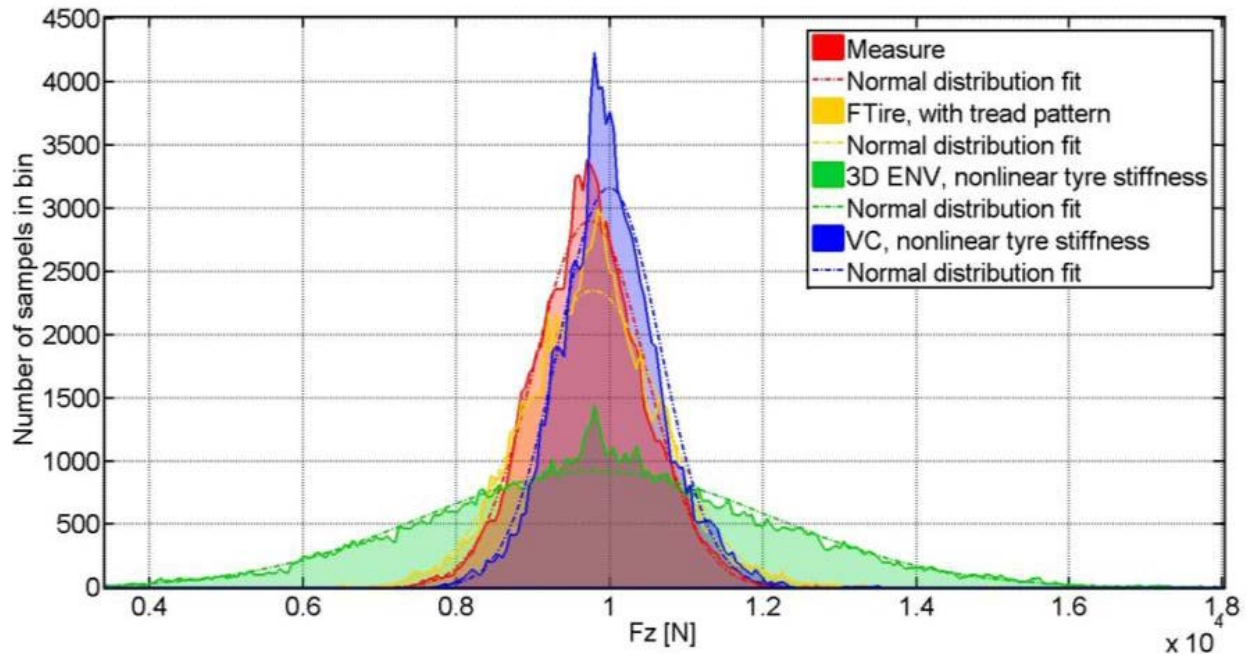
Figure 5-14 Normal load probability density of the Belgian paving test, LC 1, 3km/h

Fitting the data with a normal distribution simplified the comparison and evaluation of the tyre models. The parameters of the normal distributions of the normal loads for various tyre models are shown in Table 5-11. From the Figure 5-14 and Table 5-11 it was clear that the 3D Enveloping and the One Point Contact models could not accurately predict the normal tyre forces, and was thus omitted from the comparison. The FTire model and the 3D Equivalent Volume Contact model showed an improved accuracy.

Table 5-11 Normal distribution parameters for the Belgian paving test, LC1

	Load case 1			
	3km/h		18km/h	
	Mean percentage error, μ%err [%]	Standard deviation percentage error, σ%err [%]	Mean percentage error, μ%err [%]	Standard deviation percentage error, σ%err [%]
FTire, TP	0	24	2	48
3D ENV, nlk	1	215	3	37
OPC, nlk	1	875	4	68
VC, nlk	2	-8	5	28

The normal load, as calculated by the 3D Equivalent Volume Contact, had a lower standard deviation compared to the measured normal load and a slightly higher mean. This indicated that the normal force would be concentrated more around the mean than the measured normal Force. The simulation results

with the FTire model showed a higher standard deviation with a similar mean. Through visual inspection it was found that the FTire model approximated the normal force slightly better than the 3D Equivalent Volume Contact tyre model.

With an increase in test velocity the performance of the 3D Enveloping Contact tyre model improved. A similar behaviour was seen for the test results with an increased static load and those over different test surfaces. The accuracy of the contact model was thus speed dependent. It is not known if the accuracy of the model would further increase with an increase in velocity as no measured results could be obtained at higher speeds. At a velocity higher than 20km/h uncontrolled oscillations of the tyre test trailer resulted. The accuracy dependency of the test velocity was however unwanted and limited the range of application of the model.

At a test speed of 18km/h the 3D Equivalent Volume Contact model showed better performance than the FTire model when the normal distribution fits were compared. When the measurements were compared in the time domain, the forces predicted by FTire model showed greater resemblance to the measured results. The force probability distribution of the simulation results of the 3D Equivalent Volume Contact, One Point Contact and the 3D Enveloping Contact model could not be fitted accurately with a normal distribution. Similar to the normal force probability distribution of the LC2 simulation results, shown in Figure 5-15, the distribution showed an increased probability around the mean. This behaviour was however not captured by the normal distribution fit.

Table 5-12 Normal distribution parameters for the Belgian paving test, LC2

	Load case 2			
	3km/h		11km/h	
	Mean percentage error, μ%err [%]	Standard deviation percentage error, σ%err [%]	Mean percentage error, μ%err [%]	Standard deviation percentage error, σ%err [%]
FTire, TP	0	15	-8	6
3D ENV, nlk	0	109	-8	-9
OPC, nlk	1	534	-8	49
VC, nlk	1	-34	-7	9

When the static tyre load on the test tyre was increased, the correlation between the measured results and the predicted results was decreased for all tyre models except the FTire model. The accuracy dependency on the test velocity of the 3D Equivalent Volume Contact tyre model was especially noticeable with an increase in the static load. The tyre model predicted a smaller deviation around the mean at lower speeds and a higher deviation when the test speed is increased to 11km/h.

The simulation results of the One Point Contact, 3D Equivalent Volume Contact and the 3D Enveloping Contact model could not be fitted accurately with a normal distribution at a test speed of 11km/h.

Figure 5-15 shows the probability distribution of the generated tyre normal force for the test. It is clear that the simulation results do not show a normal distribution behaviour. The FTire model and the measured results do approximate a normal distribution with an acceptable accuracy.
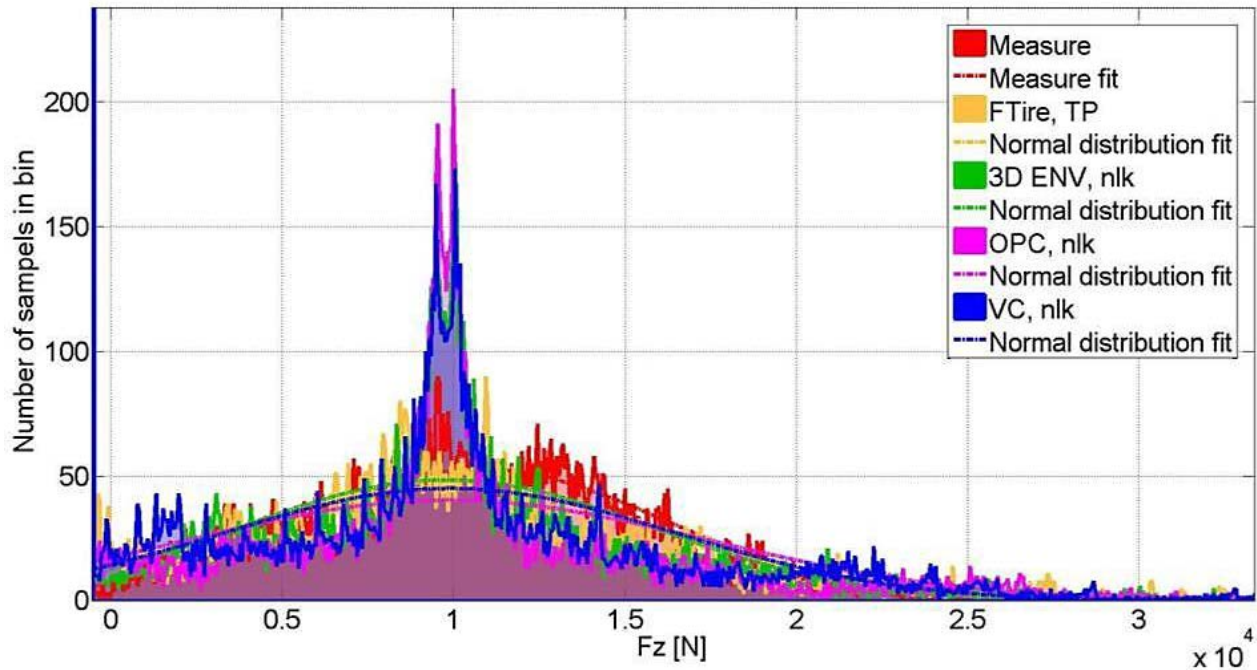

Figure 5-15 Normal load probability density of the Belgium paving test, LC 2, 11km/h

5.3.2   Fatigue track

Accurately predicting the forces generated in the tyre contact patch, while the tyre was rolling over the fatigue test track, was found to be a challenge. The forces, as predicted by all the tyre models, resulted in a rougher ride than was found during the field test with a test speed of 3km/h. The ride was a lot smoother during the 18km/h test. The accuracy of the tyre models increased during the load case two test. The reason for the extremely poor performance of the tyre models at lower speeds could not be determined but should be investigated. The validation metrics for load case 1 and 2 are listed in table Table 5-13 and Table 5-14.

Once again it was found that the FTire model performed better than all other tyre models. When the time domain results of the fatigue track test were analysed it was found that measured data showed single peak loads. A similar response was only found in the simulation results when a FTire model was used. The 3D Equivalent Volume Contact model filtered the road input in such a way that the statistical behaviour was similar to the measured results but was unable to reproduce the peak loads.

Table 5-13 Normal distribution parameters for the Fatigue track test, LC1

	Load case 1			
	3km/h		18km/h	
	Mean percentage error, μ%err	Standard deviation percentage error, σ%err	Mean percentage error, μ%err	Standard deviation percentage error, σ%err
FTire, TP	1	300	3	-48
3D ENV, nlk	1	1475	3	-59
OPC, nlk	1	1708	4	-30
VC, nlk	2	273	4	-65

Table 5-14 Normal distribution parameters for the Fatigue track test, LC2

	Load case 2			
	3km/h		11km/h	
	Mean percentage error, μ%err [%]	Standard deviation percentage error, σ%err [%]	Mean percentage error, μ%err [%]	Standard deviation percentage error, σ%err [%]
FTire, TP	0	23	-7	-4
3D ENV, nlk	1	160	-7	-21
OPC, nlk	1	224	-7	9
VC, nlk	1	-26	-7	-6

The measured time domain response of the fatigue track test and the predicted simulation results, using a 3D Equivalent Volume Contact and FTire tyre model, are shown in Figure 5-16. The peak loads are statistically not relevant but are extremely important for the outcome of the test. Tests surpassing the fatigue life of a vehicle and the peak loads will influence the outcome. To replace the physical tests with simulations it is required that the tyre models are capable of reproducing these peak loads.
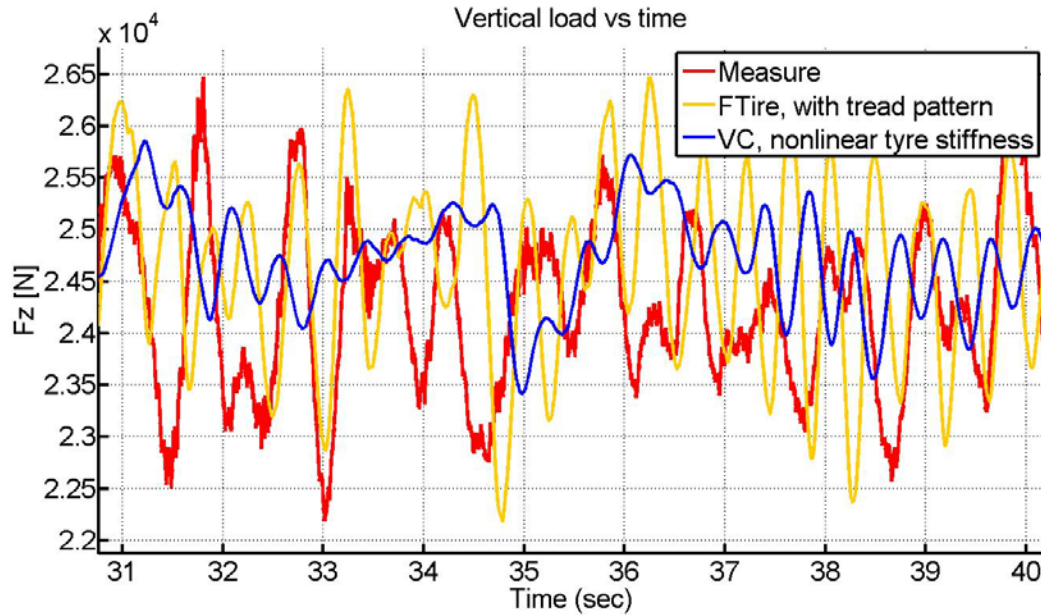
Figure 5-16 Measured and predicted vertical force over the Fatigue track, LC2, 3km/h

5.3.3   Corrugations

The corrugation test tracks were used to simulate driving manoeuvres on dirt roads that developed a series of regular bumps with short spacing on the road surface. The measured and predicted tyre forces did not conform to a normal distribution in many cases as is shown in Figure 5-17. The comparison of the different tyre models could thus not be evaluated using statistical parameters. Due to the regularly repeating obstacle it was however possible to compare the tyre models using the time domain response.

It was anticipated that the 3D Enveloping Contact model would be capable of accurately predicting the normal forces in simulations over the test track. The normal force probability density, shown in Figure 5-17, indicates that the model does not behave like the test results of the real test tyre.
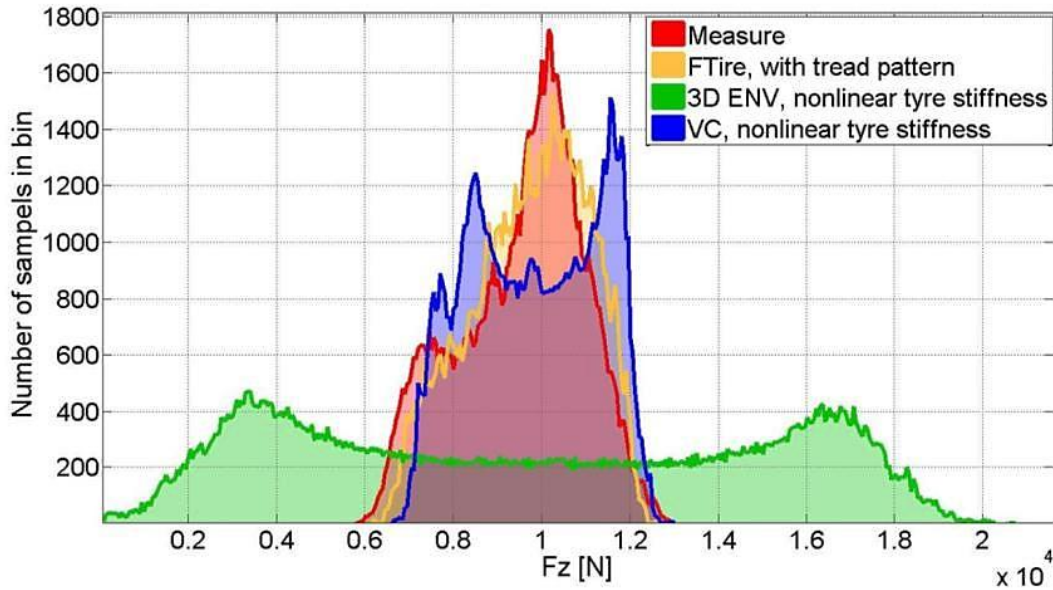
Figure 5-17 Normal load probability density of the Parallel corrugation test, LC 1, 3km/h

The time domain response of the tyre models and the results are shown in Figure 5-18. The figure clearly shows that the enveloping contact model is not capable of predicting the tyre forces. The predicted normal force of the One Point Contact model has a similar response to the 3D Enveloping Contact model but has an even larger amplitude.
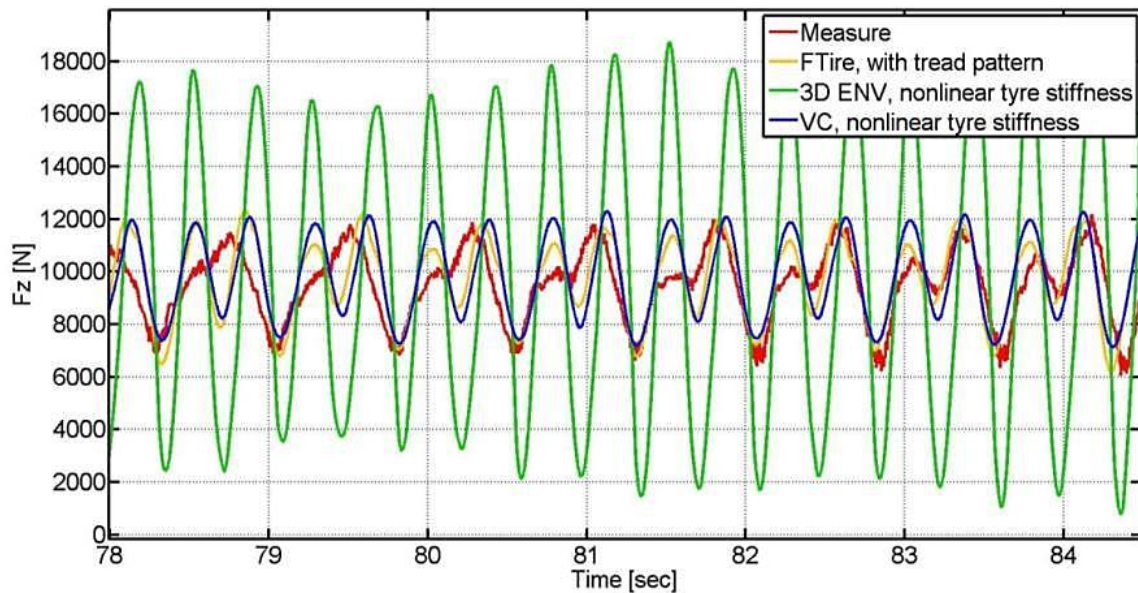

Figure 5-18 Measured and predicted normal load of the Parallel corrugation test, LC 1, 3km/h

A detailed view of the normal tyre forces is shown in Figure 5-19. The 3D Equivalent Volume Contact predicts the tyre forces fairly well, yet the FTire model is slightly better. The extremes of the forces are better represented with the FTire model.
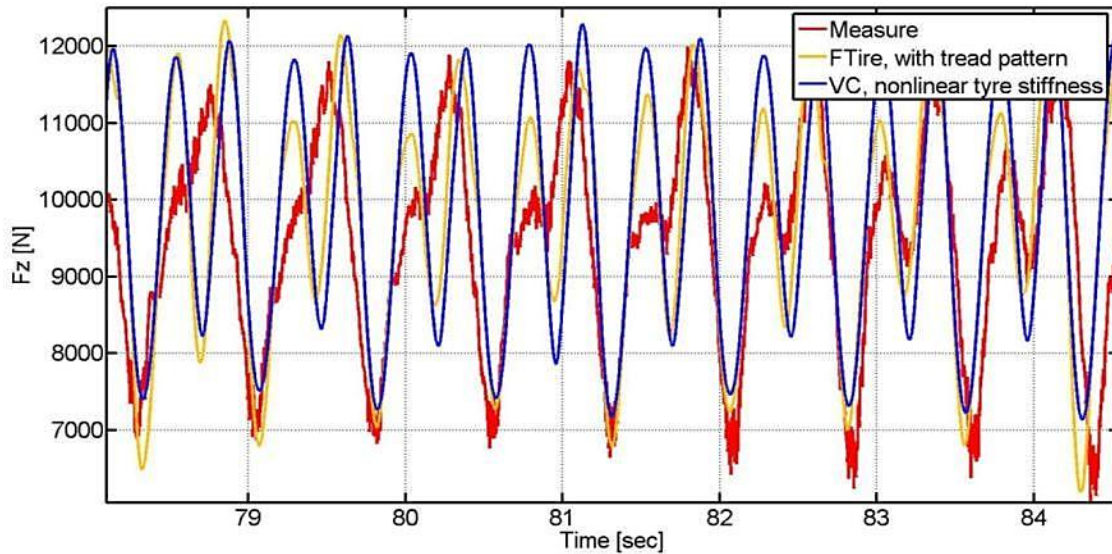
Figure 5-19 Measured and predicted normal load of the Parallel corrugation test detail, LC 1, 3km/h

To determine whether the models are able to predict the longitudinal forces that are generated when the tyre is negotiating the bumps, the measured and predicted longitudinal forces are plotted. The results are shown in Figure 5-20. It can be seen that the FTire model shows the greatest correlation between the measured and predicted forces. The 3D Enveloping and 3D Equivalent Volume Contact models predict the longitudinal force with equal magnitudes.
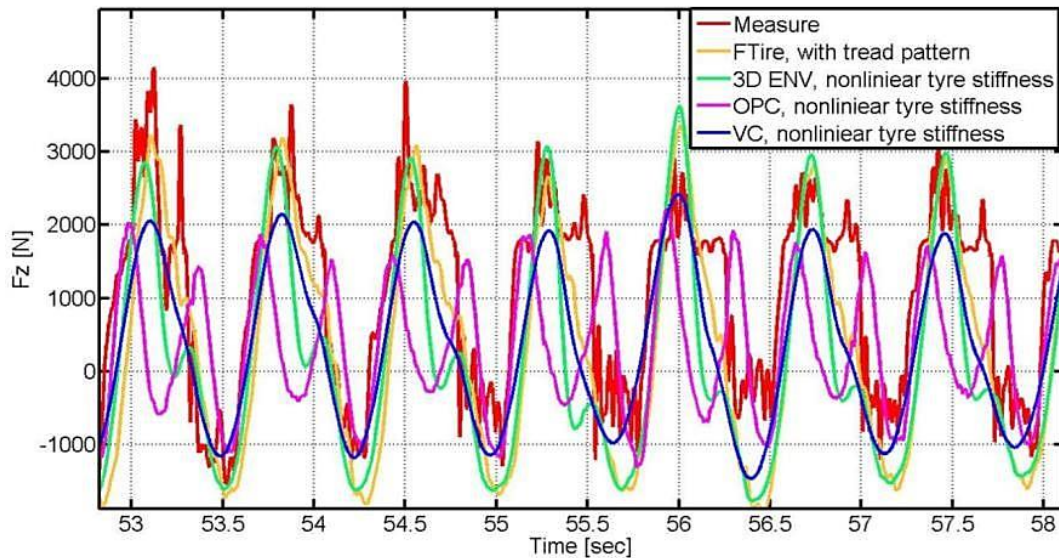
Figure 5-20 Measured and predicted longitudinal force over the Angled corrugation track, LC2, 11km/h

Figure 5-21 shows the measured and predicted normal tyre forces that are generated in the tyre while driving over the angled corrugations. The normal forces, predicted by the FTire tyre model, capture the behaviour of the tyre over the test track. The 3D Equivalent Volume Contact captures the overall tyre behaviour but cannot meet the load extremities.
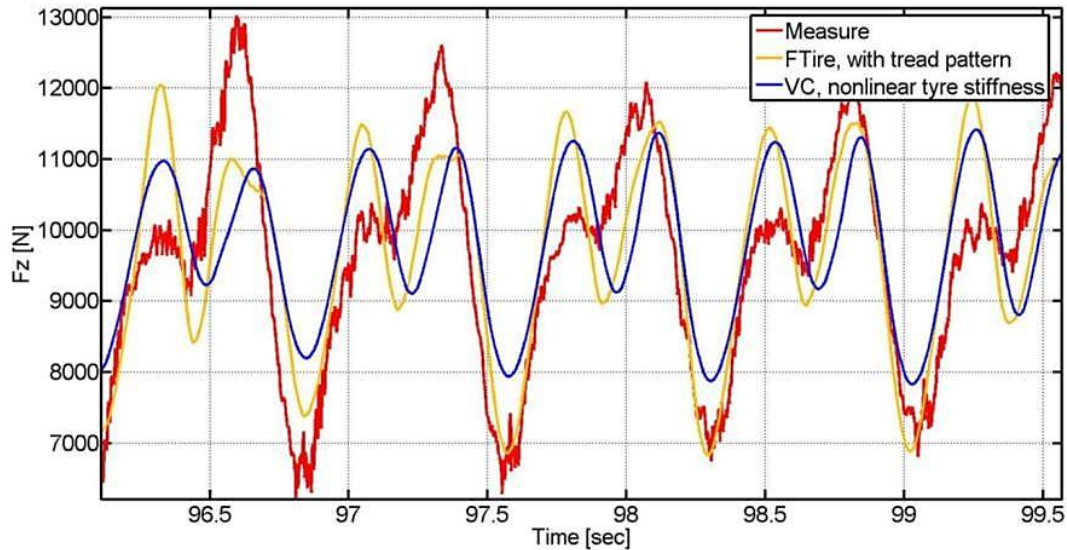
Figure 5-21 Measured and predicted normal load of the Angled corrugation test, LC 1, 3km/h

5.4   Summary

In this chapter various validation metrics were discussed. The validation metrics were useful in comparing various tyre models. It was noted that most validation measures lacked the ability to accurately quantify the correlation. The subjective comparison of the tyre models could not be avoided.

It was found that the FTire model could predict the tyre forces sufficiently accurately for all cleat and test track simulations. The model was able to predict comparable tyre forces for most test velocities and applied load cases. The model was only outperformed by the 3D Enveloping Contact model during the 42km/h 50mm cleat test.

The 3D Enveloping Contact model performed well during the cleat tests. The model however could not predict the tyre behaviour for simulations over the test tracks. This can be related to the modelling approach where the road input is only evaluated on the edges of the contact patch. Obstacles on the inside of the contact patch were disregarded. The shortcoming of this modelling approach is amplified due to the large contact area of the test tyre.

The 3D Equivalent Volume Contact model could not accurately predict the tyre behaviour for simulations over discrete obstacles, such as individual cleats. The contact model could however predict the tyre behaviour sufficiently accurate over rough terrain. The model was not capable of predicting the resulting forces for sharp disturbances. This effect was related to the modelling approach, where the total displaced volume was used to determine the effective tyre road contact point. Sharp disturbances were filtered out so that the model was not able to predict the correct tyre behaviour.

The One Point Contact tyre model was the least suited for simulations over rough terrain. The model could not be used to simulate the tyre behaviour over discrete obstacles. Acceptable results were found for simulations over the fatigue track at relatively high test velocities. This model should be avoided for all simulations where the road surface has disturbances smaller than the tyre circumference.

Table 5-15 Summary of the Validation metrics

Group	Obstacle	Tyre model/ Contact model			
		FTire	**3D ENV**	**3D VC**	**OPC**
Discrete Obstacles	**Cleats**	Comparable, best	Comparable	Not representative	Not representative
	Trapezoidal bump	Comparable, best	Not representative	Comparable	Not representative
Rough tracks	**Belgian paving**	Comparable, best	Not representative	Comparable, under certain conditions	Not representative
	Fatigue track	Comparable, best	Not representative	Comparable	Not representative
	Parallel corrugations	Comparable, best	Not representative	Comparable	Not representative
	Angled corrugations	Comparable, best	Not representative	Comparable	Not representative

The results of the validation metrics were summarized in Table 5-15. The FTire model could in most cases reproduce the best results. The 3D Enveloping Contact model can be used for simulations over discrete obstacles similar to the cleats as discussed in section 3.4.2. The 3D Equivalent Volume Contact model showed acceptable results for simulations where the tyre negotiated the trapezoidal bump, Fatigue track and the Corrugation tracks.

6. Conclusions and Recommendations

"If you cannot measure it, you cannot improve it."

-    *Lord Kelvin, 1885*

6.1   Conclusions

Tyre modelling techniques and their approaches to modelling the tyre road interface have been discussed. Four tyre models implemented in the multi body dynamics simulation software, ADAMS, were discussed detail. The One Point Contact, 3D Equivalent Volume Contact and the 3D Enveloping Contact models were developed by ADAMS. The FTire model, developed by COSIN scientific software, was also discussed.

The tyre models rely on experimental test data for the parameterization process. The amount of test data required and the effort in obtaining the required test data, varies greatly amongst the tyre models. The availability of the test data should thus be considered when selecting a tyre model. The process of acquiring the required test data was discussed in great detail.

The parameterization process of the tyre models was also discussed. The parameterization of the Pacejka contact models was found to be manageable and apparent. It was found that the description of the tyre contact patch width, as used in the 3D Enveloping Contact model, could not be used to accurately describe the footprint width of large truck tyres.

The FTire parameterization process proved to be the most difficult. Multiple parameterization iterations were completed until a tyre model with the required accuracy was created. To date, only static parameterization tests could be used in the parameterization program FTire/fit. The parameters that define the dynamic behaviour of the FTire model were determined by a crude optimization process.

Validation metrics were proposed to determine whether the tyre models could be used to accurately predict the tyre forces when driving over rough terrain. It was found that the 3D Enveloping Contact model and the FTire model were capable of predicting the tyre response for simulations over discrete obstacles. Schmeitz, who proposed the 3D Enveloping Contact tyre model, has shown similar results for passenger car tyres on drum cleat tests. It was found that FTire could predict the tyre response slightly better while negotiating the cleat.

Simulations over the test tracks have shown that the FTire model shows the best correlation between the measured and simulated tyre response. The 3D Equivalent Volume Contact model could predict the tyre behaviour with acceptable accuracy in some cases. The accuracy of the results were however dependent on the test velocity. The tyre contact model could not predict the impulse tyre response over short, high amplitude, road irregularities.

It could thus be concluded that existing tyre models could be used to predict the tyre forces over rough terrain of large off-road tyres. The best overall results were found when the FTire model was used. This tyre model predicted the tyre response accurately over a wide range of obstacles and rough test tacks.

Tyre models that use a 3D Enveloping Contact model could be used for simulations over discrete obstacles. The 3D Equivalent Volume Contact model may be useful in specific cases where the peak impulse loads were not important.

6.2   Recommendations

The model behaviour of the One Point Contact and the 3D Equivalent Volume Contact model could not be improved further. The parameters that determine the model behaviour have been determined and fit experimental data well.

To improve the filtering behaviour of the 3D Enveloping Contact model, the number of cams used should be investigated further. The cams influence the filtering behaviour and it is hypothesized that a correct number of cams would influence the accuracy of the tyre response. The number of cams needed would depend on the road surface, simulation speed and load range.

A bigger contribution can be made if further measurement procedures are investigated that can be used during the parameterization process of FTire. Currently only static tyre test data can be used directly in the parameterization process proposed. It is proposed that the following should be investigated:

I. Develop test equipment that can be used to determine dynamic tyre behaviour in a laboratory. A significant contribution to the improvement of the model can be made with the development of such test equipment. High speed tests are in many cases impractical especially for large tyres. A test rig that can be used to investigate the tyre behaviour at low speeds could hold useful information.
II. Include lateral and longitudinal test data in the parameterization process. These tests can be used to further improve the FTire model.
III. Develop test equipment that can be used to investigate camber effects. Static and dynamic test should include camber test data.
IV. Investigate the poor tyre model performance for simulations over the Fatigue track.

The repeatability of the experimental test should be further investigated. Dynamic cleat test, where the cleat is orientated parallel to the direction of travel, show good repeatability. Similar tests should be conducted to determine the repeatability of oblique orientated cleats and the test tracks.

7   Bibliography

Antoine, R.C., Schmeitz, J.C., Jansen, S.T.H., Verhoeff ,L. & Besselink, I.J.M.,2005, M*F-Swift simulation study using benchmark data*, Vehicle System Dynamics, 43:92–101.

Bekker, C.M., 2008, *Profiling of rough terrain*, Unpublished Master's Thesis, University of Pretoria, Pretoria, South Africa.

Captain, Khushroo M. et al., 1974, *The Development and Comparative Evaluation of Analytical Tire Models for Dynamic Vehicle Simulation*, Foster Miller Associates, Inc., Prepared for the Army Tank Automotive Command (ATAC), Source: National Technical Information Service, U.S. Department of Commerce.

Cremens, R., 2005, *Investigating Dynamic Tyre Model Behavior*, Unpublished Master's Thesis, Eindhoven University of Technology.

De Roon, M., 2006, *Tire modeling for for car, truck, motorcycle and heavy duty industrial applications using TNO Delft-Tyre*, Confrence presentation, European LMS Conference, Munich, Germany.

Einsle, S., 2010, *Analyse und Modelierung des Reifenubertragungsverhalten bei transienten und extremen Fahrmanovern*, PhD.Eng Thesis, Technische Universitaet Desden, Dresden, Germany.

Els, P.S. and Becker, C.M., 2010, *Characterisation and modelling of off-road tyres*, Proceedings of the Joint 9th Asia-Pacific ISTVS Conference and Annual Meeting of Japanese Society for Terramechanics, Sapporo, Japan.

Freedonia., 2012, *World Tires to 2015 - Industry Market Research, Market Share, Market Size, Sales, Demand Forecast, Market Leaders, Company Profiles, Industry Trends*, viewed 13 August 2013, from: http://www.freedoniagroup.com/DocumentDetails.aspx?ReferrerId=FG-01&studyid=2860.

Frey, W.F., 2009, *Development of a rigid ring tire model and comparison among various tire models for ride comfort simulations*, Master's Thesis, Clemson University, August 2009.

Gerotek Test Facilities, n.d., viewed 2 July 2013, from www.gerotek.co.za.

Gipser, M, n.d.,*The FTire Tire Model Family*. , viewed 2 July 2013, from http://www.cosin.eu/literature.

Gipser, M., 1999, *FTire a New Fast Tyre Model for Ride Comfort Simulations*, 1999 International and 14th European ADAS User Conference.

Gipser, M., Hofmann, G.,2010, *FTire, Modelization and Parameter Specification*, viewed 2 July 2013, from http://www.cosin.eu/literature.

Gipser, M.,2002, *ADAMS/FTire – A Tyre Model for Ride & Durability Simulations*, Proc. ADAMS User's Conf., Tokyo.

Gough, V. E. & Whitehall, S. G., 1962. *Universal tyre test machine*. Proc. FISITA 9th Int. Technical Congress.

International Standard ,1995, *ISO 8608: Mechanical Vibration – Road Surface Profiles – Reporting of Measured Data,* International Standard.

Pacejka, H.B., Bakker, E., & Lidner, L., 1987, *Tyre moddeling for use in vehicle dynamics studies*, SAE paper 870421.

Pacejka, H.B., Bakker, E., & Lidner, L., 1989, *A New Tyre Model with an Application in Vehicle Dynamics Studies*, SAE paper 890087.

Pacejka, H.B., & Sharp, R.S., 1991, *Shear force development by pneumatic tyres in steady state conditions: A review of modeling aspects.*, Vehicle System Dynamics 20. pp121-176.

Pacejka, H.B., 2002, *Tyre and Vehicle Dynamics*, Butterworth-Heinemann.

Kat,C. & Els, P.S., 2012, *Validation metric based on relative error, Mathematical and Computer Modelling of Dynamical Systems: Methods*, Tools and Applications in Engineering and Related Sciences, 18:5, 487-520.

Michelin, n.d., Michelin Americas Truck Tires XZL, viewed 13 August 2013, from http://www.michelintruck.com/michelintruck/tires-retreads/tireInfo.do?tread=XZL.

Mohammadi, F., 2012, *Tire Characteristics Sensitivity Study*, Master's Thesis, Chalmers University of Technology

MSC Sotfware (a), n.d., *DOC 10023- Help Document for Adams/Tire*, viewed 2 July 2013, from http://simcompanion.mscsoftware.com/infocenter.

MSC Sotfware (b), n.d.,*ADM740 Seminar Class: Adams/Car, Seminar handout distributed in the unit ADM740 MSC.ADAMS Training Course*, Esteq, Pretoria on June 2010.

MTS., n.d., *Flat-Trac®Tire Test Systems*, viewed 10 August 2013, from http://www.mts.com/ucm/groups/public/documents/library/dev_002227.pdf

Mullineux, N., 2011, *History of the Tire-World Tire Industry Report*, viewed 10 August 2013, from http://www.worldtirereport.com/Contents/SectionOneIntroduction/TireHistory

Oosten, J., 2001, *How to get tire model parameters*, MSC Software Office, Munich, Germany.

OpenCRG, 2011., *User Manual*, viewed 10 August 2013, from http://www.vires.com/opencrg/docs/OpenCRGUserManual.pdf.

Rill, G., 2006, *Vehicle Dynamics*, Lecture notes, Fachhochschule Regensburg, viewed 10 August 2013, from https://hps.hs-regensburg.de/~rig39165/.

SAE International, 2013, SAE standard: Tire Performance Technology, (SAE J 2047) SAE International, Troy, Michigan.

Schmeitz, A.J.C., 2004. *A Semi-Empirical Three-Dimensional Model of the Pneumatic Tyre Rolling over Arbitrarily Uneven Road Surfaces*, PhD Thesis, Delft University of Technology, Delft, The Netherlands.

Schwalbe, G., n.d., *TYROSAFE 1st workshop* , viewed 10 August 2013, from http://tyrosafe.fehrl.org/?m=49&mode=download&id_file=7796

Tianjin Jiurong Wheel Tech Company, n.d., *Off the Road Tire Durability Test Machine* , viewed 10 August 2013, from http://www.chinajiurong.com/EngLish/ProShow.asp?id=44.

TÜV SÜD., n.d., *Test Rigs for Tires/Wheels*, viewed 10 August 2013, from http://www.tuev-sued.de/uploads/images/1263905646961806440579/Produktblatt-Test-Rigs-Tires--Wheels-englisch.pdf

Unrau, H.-J., Riedel, A., van Oosten, J. J. M., & Bakker, E.,1999, *Standardization in Tire Modeling and Tire Testing — TYDEX Workgroup, TIME Project*. Tire Science and Technology: July 1999, Vol. 27, No. 3, pp. 188-202.

Zegelaar, P.W.A., 1998, *The dynamic response of tyres to brake torque variations and road unevenness,* PhD Thesis, Delft University of Technology, Delft, The Netherlands.